Higher order corrections to deeply virtual Compton scattering

Dissertation zur Erlangung des Doktorgrades der Naturwissenschaften (Dr. rer. nat.) der Fakultät Physik

der Universität Regensburg

vorgelegt von

Jakob Christoph Schönleber aus

Regensburg

im Jahr 2023

Promotionsgesuch eingereicht am: 10. März 2023

Die Arbeit wurde angeleitet von: *Prof. Dr. Vladimir Braun*

Prüfungsausschuss:

Vorsitzender:	*Prof. Dr. Jascha Repp*
1. Gutachter:	*Prof. Dr. Vladimir Braun*
2. Gutachter:	*Prof. Dr. Gunnar Bali*
weiterer Prüfer:	*Prof. Dr. Jaroslav Fabian*

Das Kolloquium fand statt am 01.06.2023.

Gesamtnote: **summa cum laude**.

Abstract

This dissertation is devoted to the calculation of perturbative corrections to deeply virtual Compton scattering. This reaction is the gold-plated process for studying generalized parton distributions that encode information on the three-dimensional tomographic imaging of the nucleon, which is a significant part of the experimental program at major hadron physics experimental facilities at Jefferson Laboratory and the upcoming Electron-Ion Collider at Brookhaven National Laboratory. In this thesis I present the theoretical foundations and shortly describe the methods that were used to obtain the main results: the complete next-to-next-to-leading order coefficient functions and the resummation formula for threshold logarithms at the next-to-next-to-leading logarithmic order. These results are expected to substantially improve the accuracy of the extraction of generalized parton distributions from current and future experimental data.

Contents

List of Figures

List of Tables

1 Introduction

The description of the hydrogen atom from the non-relativistic Schrödinger equation yields the complete information about the electron's energy eigenstates. For each state, a probability distribution of the electron position with respect to the proton can be calculated and is visualized for the first few states in Fig. 1.1. These pictures provide an illustrative example for the imaging of quantum objects, in this case the spatial probability densities in a cross section of an hydrogen atom. Similar probability distributions can be obtained for more complicated atoms and molecules. The importance of the quantitative understanding of atoms for science and technology is hard to understate.

In the usual treatment of the hydrogen atom, the proton is viewed as as static positively charged massive object, whose internal structure is not relevant for atomic physics phenomena. This approximation has high accuracy and is justified by vastly different energy scales associated to atomic and nuclear physics, with the ground state energy of hydrogen being about 10 eV and the mass of the proton being about 1 GeV. Conversely, in order to uncover the proton structure one needs much larger energies than are typical in atomic physics.

It is well known that the proton is not an elementary particle, but a bound state of quarks and gluons. In the quark model of the 1960s the constituents are two up- and one down-quark, as shown on the left in Fig. 1.2. The early quark model was essentially a classification scheme for hadrons and successfully predicted for example the existence of the Ω^- baryon [2–4]. However, it does not give any quantitative tools to investigate hadron structure from first principles. Our current fundamental theory governing particle interactions is the standard model of particle physics. Quantum chromodynamics (QCD), being part of the standard model, is the dynamic theory governing the interactions of quark and gluons in the proton.

The question arises whether one can obtain the multi-particle bound state wave functions of the energy eigenstates in terms of those elementary constituents. Unfortunately, the QCD Hamiltonian is much more complicated than any Hamiltonian in non-relativistic quantum mechanics. First of all, like in any relativistic quantum field theory, particle number is not conserved. Thus, in addition to the three so-called valence quarks predicted by the quark model, any number of quark-antiquark pairs, called sea quarks, and gluons may pop into existence inside the proton in accordance with the uncertainty principle. A visualization is shown on the right in Fig. 1.2. As it turns out sea quarks and gluons make a significant contribution to the bound state structure of the proton. An exception to this is for example the electric charge, which is the sum of charges of the valence quarks, since quark-antiquark pairs and gluons have zero electric charge. The sea quarks and gluons do, however, contribute to the total spin of the proton through their angular momentum and spin, as is illustrated in Fig. 1.2.

The problem of particle number not being conserved is however the lesser problem when investigating the proton in QCD. In any quantum field theory (QFT), such as QCD, observables can generally only be calculated approximately. With an exception of first principles numerical simulations of some key observables, using lattice QCD techniques, most of the interesting quantities can only be calculated using perturbation theory. More precisely, an observable $\mathcal{O}$ is given by an

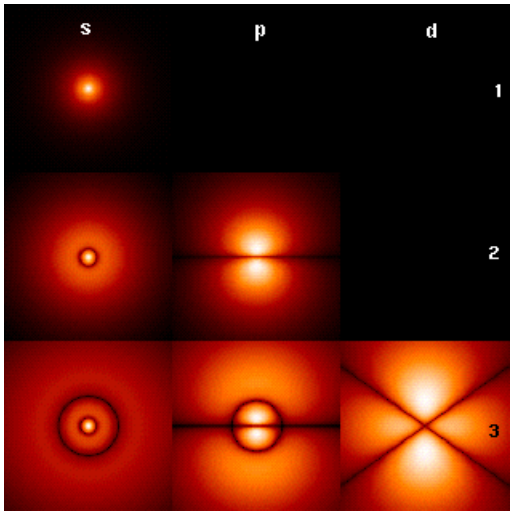

Figure 1.1: Spatial probability densities in the xz-plane of the electron in the hydrogen atom at different quantum numbers (ℓ, across top; n, down side; $m = 0$), Taken from `https://en.wikipedia.org/wiki/Hydrogen_atom`

infinite power series in the coupling constant α

$$\mathcal{O} = \sum_{n=0}^{\infty} \alpha^n c_n.$$

Most of the time only the first few coefficients c_n in this expansion are calculated. The approximation is of course only appropriate if the series is converging sufficiently fast. This is for example ensured if $\alpha \ll 1$ and $c_n \sim 1$. But in reality, any perturbative expansion for quantum systems is only an asymptotic expansion in the mathematical sense and does not converge (has zero radius of convergence) due to factorial growth of the coefficients $c_n \sim n!$ at very high orders [5–8]. The ultimate accuracy of the perturbative description is usually assumed to be of the order of the minimum term in the series which can be an acceptably small number, suppressed by a power of the large momentum.

The situation in QCD is, however, additionally complicated by the strong coupling becoming "too strong", of the order of unity at energy scales of the inverse proton size, so that no perturbative description is possible at all.

There exist approaches to obtaining information about proton structure without the use of QCD, most prominently the quark model, see Ref. [9] for a recent review. Such approaches have some predictive power, but are generally unsatisfactory since they are not derived from the fundamental principles. Lattice QCD on the other hand has this feature and though it had many successes, the uses are limited and it should be viewed as complementary to perturbative QCD.

The bulk of the applications of QCD to the physics of hadrons exploit the "asymptotic freedom" property, meaning that the interaction strength decreases with energy. The basic idea is that the process of interest can be separated in subprocesses occurring at small and large distances (or equivalently at large and small energies) which can be treated using different methods. This

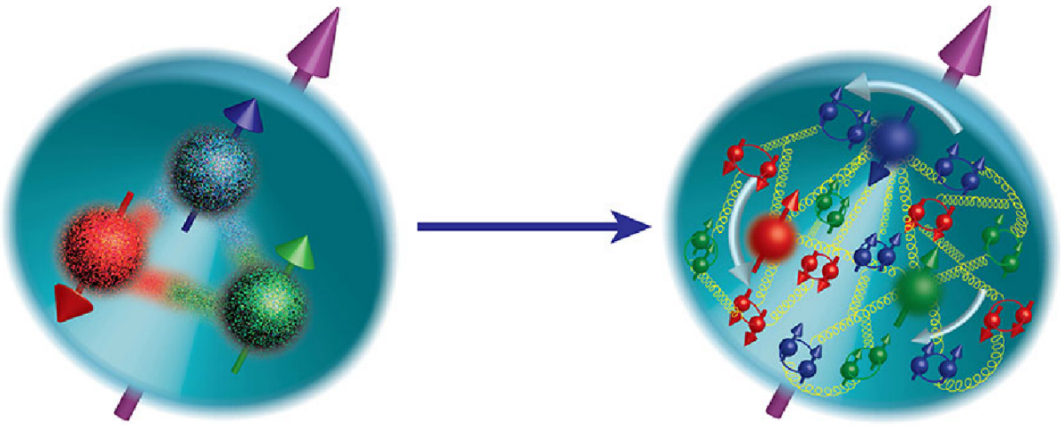

Figure 1.2: Evolution of our understanding of the nucleon. The arrows indicate how the total spin of the proton arises in terms of its constituents. Left: The quark model picture, where the nucleon consists of three quarks. Right: In QCD the nucleon is a complex object with many quark-antiquark pairs and gluons in addition to the three valence quarks. Picture taken from [1].

approach is referred to as factorization. Short-distance/large-energy effects are treated using QCD perturbation theory, whereas large-distance/small-energy physics input is obtained by matching theory to experiment, or from lattice calculations.

The important point is that the non-perturbative physics can be encoded in certain universal functions that encode information on hadronic structure. The historically first example of this approach is Feynman's parton model, applied, for example, to deep inelastic scattering (DIS). In this process a highly energetic electron scatters off the proton. In a suitable frame of reference, the proton can be viewed as a Lorentz-contracted "pancake" shaped composite system, with the interaction between the constituents (partons) slowed down by relativistic time-dilation, such that the partons can be considered to be quasi-free at the time scales relevant for the interaction with an energetic (high-frequency) photon. This implies that the photon-proton interaction proceeds via photon scattering from a single parton (quark or gluon) and the DIS cross section is given by a sum of probabilities of scattering from different partons, i.e. there is no quantum interference. The probability density to find a parton of a given species and with given longitudinal momentum fraction inside a given hadron is called a parton distribution function (PDF). These functions are key non-perturbative inputs for most QCD applications.

On a more detailed level, the proton structure can be described through a multitude of quantum correlation functions (QCFs). An important subclass of QCFs, see Fig. 1.3, can be obtained from the so-called Wigner distribution $W(x, \vec{b}_T, \vec{k}_T)$ [11], which is the QCD analog of the Wigner quasi-probability distribution $W(\vec{x}, \vec{p})$ [12], which in some sense encodes the maximum amount of information on the wave-function of the system. In particular $\int d^3\vec{p}\, W(\vec{r}, \vec{p})$ and $\int d^3\vec{x}\, W(\vec{x}, \vec{p})$ give the usual quantum mechanical probability distributions in position and momentum, respectively. Correspondingly, integrating $W(x, \vec{b}_T, \vec{k}_T)$ over $\vec{b}_T$ and $\vec{k}_T$ gives the transverse momentum distributions (TMDs) and impact parameter distributions (IPDs), respectively. The TMDs integrated over

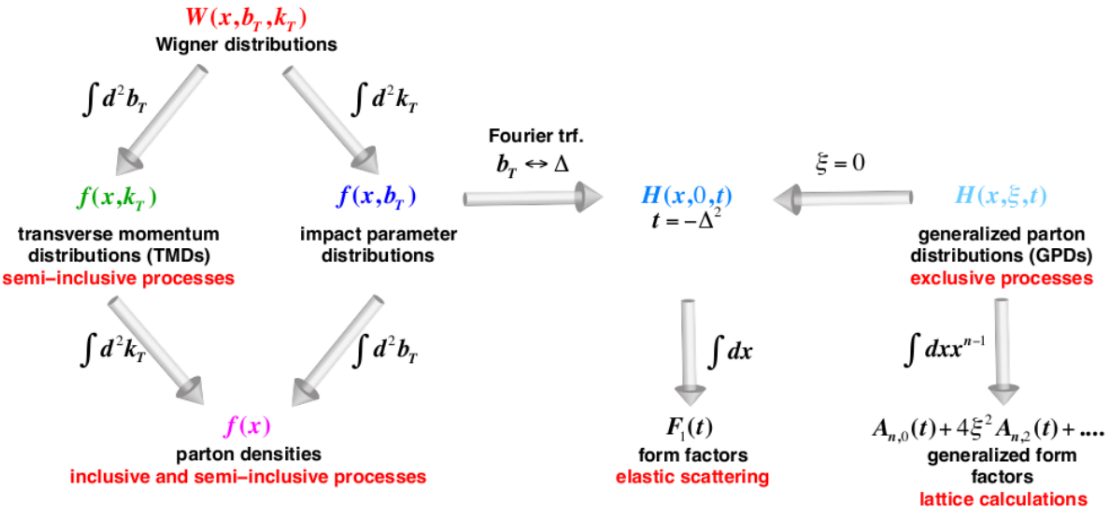

Figure 1.3: Connections between different QCFs describing the distribution of partons inside the proton. Taken from [1].

$\vec{k}_T$ and the IPDs integrated over $\vec{b}_T$ in turn give the PDFs. $W(x, \vec{b}_T, \vec{k}_T)$ of the proton is however currently unattainable through experiment.

In this thesis we will focus on the generalized parton distributions (GPDs) [13–17], from which the IPDs can be obtained directly. The IPDs are the spatial probability distributions for a given parton with given longitudinal momentum fraction in the plane perpendicular to the hadron momentum. A schematic representation is shown in Fig. 1.4 and an example from a lattice QCD calculation is shown in Fig. 1.5. These studies, together with the momentum space picture of the TMDs, are broadly gathered under the three-dimension "tomographic" imaging of the proton. The physics program of the planned Electron-Ion Collider (EIC) [1, 18, 19] states this as a major goal. It should be noted that this is not the only information that GPDs give about proton structure. Indeed, they yield information on the decomposition of proton spin in terms of its constituents [14] and various inter- and multi-parton correlations [20].

The most prominent process that gives access to GPDs is Deeply Virtual Compton Scattering (DVCS) [14–16], which is the scattering of an electron from a proton, where the proton remains intact and in addition an outgoing photon in the final state is measured. DVCS has been studied at experimental facilities at DESY [21–32], JLAB [33–40] and CERN [41]. Further experiments are planned at JLAB, CERN and the upcoming EIC. A good control over the perturbative physics will be necessary to match the precision of these experiments. In particular, since GPDs are usually determined from inventing models and matching the model parameters to data, the extraction of the GPDs may depend strongly on small variations of the perturbative calculations.

There are two directions in which QCD theory predictions can be improved. The first one is to consider higher order perturbative corrections to the leading power in α_s of the underlying

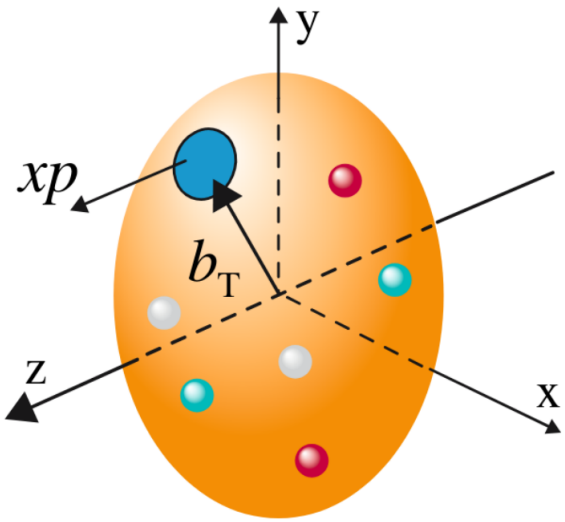

Figure 1.4: Schematic view of a parton with longitudinal momentum fraction x and transverse position $\vec{b}_T$ in the proton. Taken from [1].

short-distance subprocess, which are usually termed radiative corrections [1] These corrections are the subject of this thesis, with the main goal to achieve the so-called next-to-next-to leading order (NNLO) accuracy. The second one is to include power corrections corresponding to kinematic effects and quark-gluon correlations. These terms generally involve more complicated QCFs and are very poorly understood. They will be omitted in what follows. Although, in order to obtain an acceptable theoretical precision, a good control of both types of corrections is needed in general.

To obtain α_s corrections one needs to compute Feynman diagrams of increasing complexity. We are way beyond the point where state-of-the-art calculations are feasible to do by hand. Instead, computer algebra based methods are used to obtain results for Feynman diagrams. Probably the most powerful method are the integration-by-parts (IBP) identities [46], which reduce a large set of diagrams to a manageable set of master integrals. These integrals can then be calculated by various methods, the most prominent being the method of differential equations [47].

This text is organized as follows. In Cha. 2 we present a review of DVCS at leading power. In particular, we perform the leading twist expansion of the hadronic off-forward Compton tensor and describe how it can be parameterized in terms of Compton form factors (CFFs). We also discuss evolution equations for GPDs and the finite renormalization for the axial-vector GPD.

In Cha. 3 we first briefly introduce computer algebra methods for Feynman integrals and then describe the calculation of the two-loop coefficient function (CF) of DVCS as it was performed in Ref. [48]. We also introduce an alternative method, based on conformal symmetry, to calculate the CF. Then we introduce the Goncharov polylogarithms [49] and their subset, the harmonic polylogarithms (HPLs) [50]. The HPLs serve as a convenient basis of functions in which the CF can be expressed.

In Cha. 4 we first discuss some aspects of DVCS phenomenology. Then we introduce the

[1]Sometimes the term "radiative corrections" also refers to electromagnetic $\alpha_{\rm em}$ corrections. These have been discussed in the context of DVCS in Refs. [42–45]

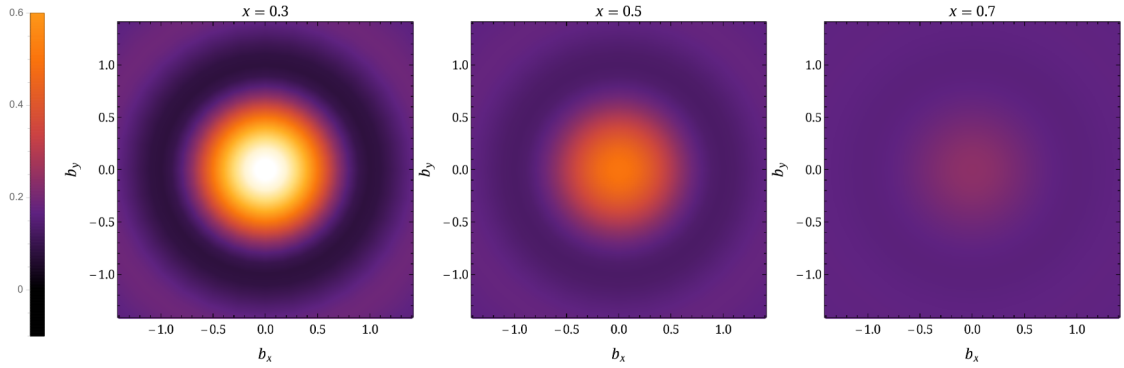

Figure 1.5: Nucleon IPD of a quark for $x = 0.3,\ 0.5$ and 0.7 from lattice QCD calculation at the scale of the physical pion mass [10].

Goloskokov-Kroll (GK) model [51] for the GPDs H_q, H_g and describe how one can perform the convolution integral with the CF. We discuss some numerical results for NNLO corrections using the GK model, in order to get an idea of the size of radiative corrections to DVCS.

Finally, in Cha. 5 we explain how contributions to the CFs that are logarithmically enhanced in the threshold regions $x \to \pm\xi$ can be resummed to all orders [52]. Then we briefly discuss the numerical impact.

Basic notation and conventions

Throughout this work we use dimensional regularization with the space-time dimension denoted by $d = 4 - 2\epsilon$ and we use the $\overline{\text{MS}}$-scheme. Feynman gauge is used throughout. We define

$$a_s = \frac{\alpha_s}{4\pi} = \frac{g^2}{(4\pi)^2}, \tag{1.1}$$

where g is the renormalized QCD coupling constant. We define the β function as

$$\beta(a_s) = \mu \frac{da_s}{d\mu} = -2a_s\Big(\epsilon + \sum_{j=0}^{\infty} \beta_j a_s^j\Big), \tag{1.2}$$

so that

$$\beta_0 = \frac{11}{3}C_A - \frac{2}{3}n_f, \qquad \beta_1 = \frac{2}{3}\Big(17C_A^2 - 5n_f C_A - 3n_f C_F\Big), \qquad \ldots, \tag{1.3}$$

where n_f is the number of quark flavors. In terms of the number of colors N_c the quadratic Casimirs of the SU(N_c) group in the fundamental and adjoint representation are given by

$$C_F = \frac{N_c^2 - 1}{2N_c} \qquad \text{and} \qquad C_A = N_c, \tag{1.4}$$

respectively. For a general perturbative quantity X, we define

$$X = \sum_{j=0}^{\infty} a_s^j X^{(j)} = \sum_{j=0}^{\infty} \sum_{k=-2j}^{\infty} a_s^j \epsilon^k X^{(j,k)}, \tag{1.5}$$

where we assumed that any relevant quantity diverges no worse than ϵ^{-2j} for $\epsilon \to 0$, where j is the order in a_s.

We denote by a bar over $z \in \mathbb{C}$ the number $\bar{z} = 1 - z$. We will frequently use the variables

$$z = \frac{1}{2}(1 - x/\xi), \qquad L = \log \frac{\mu^2}{Q^2}, \tag{1.6}$$

where x, ξ, μ, Q are standard notation used in the DVCS literature.

We use light-cone coordinates with respect to two light-like vectors $n, \bar{n}$ with $n^2 = \bar{n}^2 = 0$ and $n \cdot \bar{n} = 1$. Without loss of generality we can define

$$n^\mu = \frac{1}{\sqrt{2}} \begin{pmatrix} 1 \\ 0 \\ 0 \\ 1 \end{pmatrix}^\mu, \qquad \bar{n}^\mu = \frac{1}{\sqrt{2}} \begin{pmatrix} 1 \\ 0 \\ 0 \\ -1 \end{pmatrix}^\mu. \tag{1.7}$$

For a generic vector V we define $V^+ = n \cdot V$, $V^- = \bar{n} \cdot V$ and $V_\perp - V^+\bar{n} - V^- n$. We will commonly denote a vector V in terms of its light-cone components by

$$V = (V^+, V^-, V_\perp). \tag{1.8}$$

2 Deeply virtual Compton scattering at leading power

2.1 Preliminaries

In the DVCS process a highly energetic photon γ^*, produced by an energetic lepton ℓ, scatters of a nucleon N, without destroying it while producing a real photon γ,

$$\gamma^*(q)N(p) \to \gamma(q')N(p'). \tag{2.1}$$

It is fully exclusive, meaning that the recoiled proton and lepton as well as the real photon must be measured. DVCS is part of the more general process of leptoproduction of a photon from a nucleon target [14, 16, 53–62]

$$\ell(k)N(p) \to \ell(k')\gamma(q')N(p'), \tag{2.2}$$

where in addition also the Bethe-Heitler (BH) process

$$\ell(k) \to \gamma^*(\Delta)\gamma(q')\ell(k'), \tag{2.3}$$

with $\Delta = k - q' - k'$, contributes. The total scattering amplitude is the sum of the DVCS and BH amplitudes

$$\mathcal{M} = \mathcal{M}_{\text{DVCS}} + \mathcal{M}_{\text{BH}}. \tag{2.4}$$

At leading order in the electromagnetic interactions and neglecting contributions from the exchange of a massive vector boson, the corresponding Feynman diagrams are shown in Fig. 2.1. Applying

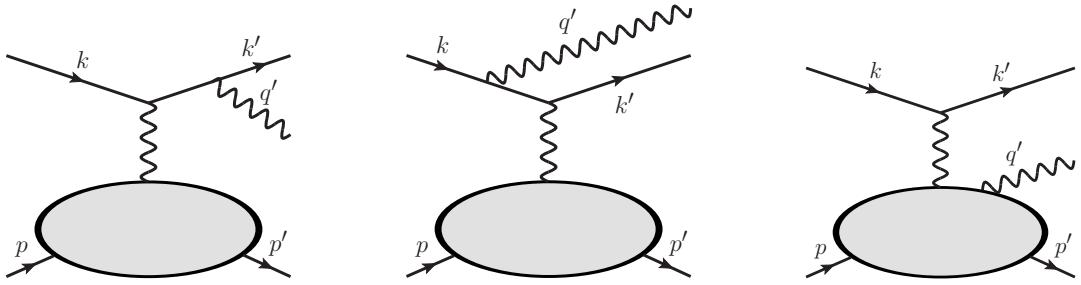

Figure 2.1: Leading order diagrams in electromagnetic interactions of electroproduction of a photon from a nucleon target. First two graphs from the left: Bethe-Heitler process, Right-most graph: Deeply virtual Compton scattering.

the Feynman rules yields the expressions for the scattering amplitudes

$$i\mathcal{M}_{\rm BH} = -\frac{e^3}{\Delta^2} e_\ell^2 \bar{u}_{\lambda'}(k') \left(\not{\ell} \frac{1}{\not{k}' + \not{\Delta} - m_\ell} \not{\varepsilon}^*_{h'}(q') + \not{\varepsilon}^*_{h'}(q') \frac{1}{\not{k} - \not{\Delta} - m_\ell} \not{\ell} \right) u_\lambda(k),$$
$$i\mathcal{M}_{\rm DVCS} = -\frac{ie^3}{q^2} e_\ell \bar{u}_{\lambda'}(k') \gamma_\mu u_\lambda(k) \varepsilon^*_{h',\nu}(q') T^{\mu\nu}, \tag{2.5}$$

where we introduced the nucleon electromagnetic current

$$J^\mu = \langle N(p',s')|j^\mu(0)|N(p,s)\rangle \tag{2.6}$$

and the hadronic tensor

$$T^{\mu\nu} = i \int d^4x \; e^{-iqx} \langle N(p',s')|T\{j^\mu(x) j^\nu(0)\}|N(p,s)\rangle. \tag{2.7}$$

We also introduced the (quark) electromagnetic currents

$$j^\mu(x) = \sum_q e_q \bar{q}(x) \gamma^\mu q(x), \tag{2.8}$$

with the sums over quark flavors q and corresponding charges e_q.

Let us introduce the kinematical parameters of the DVCS process. It is conventional to define the four-vectors

$$P = \frac{p+p'}{2}, \qquad \Delta = p' - p, \qquad Q^2 = -q^2 \tag{2.9}$$

and the Lorentz scalars

$$x_B = \frac{Q^2}{2p\cdot q}, \qquad t = \Delta^2, \qquad m^2 = p^2 = p'^2, \tag{2.10}$$

where x_B is the Bjorken variable and m is nucleon mass.

It is useful to choose a preferred frame of reference to analyze the process. Our choice of frame in this thesis is defined by requirement that $q'^+, q'_\perp, P_\perp = 0$. In particular, q' is taken to be proportional to the light-like vector n, whereas the nucleon momenta are proportional to $\bar{n}$ for $m^2, t = 0$. Explicitly

$$\begin{aligned}
p &= \Big((1+\xi) P^+, (1-\xi) \frac{4m^2 - t}{8P^+}, \frac{\Delta_\perp}{2} \Big), \\
p' &= \Big((1-\xi) P^+, (1+\xi) \frac{4m^2 - t}{8P^+}, -\frac{\Delta_\perp}{2} \Big), \\
q &= \Big(-2\xi P^+, \frac{Q^2 + t + (4m^2 - t)\xi^2}{4\xi P^+}, -\Delta_\perp \Big), \\
q' &= \Big(0, \frac{Q^2 + t}{4\xi P^+}, 0 \Big).
\end{aligned} \tag{2.11}$$

Here the transverse components of Δ are defined only up to rotations in the transverse plane with the constraint that

$$\Delta_\perp^2 = 4m^2\xi^2 + t(1-\xi^2). \tag{2.12}$$

We also introduced the skewness variable $\xi = \frac{p^+ - p'^+}{p^+ + p'^+}$. It is related to the Bjorken variable x_B by

$$\xi = \frac{x_B(Q^2 + t)}{2Q^2 - x_B(Q^2 - t)}. \tag{2.13}$$

If we say that both p, p' are particles (i.e. not antiparticles) we must have $-1 < \xi < 1$. Throughout this work we will additionally assume that $p'^+ < p^+$, so that $0 < \xi < 1$. Then the obvious statement $\Delta_\perp^2 < 0$ implies the maximum value t for a given ξ and m^2

$$t < -\frac{4m^2\xi^2}{1 - \xi^2} < 0. \tag{2.14}$$

2.2 Factorization of the Compton tensor

In order to deal with the non-perturbative object $T^{\mu\nu}$ we need to demand certain kinematical order-of-magnitude restrictions to make use of factorization, which allows to encode non-perturbative physics in the QCFs, in this case the GPDs. These kinematical restrictions are

$$Q^2 \gg -t, m^2, \qquad P^+ \sim Q. \tag{2.15}$$

Contributions that are suppressed by powers of $\lambda \sim \sqrt{-t}/Q,\ m/Q$ are called higher-twist corrections or power-corrections. Here the relation $\sim$ means that $a \sim b$ if and only if $a = O(b)$ and $b = O(a)$ as $Q \to \infty$. In this work we will only consider terms of leading power in λ, also called leading twist. The standard proof of the factorization theorem of the $T^{\mu\nu}$ [63, 64] uses the analysis of Libby and Sterman [65], where leading regions of loop momentum space are identified through the Landau criterion [66–68]. The standard arguments [63, 69] culminate in the leading regions represented by the reduced graphs in Fig. 2.2. Two additional subtleties regard the possible q' collinear subgraph at the outgoing photon vertex and a soft subgraph that may attach to the collinear subgraphs. However, it can be shown that these contributions are power suppressed [63].

Consider a generic graph Γ contributing to the $T^{\mu\nu}$ written in a form corresponding to Fig. 2.2 a), where a reference to a specific region $R(H, A)$ is suggested. Formally, in the region $R(H, A)$ the momenta of lines in the subgraph H are hard $l \sim q$ and the line momenta in the subgraph A are $\bar{n}$-collinear $l \sim P$. The diagram may be written as

$$\begin{aligned}\Gamma(H, A) = \int d^d k \Big(\int \prod_{j=1}^{N} d^d l_j \Big) H^{\mu\nu\mu_1 \dots \mu_N}_{\alpha_1, c_1, \alpha_2, c_2, a_1, \dots, a_N}(q, q', k, l_1, \dots, l_N) \delta_{\alpha_1\beta_1} \delta_{\alpha_2\beta_2} \delta_{c_1 d_1} \delta_{c_2 d_2} \\ \times \Big(\prod_{j=1}^{N} g_{\mu_j\nu_j} \delta_{a_j b_j} \Big) A^{\nu_1 \dots \nu_N}_{\beta_1, d_1, \beta_2, d_2, b_1, \dots, b_N}(p, p', k, l_1, \dots, l_N),\end{aligned} \tag{2.16}$$

where μ_j, ν_j are Lorentz indices, a_j, b_j, c_j, d_j are color indices (in the fundamental or adjoint representation) and α_j, β_j are spin/Lorentz indices corresponding to the two outer parton lines, quarks or transversely polarized gluons. Applying the region approximator $T_{R(H,A)}$ amounts to the following replacements.

- For the two outer parton lines insert projectors on the leading components of spin/Lorentz indices between the contraction of indices between H and A.

$$\delta_{\alpha_1\beta_1} \to \mathcal{P}_{\alpha_1\beta_1}, \qquad \delta_{\alpha_2\beta_2} \to \bar{\mathcal{P}}_{\alpha_2\beta_2} \tag{2.17}$$

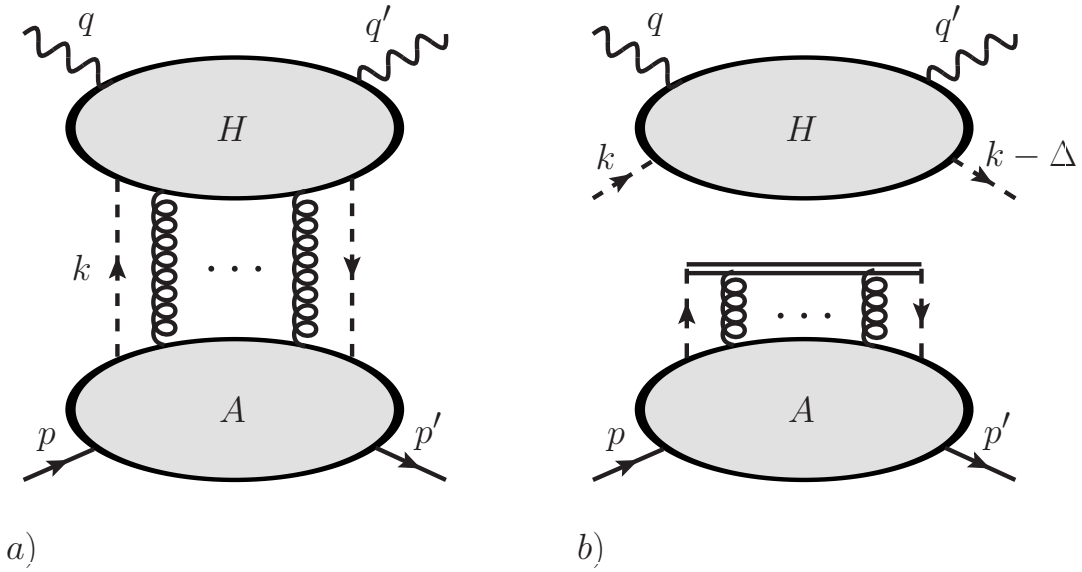

Figure 2.2: a) Leading regions of the hadronic tensor $T^{\mu\nu}$. The dashed lines may be quark lines or transversely polarized gluon lines. b) $T^{\mu\nu}$ after application of the region approximation.

For quarks

$$\mathcal{P}_{\alpha_1\beta_1} = \frac{1}{2}(\gamma^+\gamma^-)_{\alpha_1\beta_1}, \qquad \bar{\mathcal{P}}_{\alpha_2\beta_2} = \frac{1}{2}(\gamma^-\gamma^+)_{\alpha_2\beta_2}, \tag{2.18}$$

while for gluons

$$\mathcal{P}_{\alpha_1\beta_1} = g_{\perp,\alpha_1\beta_1}, \qquad \bar{\mathcal{P}}_{\alpha_2\beta_2} = g_{\perp,\alpha_2\beta_2}, \tag{2.19}$$

where $g_\perp^{\mu\nu} = g^{\mu\nu} - n^\mu\bar{n}^\nu - \bar{n}^\mu n^\nu$.

- In the hard subgraph H replace all momenta by their leading twist approximations, i.e. $\lambda \to 0$, denoted by a hat over the symbol. For the loop momenta in H we must make the replacement

$$\begin{aligned} k^\mu &\to \hat{k}^\mu = k^+\bar{n}^\mu, \\ l_j &\to \hat{l}_j^\mu = l_j^+\bar{n}^\mu. \end{aligned} \tag{2.20}$$

  I.e. we replace $H(q, q', k, l_1, ..., l_N) \to H(\hat{q}, \hat{q}', \hat{k}, \hat{l}_1, ..., \hat{l}_N)$.

- For the contraction of an μ_j index between H and A, replace the corresponding metric tensor by

$$g_{\mu_j\nu_j} \to \frac{\hat{l}_{j,\mu_j} n_{\nu_j}}{\hat{l}_j \cdot n + i0}. \tag{2.21}$$

  Then use Ward identities to decouple the collinear gluons from the hard subgraph. This requires to sum over hard subgraphs $\sum_H$ with the same number of collinear gluon insertions.

Proving this decoupling rigorously in the graphical approach is very complicated in the case of QCD. However, the results have become standard. We get

$$\sum_H H^{\mu\nu\mu_1\ldots\mu_N}_{\alpha_1\alpha_2,a_1\ldots a_N}(\hat{q},\hat{q}',\hat{k},\hat{l}_1,...,\hat{l}_n) \to \sum_{\hat{H}} \hat{H}^{\mu\nu}_{\alpha_1\alpha_2}(\hat{q},\hat{q}',\hat{k})\ \mathcal{W}^{\mu_1\ldots\mu_N}_{a_1\ldots a_N}(l_1^+,...,l_N^+), \tag{2.22}$$

where

$$\mathcal{W}^{\mu_1\ldots\mu_N}_{a_1\ldots a_N}(l_1^+,...,l_N^+) = \sum_{\substack{\text{permutations}\\ \text{of } \{1,\ldots,N\}}} (-g)^N \frac{n^{\mu_1}t_{a_1}\ldots n^{\mu_N}t_{a_N}}{(l_1^+ + i0)\ldots(\sum_{j=1}^N l_j^+ + i0)} \tag{2.23}$$

is the g^N contribution to a momentum space Wilson line that factors into the GPD. The remaining sum $\sum_{\hat{H}}$ is over all possible hard subgraphs without the collinear gluon insertions.

We obtain an expression of the form

$$\begin{aligned}\sum_H T_{R(H,A)}\Gamma(H,A) = \int \frac{dk^+}{2\pi} \sum_{\hat{H}} \hat{H}^{\mu\nu}_{\alpha_1\alpha_2}(\hat{q},\hat{q}',\hat{k})\mathcal{P}_{\alpha_1\beta_1}\bar{\mathcal{P}}_{\alpha_2\beta_2}\\ \times \int \frac{dk^-}{2\pi} \int \frac{d^{d-2}k_\perp}{(2\pi)^{d-2}} \mathcal{W}^{\mu_1\ldots\mu_N}_{a_1\ldots a_N}(l_1^+,...,l_N^+) A^{\mu_1\ldots\mu_N}_{\beta_1,\beta_2,a_1,\ldots,a_N}(p,p',k,l_1,...,l_N) + O(\lambda)\end{aligned} \tag{2.24}$$

When summing over all graphs and regions one has to subtract the resulting double counting contributions. On the graphical level one can define a subtraction procedure defined recursively from smaller to larger regions in the sense of set inclusion. Comparing this procedure to alternative formulations that use an approach in terms of an operator expansion, such as soft-collinear effective theory, one obtains that these double counting subtractions correspond to subdivergence subtractions with respect to the UV renormalization of parton densities, which are implicit when the factorization formula is viewed in its operator form. We elaborate more on this in Sec. 2.6.

Considering these statements as given, we obtain the factorization theorem

$$T^{\mu\nu} = \sum_j \int dk^+ \ \mathrm{tr}\Big[\mathcal{P}_j \mathcal{C}_j^{\mu\nu}(\hat{q},\hat{q}',k^+)\bar{\mathcal{P}}_j \mathcal{F}_j(p,p',k^+)\Big] + O(\lambda) \tag{2.25}$$

where the sum $\sum_j$ runs over parton species and the trace goes over all remaining Dirac or color indices. The trace over color indices can be simplified by noticing that $\mathcal{C}_j$ must be diagonal in color, since photons do not carry color. Hence we may define $\mathcal{F}_j$ to be traced in the color indices.

2.3 Breakpoints at $k^+ = 0$ and $k^+ = \Delta^+$

Before continuing we discuss a subtlety concerning the above derivation. Recall that we classified the two parton legs connecting the subgraphs $\hat{H}$ to A, carrying momenta k and $k' = k - \Delta$, respectively, as being $\bar{n}$-collinear. In Eq. (2.25) we are naively integrating over $k^+ \in \mathbb{R}$, which includes regions where $k^+, k'^+ \ll Q$, so that we can not count them as being $\bar{n}$-collinear. This seemingly contradicts the assumption that both parton legs are collinear which would be the case if $q'^2 \sim Q^2$. Indeed the region of collinear k includes the region of soft k' and vice versa. This phenomenon arises only in

the DVCS case $q'^2 = 0$ and was first pointed out by Radyushkin Ref. [70] and then addressed by Collins and Freund [63]. We summarize the arguments made in Ref. [63] in the following.

To illustrate the issue, consider the leading order s-channel contribution to the leading order handbag diagram and in particular the denominator of the hard line connecting the electromagnetic currents

$$(k+q)^2 + i0 = 2(x-\xi)(k^- + q^-)P^+ + k_\perp^2 + O(-t, m^2) + i0, \tag{2.26}$$

where we wrote $k^+ = (x+\xi)P^+$. The collinear approximation, i.e. setting $k^-, k_\perp, -t, m^2$ in the hard subgraph to zero, is therefore only correct if $|x-\xi| \gg \max(-t, m^2, -k_\perp^2)/Q^2$. From Eq. (2.26) one can observe that in the region of soft $k' \sim (\lambda, \lambda, \lambda)Q$, i.e. $x - \xi \sim \lambda$ and $k_\perp^2 + O(-t^2, m^2) \sim \lambda^2 Q^2$, the collinear approximation remains correct, but in the Glauber region $k' \sim (\lambda^2, \lambda^2, \lambda)Q$, i.e. $x - \xi \sim \lambda^2$, we can not neglect $k_\perp^2 + O(-t, m^2) \sim \lambda^2 Q^2$. However, a deformation out of the Glauber region is possible [63], so the collinear approximation remains correct.

In fact, this contour deformation must be performed explicitly when evaluating the k^+ integral in Eq. (2.25) because the CF $\mathcal{C}_j$ has a pole at $x = \xi$. The direction of the deformation can be fixed by considering the Feynman pole prescription in Eq. (2.26). For $\xi > 0$ we have $q^- > 0$, so the k^+ integration contour, or equivalently, the x integration contour, must be deformed into the upper half plane, whereas for $\xi < 0$ the integration contour must be performed into the lower half plane.

The discussion of the region $k^+ \ll Q$ is analogous. For this we need to consider the handbag diagram with crossed photon legs, where the hard denominator reads

$$(k - q')^2 + i0 = -2(x+\xi)q'^- + k_\perp^2 + i0. \tag{2.27}$$

Thus, for the pole at $k^+ = 0$, the integration contour must be deformed into the lower half plane for $\xi > 0$ and upper half plane for $\xi < 0$. It is convenient to introduce the $\xi \to \xi - i0$ prescription for the evaluation of the integral in Eq. (2.25), which ensures that the contour is deformed in the correct way for all cases.

There is one possible objection to the above contour deformation argument. It can be shown [70] that $\mathcal{F}_j$ in Eq. (2.25) is supported only for $-p'^+ < k^+ < p^+$, i.e. $-1 < x < 1$, and it is in general non-analytic, but continuous, at $x = \pm\xi$. In order to apply the contour deformation argument we can perform the following manipulations to the convolution integral. For simplicity, let us only consider the region $1 > x > 0$. The case $-1 < x < 0$ can be handled analogously. It can be shown [70] that we can write

$$\mathcal{F}(x,\xi) = \Theta(x-\xi)\mathcal{F}_{x>\xi}(x,\xi) + \Theta(\xi - x)\mathcal{F}_{x<\xi}(x,\xi), \tag{2.28}$$

where $\mathcal{F}_{x>\xi}$ and $\mathcal{F}_{x<\xi}$ can be analytically continued to the complex x-plane. Thus

$$\begin{aligned}\int_0^1 dx\, \mathcal{C}(x, \xi - i0)\mathcal{F}(x,\xi) = &\int_0^1 dx\, \mathcal{C}(x,\xi - i0)\mathcal{F}_{x<\xi}(x,\xi) \\ &+ \int_\xi^1 dx\, \mathcal{C}(x,\xi - i0)\Big(\mathcal{F}_{x>\xi}(x,\xi) - \mathcal{F}_{\xi<x}(x,\xi)\Big).\end{aligned} \tag{2.29}$$

For the first term of Eq. (2.29) the contour deformation argument can be applied literally, while the integrand of the second term of Eq. (2.29) goes to zero like $(x-\xi)^p$ for $x \to \xi$ for some $p > 0$. But looking back at Eq. (2.26) it is clear that we can not deform out of the Glauber region for

this term, since the point $x = \xi$ is at the endpoint of the integral. Thus we can not apply the collinear approximation strictly speaking. However, with the suppression at $x \to \xi$ due to the factor $\mathcal{F}_{x>\xi} - \mathcal{F}_{\xi<x}$, the Glauber region is power-suppressed. Consequently, the errors of making the collinear approximation in the second term of Eq. (2.29) are power-suppressed.

2.4 Form factor decomposition

We continue to decompose the leading twist contribution to $T^{\mu\nu}$ in Eq. (2.25) in terms of form factors.

2.4.1 Projections of the photon indices

Not all components of the tensor on the right-hand side of Eq. (2.25) are in fact of the leading power in λ, i.e. of leading twist. Using the Ward identity $q_\mu T^{\mu\nu} = q'_\mu T^{\nu\mu} = 0$, we can write

$$\begin{aligned} T^{\mu\nu} = &\Big(n^\mu - \frac{n\cdot q}{\bar n\cdot q}\bar n^\mu\Big) n^\nu T^{--} + \Big(n^\mu - \frac{n\cdot q}{\bar n\cdot q}\bar n^\mu\Big) g_\perp^{\nu\nu'} T^-{}_{\nu'} + n^\nu g_\perp^{\mu\mu'} T_{\mu'}{}^- \\ &+ \frac{1}{2} g_\perp^{\mu\nu} g_\perp^{\mu'\nu'} T_{\mu'\nu'} + \frac{1}{2}\varepsilon_\perp^{\mu\nu}\varepsilon_\perp^{\mu'\nu'} T_{\mu'\nu'} + \tau_\perp^{\mu\nu\mu'\nu'} T_{\mu'\nu'}, \end{aligned} \tag{2.30}$$

where

$$\begin{aligned} g_\perp^{\mu\nu} &= g^{\mu\nu} - n^\mu \bar n^\nu - \bar n^\mu n^\nu, \\ \varepsilon_\perp^{\mu\nu} &= \varepsilon^{\mu\nu\rho\sigma} n_\rho \bar n_\sigma, \\ \tau_\perp^{\mu\nu\rho\sigma} &= \frac{1}{2}\Big(g_\perp^{\mu\rho} g_\perp^{\nu\sigma} + g_\perp^{\mu\sigma} g_\perp^{\nu\rho} - g_\perp^{\mu\nu} g_\perp^{\rho\sigma}\Big) \end{aligned} \tag{2.31}$$

and we have used the identity [71]

$$g_\perp^{\mu\mu'} g_\perp^{\nu\nu'} = \frac{1}{2} g_\perp^{\mu\nu} g_\perp^{\mu'\nu'} + \frac{1}{2}\varepsilon_\perp^{\mu\nu}\varepsilon_\perp^{\mu'\nu'} + \tau_\perp^{\mu\nu\mu'\nu'}. \tag{2.32}$$

Firstly, note that the T^{--} component does not contribute to DVCS. Indeed, this follows immediately from (2.5) and the transversity of the photon polarization vector, which implies $\varepsilon^*_{h',\nu} n^\nu = 0$. The same applies of course to $g_\perp^{\mu\mu'} T_{\mu'}{}^-$. Therefore, we will ignore these contributions for the rest of this work.

Secondly, the projection $g_\perp^{\nu\nu'} T^-{}_{\nu'}$ (and also $g_\perp^{\mu\mu'} T_{\mu'}{}^-$) is twist-three. Indeed, if one applies the corresponding projections on the λ^0 term on the right-hand-side of Eq. (2.25) one obtains $g_\perp^{\nu\nu'} \mathcal{C}^-{}_{\nu'}$. The only possible tensors that can carry the single index in $\mathcal{C}^{-\mu}$ that can appear are $\hat q^\mu, \hat q'^\mu, \hat k$, but they all have zero transverse components, so $g_\perp^{\nu\nu'} \mathcal{C}^-{}_{\nu'} = 0$, proving that $g_\perp^{\nu\nu'} T^-{}_{\nu'}$ is $O(\lambda)$. In fact it is of size λ^1, i.e. twist-three, see for example Ref. [20] for a detailed discussion.

In this work, we focus on the twist-two quantities

$$\begin{aligned}
\mathcal{V} &= -\frac{1}{2} g_\perp^{\mu\nu} \sum_j \int dk^+ \ \mathrm{tr}\Big[\mathcal{P}_j \mathcal{C}_{j,\mu\nu}(\hat{q},\hat{q}',k^+)\bar{\mathcal{P}}_j \mathcal{F}_j(p,p',k^+)\Big], \\
\mathcal{A} &= \frac{1}{2} \varepsilon_\perp^{\mu\nu} \sum_j \int dk^+ \ \mathrm{tr}\Big[\mathcal{P}_j \mathcal{C}_{j,\mu\nu}(\hat{q},\hat{q}',k^+)\bar{\mathcal{P}}_j \mathcal{F}_j(p,p',k^+)\Big], \\
\mathcal{T}^{\mu\nu} &= \tau_\perp^{\mu\nu\mu'\nu'} \sum_j \int dk^+ \ \mathrm{tr}\Big[\mathcal{P}_j \mathcal{C}_{j,\mu'\nu'}(\hat{q},\hat{q}',k^+)\bar{\mathcal{P}}_j \mathcal{F}_j(p,p',k^+)\Big].,
\end{aligned} \tag{2.33}$$

which parameterize the leading power contribution to the hadronic tensor

$$T^{\mu\nu} = -g_\perp^{\mu\nu}\mathcal{V} + \varepsilon_\perp^{\mu\nu}\mathcal{A} + \mathcal{T}^{\mu\nu} + O(\lambda). \tag{2.34}$$

Note that while the vector $\mathcal{V}$ and axial-vector contribution $\mathcal{A}$ are also present in this forward case for spin-1/2 targets, the transversity contribution $\mathcal{T}^{\mu\nu}$ is not. But it does contribute to DVCS at twist-two, even for spin-1/2 targets [71].

2.4.2 Quark contribution

We now insert the projectors $\mathcal{P}, \bar{\mathcal{P}}$ in Eq. (2.25) and Eq. (2.33) for the quark contribution. The quark projectors were defined in Eq. (2.18). In the process, we will define the corresponding projection of the conventional GPDs and CFs. To distinguish them from the general tensor-valued object $\mathcal{F}$, we call $\mathcal{F}$ the parent GPD. Correspondingly, we call $\mathcal{C}$ the parent CF.

Consider now the contribution from quarks in Eq. (2.25). The lower subgraph amplitude can be written as a non-local time-ordered (connected) correlator of two quark fields, which interpolate the parton coming from the nucleon with the partonic scattering amplitude $\mathcal{C}_q$. Furthermore, it is integrated over the minus and transverse components of the parton momentum

$$\begin{aligned}
\mathcal{F}_{q,\alpha\beta} = \frac{1}{2\pi}\int \frac{dk^-}{2\pi} \int \frac{d^{d-2}k_\perp}{(2\pi)^{d-2}} \int d^d z \ e^{ik\cdot z} \\
\times \langle N(p',s')|\, T\bar{q}_\beta(0) W_n(0)^\dagger W_n(z) q_\alpha(z)\, |N(p,s)\rangle\,.
\end{aligned} \tag{2.35}$$

Clearly, the parent quark CF $\mathcal{C}_q$ must be diagonal in color, so an average of color in $\mathcal{C}_q$ and $\mathcal{F}_q$ is always implied. The collinear Wilson lines

$$W_n(x) = \mathrm{P}\exp\Big[ig\int_{-\infty}^0 ds \ A^+(x+sn)\Big] \tag{2.36}$$

arise from the scalar-polarized collinear gluons and can be fixed by requiring gauge invariance of the $\mathcal{F}_q$. After performing the $k^-, k_\perp$ integration the quark correlator is projected onto the light-ray spanned by n and the Wilson lines combine to a single Wilson line connecting the two quark fields

$$\begin{aligned}
\mathcal{F}_{q,\alpha\beta} &= \int \frac{dz^-}{2\pi} e^{ik^+z^-} \ \langle N(p',s')|\, T\bar{q}_\beta(0) W_n(0,z^-n) q_\alpha(z^-n)\, |N(p,s)\rangle \\
&= \int \frac{dz^-}{2\pi} e^{ixP^+z^-} \ \langle N(p',s')|\, T\bar{q}_\beta(-z^-/2) W_n(-z^-/2,z^-/2) q_\alpha(z^-n/2)\, |N(p,s)\rangle \\
&= \int \frac{dz^-}{2\pi} e^{ixP^+z^-} \ \langle N(p',s')|\, \bar{q}_\beta(-z^-/2) W_n(-z^-/2,z^-/2) q_\alpha(z^-n/2)\, |N(p,s)\rangle
\end{aligned} \tag{2.37}$$

where

$$W_n(z_1, z_2) = \mathrm{P}\exp\Big[ig\int_{z_2}^{z_1} ds\ A^+(sn)\Big] \tag{2.38}$$

and we defined $x = k^+/P^+ - \xi$. In the last equality of Eq. (2.37) we have used the fact that one can drop the time-ordering in the light-cone correlator [72]. To summarize, the parent GPD $\mathcal{F}_{q,\alpha\beta}$ can be written as a Fourier transformed hadronic matrix element of the light-ray operator

$$\mathcal{O}_{q,\alpha\beta}(z^-) = \bar{q}_\beta(-z^-/2)W_n(-z^-/2, z^-/2)q_\alpha(z^- n/2). \tag{2.39}$$

On the other hand, the parent CF can be written as

$$\begin{aligned}\mathcal{C}^{\mu\nu}_{q,\alpha\beta} = i\int d^d z_1\ e^{-i\hat{q}\cdot z_1}\int d^d z_2\ e^{i\hat{q}'\cdot z_2}\int d^d z_3\ e^{-i\hat{k}\cdot z_3}\\ \times \langle\Omega|\, T q_\beta(0) j^\nu(z_2) j^\mu(z_1)\bar{q}_\alpha(z_3)\,|\Omega\rangle_{\text{connected, amputated}}\,.\end{aligned} \tag{2.40}$$

The trace in Eq. (2.25) becomes

$$\frac{1}{4}\mathrm{tr}\Big[\gamma^-\mathcal{C}^{\mu\nu}_q\gamma^-\gamma^+\mathcal{F}_q(p,p',k^+)\gamma^+\Big]. \tag{2.41}$$

Decomposing the $\mathcal{C}^{\mu\nu}_q$ and $\mathcal{F}_q$ in terms of a basis of Dirac structures, we observe that, after the light-cone projection, there are only three linearly independent structures that are possible, namely $\gamma^\pm, \gamma^\pm\gamma_5$ and $\sigma^{\pm j} = \frac{i}{2}[\gamma^\pm, \gamma^j]$ ($j \in \{1, 2\}$), where the plus sign applies to $\mathcal{C}^{\mu\nu}_q$ while the minus sign applies to $\mathcal{F}_q$. Hence we can exchange

$$\begin{aligned}\mathcal{F}_q &\to \frac{1}{4}\mathrm{tr}(\gamma^+\mathcal{F}_q)\gamma^- + \frac{1}{4}\mathrm{tr}(\gamma^+\gamma_5\mathcal{F}_q)\gamma_5\gamma^- + \frac{1}{4}\mathrm{tr}(\sigma^{+j}\mathcal{F}_q)\sigma^{-j},\\ \mathcal{C}^{\mu\nu}_q &\to \frac{1}{4}\mathrm{tr}(\gamma^-\mathcal{C}^{\mu\nu}_q)\gamma^+ + \frac{1}{4}\mathrm{tr}(\gamma^-\gamma_5\mathcal{C}^{\mu\nu}_q)\gamma_5\gamma^+,\end{aligned} \tag{2.42}$$

where we used that $\mathrm{tr}(\sigma^{-j}\mathcal{C}^{\mu\nu}_q) = 0$, since it involves a trace over an odd number of gamma matrices.

Note that we can choose the light-like vectors $n, \bar{n}$ such that $n \leftrightarrow \bar{n}$ under a parity transformation. Then we find that

$$\begin{aligned}\mathrm{tr}(\gamma^-\mathcal{C}^{\mu\nu}_q) &\to (-1)^\mu(-1)^\nu\mathrm{tr}(\gamma^+\mathcal{C}^{\mu\nu}_q|_{n\leftrightarrow\bar{n}}),\\ \mathrm{tr}(\gamma^-\gamma_5\mathcal{C}^{\mu\nu}_q) &\to -(-1)^\mu(-1)^\nu\mathrm{tr}(\gamma^+\gamma_5\mathcal{C}^{\mu\nu}_q|_{n\leftrightarrow\bar{n}})\end{aligned} \tag{2.43}$$

under a parity transformation, where $(-1)^\mu = 1$ for $\mu = 0$ and -1 else. In Eq. (2.43) we have used that QCD is invariant under parity. Note that $\varepsilon^{\mu\nu}_\perp$ is odd while $g^{\mu\nu}_\perp$ and $\tau^{\mu\nu\mu'\nu'}_\perp$ are even under $n \leftrightarrow \bar{n}$. On the other hand, $\varepsilon^{\mu\nu}_\perp\mathcal{A}$ must transform covariantly under a parity transformation with a sequential spatial rotation that takes $n \leftrightarrow \bar{n}$. But in order to compensate the minus sign from $\varepsilon^{\mu\nu}_\perp$ the structure $\mathcal{A}$ can only depend on the projection $\mathrm{tr}(\gamma^-\gamma_5\mathcal{C}^{\mu\nu}_q)$. By the same reasoning this projection can not occur in $\mathcal{V}$.

Furthermore, note that the projection $\tau^{\mu\nu}_{\perp,\,\mu'\nu'}\mathrm{tr}(\gamma^-\mathcal{C}^{\mu'\nu'}_q)$ has two free indices and the only possibility to obtain an invariant is to contract them. In $d = 4$ we have $g_{\mu\nu}\tau^{\mu\nu\rho\sigma}_\perp = 0$, so the projection vanishes. For general d, this is not the case, but suffice it to say that one can redefine $\tau_\perp$

such that $g_{\mu\nu}\tau_\perp^{\mu\nu\rho\sigma} = 0$ for arbitrary d. This is discussed in Sec. 2.5. Hence the only contribution to $\mathcal{V}$ comes from $\mathrm{tr}(\gamma^- \mathcal{C}_q^{\mu\nu})$ and we get the two CFs

$$\begin{aligned} C_q(x/\xi, Q, \mu) &= -\frac{\xi}{4}\frac{g_{\perp,\mu\nu}}{2}\mathrm{tr}(\gamma^- \mathcal{C}_q^{\mu\nu}), \\ \widetilde{C}_q(x/\xi, Q, \mu) &= \frac{\xi}{4}\frac{\varepsilon_{\perp,\mu\nu}}{2}\mathrm{tr}(\gamma_5\gamma^- \mathcal{C}_q^{\mu\nu}), \end{aligned} \tag{2.44}$$

where we introduced the factor ξ to make the CFs depend only on the ratio x/ξ. This must be the case, since all possible scalar products of the vectors $\hat{q}, \hat{q}', \hat{k}$ depend only on the ratio x/ξ.

The formulae in Eq. (2.44) apply in $d = 4$, but when using dimensional regularization, some modifications must be made. This is discussed in Sec. 2.5.

We mention that another implication of symmetry for the CFs comes from charge conjugation symmetry, under which the field bilinear in the correlator transforms as

$$\bar{q}(z_3)\gamma^\mu q(0) \to -\bar{q}(0)\gamma^\mu q(z_3), \qquad \bar{q}(z_3)\gamma^\mu\gamma_5 q(0) \to +\bar{q}(0)\gamma^\mu\gamma_5 q(z_3). \tag{2.45}$$

Since QCD is invariant under charge conjugation and so is the product of two electromagnetic currents, this implies that C_q is anti-symmetric with respect to exchanging the quark legs or equivalently $x \to -x$, while $\widetilde{C}_q$ is symmetric.

We define the quark GPDs as

$$\begin{aligned} F_q(x,\xi,t) &= \frac{1}{2}\int \frac{dz^-}{2\pi} e^{ixP^+z^-} \left\langle N(p',s')\right| \mathrm{tr}(\gamma^+ \mathcal{O}_q(z^-)) \left|N(p,s)\right\rangle, \\ \widetilde{F}_q(x,\xi,t) &= \frac{1}{2}\int \frac{dz^-}{2\pi} e^{ixP^+z^-} \left\langle N(p',s')\right| \mathrm{tr}(\gamma^+\gamma_5 \mathcal{O}_q(z^-)) \left|N(p,s)\right\rangle. \end{aligned} \tag{2.46}$$

Technically there is also the so-called quark transversity GPD $F_{q,T}^j$, given by tracing $\mathcal{F}_q$ with σ^{+j}, although it clearly does not contribute to the DVCS amplitude, since the corresponding CF vanishes.

We conclude that the twist-two quark contributions to the hadronic tensor read

$$\begin{aligned} \mathcal{V}_q(\xi,Q,t) &= \int_{-1}^{1} \frac{dx}{\xi} C_q(x/\xi, Q) F_q(x,\xi,t), \\ \mathcal{A}_q(\xi,Q,t) &= \int_{-1}^{1} \frac{dx}{\xi} \widetilde{C}_q(x/\xi, Q) \widetilde{F}_q(x,\xi,t). \end{aligned} \tag{2.47}$$

The quark GPDs $F_q, \widetilde{F}_q$ can be further decomposed into four GPDs $H_q, E_q, \widetilde{H}_q, \widetilde{E}_q$, by the Gordon decomposition

$$\begin{aligned} F_q(x,\xi,t) &= \frac{1}{2P^+}\left[H_q(x,\xi,t)\bar{u}_{s'}(p')\gamma^+ u_s(p) + E_q(x,\xi,t)\bar{u}_{s'}(p')\frac{i\sigma^{+\alpha}\Delta_\alpha}{2m}u_s(p)\right], \\ \widetilde{F}_q(x,\xi,t) &= \frac{1}{2P^+}\left[\widetilde{H}_q(x,\xi,t)\bar{u}_{s'}(p')\gamma^+\gamma_5 u_s(p) + \widetilde{E}_q(x,\xi,t)\bar{u}_{s'}(p')\frac{\gamma_5\Delta^+}{2m}u_s(p)\right], \end{aligned} \tag{2.48}$$

where $u_s(p)$ is the nucleon spinor. Thus the quark contribution to $T^{\mu\nu}$ is, at leading twist, entirely determined by the four quark CFFs, defined by

$$\begin{aligned}
\mathcal{H}_q &= \int \frac{dx}{\xi} C_q(x/\xi, Q) H_q(x,\xi,t), & \mathcal{E}_q &= \int \frac{dx}{\xi} C_q(x/\xi, Q) E_q(x,\xi,t), \\
\widetilde{\mathcal{H}}_q &= \int \frac{dx}{\xi} \widetilde{C}_q(x/\xi, Q) \widetilde{H}_q(x,\xi,t), & \widetilde{\mathcal{E}}_q &= \int \frac{dx}{\xi} \widetilde{C}_q(x/\xi, Q) \widetilde{E}_q(x,\xi,t).
\end{aligned} \tag{2.49}$$

2.4.3 Gluon contribution

The gluonic contribution to $T^{\mu\nu}$ can be determined similarly. Demanding gauge invariant twist-two gluon operators, we want to write the gluon GPDs as matrix elements of the light-ray operator

$$\mathcal{O}_g^{\mu\nu}(z^-) = G^{\mu+}(-z^- n/2) W_{n,A}(-z^-/2, z^-/2) G^{+\nu}(z^- n/2), \tag{2.50}$$

where $G^{\mu\nu}$ is the gluon field strength tensor. The trace over color is implicit and $W_{n,A}$ denotes a n-collinear Wilson line in the adjoint representation. Due to the projection $\mathcal{P}\mathcal{O}_g\bar{\mathcal{P}}$ we can treat μ, ν as transverse indices. One can then define the gluon parent GPD as

$$\mathcal{F}_g^{ij}(x,\xi,t) = \frac{1}{P^+} \int \frac{dz^-}{2\pi} e^{ixP^+z^-} \left\langle N(p',s') \right| \mathcal{O}_g^{ij}(z^-) \left| N(p,s) \right\rangle, \tag{2.51}$$

where $i, j \in \{1, 2\}$ and the factor $1/P^+$ is introduced to make $\mathcal{F}_g$ dimensionless. The particular gauge-invariant choice in Eq. (2.50) implies additional factors due to the derivatives in the gluon field strengths that have to be taken into account in the CFs. The additional two factors of ∂^+ produce a factor of $\frac{k^+k'^+}{(P^+)^2} = x^2 - \xi^2$. We have

$$\begin{aligned}
\mathcal{C}_g^{\mu\nu,ij} = \frac{i}{2(x^2-\xi^2)} \int d^d z_1 \; e^{-iq\cdot z_1} \int d^d z_2 \; e^{iq'\cdot z_2} \int d^d z_3 \; e^{-i\hat{k}\cdot z_3} \\
\times \left\langle \Omega \right| T A^{a,i}(0) j^\nu(z_2) j^\mu(z_1) A^{a,j}(z_3) \left| \Omega \right\rangle_{\text{connected, amputated}}.
\end{aligned} \tag{2.52}$$

Applying the decomposition of tensors in transverse space, Eq. (2.32), to the indices of the parent GPD $\mathcal{F}_g^{\mu\nu}$ leads to the following definition of the gluon GPDs

$$\begin{aligned}
F_g(x,\xi,t) &= \frac{1}{P^+} \int \frac{dz^-}{2\pi} e^{ixP^+z^-} \left\langle N(p',s') \right| g_\perp^{\mu'\nu'} \mathcal{O}_{g,\mu'\nu'}(z^-) \left| N(p,s) \right\rangle, \\
\widetilde{F}_g(x,\xi,t) &= -\frac{i}{P^+} \int \frac{dz^-}{2\pi} e^{ixP^+z^-} \left\langle N(p',s') \right| \varepsilon_\perp^{\mu'\nu'} \mathcal{O}_{g,\mu'\nu'}(z^-) \left| N(p,s) \right\rangle, \\
F_{g,T}^{\rho\sigma}(x,\xi,t) &= \frac{2}{P^+} \int \frac{dz^-}{2\pi} e^{ixP^+z^-} \left\langle N(p',s') \right| \tau_\perp^{\mu'\nu'\rho\sigma} \mathcal{O}_{g,\mu'\nu'}(z^-) \left| N(p,s) \right\rangle.
\end{aligned} \tag{2.53}$$

It remains to identify which of the projections of Lorentz indices, see Eq. (2.33), matches to which gluon GPD in Eq. (2.53). Firstly, parity invariance implies that the $\varepsilon_\perp^{\mu\nu}$ structure can only appear in combination with $\widetilde{F}_g$, by similar arguments as for the quark case. Secondly, the $\tau_\perp$ structure must go together with $F_{g,T}$, since there is no other way to contract the remaining Lorentz indices.

Finally, we find that gluon CFs can be written as

$$\begin{aligned} C_g(x/\xi,Q) &= -\frac{\xi^2}{4}\frac{g_{\perp,\mu\nu}g_{\perp,\rho\sigma}}{4}\mathcal{C}_g^{\mu\nu,\rho\sigma}, \\ \widetilde{C}_g(x/\xi,Q) &= \frac{\xi^2}{4}\frac{\varepsilon_{\perp,\mu\nu}\varepsilon_{\perp,\rho\sigma}}{4}\mathcal{C}_g^{\mu\nu,\rho\sigma}, \\ C_{g,T}(x/\xi,Q) &= \frac{\xi^2}{4}\frac{\tau_{\perp,\mu\nu\rho\sigma}}{2}\mathcal{C}_g^{\mu\nu,\rho\sigma}, \end{aligned} \tag{2.54}$$

where we introduced the factor ξ^2 in order to make the CFs depend on the ratio x/ξ and again, the definition for arbitrary d is discussed in Sec. 2.5. Furthermore, an argument based charge conjugation symmetry, analogous to the quark case, implies that $C_g, C_{g,T}$ are even under $x/\xi \to -x/\xi$, while $\widetilde{C}_g$ is odd.

Note that, in contrast to the quark case, $C_{g,T}$ is in fact not zero in DVCS, so the gluon transversity GPD $F_{g,T}^{\mu\nu}$ does contribute at leading twist. The gluon contribution to the hadronic tensor therefore reads

$$\begin{aligned} \mathcal{V}_g(\xi,Q,t) &= \int_{-1}^{1}\frac{dx}{\xi^2}C_g(x/\xi,Q)F_g(x,\xi,t), \\ \mathcal{A}_g(\xi,Q,t) &= \int_{-1}^{1}\frac{dx}{\xi^2}\widetilde{C}_g(x/\xi,Q)\widetilde{F}_g(x,\xi,t), \\ \mathcal{T}_g^{\mu\nu}(\xi,Q,t) &= \int_{-1}^{1}\frac{dx}{\xi^2}C_{g,T}(x/\xi,Q)F_{g,T}^{\mu\nu}(x,\xi,t). \end{aligned} \tag{2.55}$$

The gluon GPDs $F_g, \widetilde{F}_g$ can be further decomposed similarly to the quark GPDs in Eq. (2.48)

$$\begin{aligned} F_g(x,\xi,t) &= \frac{1}{2P^+}\left[H_g(x,\xi,t)\bar{u}_{s'}(p')\gamma^+u_s(p) + E_g(x,\xi,t)\bar{u}_{s'}(p')\frac{i\sigma^{+\alpha}\Delta_\alpha}{2m}u_s(p)\right], \\ \widetilde{F}_g(x,\xi,t) &= \frac{1}{2P^+}\left[\widetilde{H}_g(x,\xi,t)\bar{u}_{s'}(p')\gamma^+\gamma_5u_s(p) + \widetilde{E}_g(x,\xi,t)\bar{u}_{s'}(p')\frac{\gamma_5\Delta^+}{2m}u_s(p)\right]. \end{aligned} \tag{2.56}$$

The object $F_{g,T}$ can be decomposed into four GPDs [72]

$$\begin{aligned} F_{g,T}^{ij} = \frac{\tau_{\perp,\ i'j'}^{ij}}{2P^+}\frac{P^+\Delta^{j'} - \Delta^+P^{j'}}{2mP^+}\bar{u}_{s'}(p') \\ \times\left[H_{g,T}i\sigma^{+i'} + \widetilde{H}_{g,T}\frac{P^+\Delta^{i'} - \Delta^+P^{i'}}{m^2}\right. \\ \left. + E_{g,T}\frac{\gamma^+\Delta^{i'} - \Delta^+\gamma^{i'}}{2m} + \widetilde{E}_{g,T}\frac{\gamma^+P^{i'} - P^+\gamma^{i'}}{m}\right]u_s(p). \end{aligned} \tag{2.57}$$

We define the gluon CFFs as

$$\begin{aligned}
\mathcal{H}_g &= \int \frac{dx}{\xi^2} C_g(x/\xi, Q) H_g(x,\xi,t), & \mathcal{E}_g &= \int \frac{dx}{\xi^2} C_g(x/\xi, Q) E_g(x,\xi,t), \\
\widetilde{\mathcal{H}}_g &= \int \frac{dx}{\xi^2} \widetilde{C}_g(x/\xi, Q) \widetilde{H}_g(x,\xi,t), & \widetilde{\mathcal{E}}_g &= \int \frac{dx}{\xi^2} \widetilde{C}_g(x/\xi, Q) \widetilde{E}_g(x,\xi,t), \\
\mathcal{H}_{g,T} &= \int \frac{dx}{\xi^2} C_{g,T}(x/\xi, Q) H_{g,T}(x,\xi,t), & \mathcal{E}_{g,T} &= \int \frac{dx}{\xi^2} C_{g,T}(x/\xi, Q) E_{g,T}(x,\xi,t), \\
\widetilde{\mathcal{H}}_{g,T} &= \int \frac{dx}{\xi^2} C_{g,T}(x/\xi, Q) \widetilde{H}_{g,T}(x,\xi,t), & \widetilde{\mathcal{E}}_{g,T} &= \int \frac{dx}{\xi^2} C_{g,T}(x/\xi, Q) \widetilde{E}_{g,T}(x,\xi,t).
\end{aligned} \tag{2.58}$$

2.4.4 Total contribution

We conclude that the form factors defined in Eq. (2.33) are given by

$$\mathcal{V} = \sum_q \mathcal{V}_q + \mathcal{V}_g, \qquad \mathcal{A} = \sum_q \mathcal{A}_q + \mathcal{A}_g, \qquad \mathcal{T}^{\mu\nu} = \mathcal{T}_g^{\mu\nu}. \tag{2.59}$$

Note that the running of the factorization scale μ, which was omitted from notation so far, mixes between quark and gluon contribution, so in fact only the sum of quark and gluon contributions is invariant under the running of μ.

Decomposing $\mathcal{V}, \mathcal{A}, \mathcal{T}^{\mu\nu}$ into CFFs leads to

$$\begin{aligned}
\mathcal{V} &= \frac{1}{2P^+}\left[\mathcal{H}\bar{u}_{s'}(p')\gamma^+ u_s(p) + \mathcal{E}\bar{u}_{s'}(p')\frac{i\sigma^{+\alpha}\Delta_\alpha}{2m}u_s(p)\right], \\
\mathcal{A} &= \frac{1}{2P^+}\left[\widetilde{\mathcal{H}}\bar{u}_{s'}(p')\gamma^+\gamma_5 u_s(p) + \widetilde{\mathcal{E}}\bar{u}_{s'}(p')\frac{\gamma_5\Delta^+}{2m}u_s(p)\right] \\
\mathcal{T}^{ij} &= \frac{\tau_{\perp,\, i'j'}^{ij}}{2P^+}\frac{P^+\Delta^{j'} - \Delta^+ P^{j'}}{2mP^+}\bar{u}_{s'}(p') \\
&\quad \times \Bigg[\mathcal{H}_{g,T} i\sigma^{+i'} + \widetilde{\mathcal{H}}_{g,T}\frac{P^+\Delta^{i'} - \Delta^+ P^{i'}}{m^2} \\
&\qquad + \mathcal{E}_{g,T}\frac{\gamma^+\Delta^{i'} - \Delta^+\gamma^{i'}}{2m} + \widetilde{\mathcal{E}}_{g,T}\frac{\gamma^+ P^{i'} - P^+\gamma^{i'}}{m}\Bigg] u_s(p),
\end{aligned} \tag{2.60}$$

where

$$\begin{aligned}
\mathcal{H} &= \sum_q \mathcal{H}_q + \mathcal{H}_g, & \widetilde{\mathcal{H}} &= \sum_q \widetilde{\mathcal{H}}_q + \widetilde{\mathcal{H}}_g, \\
\mathcal{E} &= \sum_q \mathcal{E}_q + \mathcal{E}_g, & \widetilde{\mathcal{E}} &= \sum_q \widetilde{\mathcal{E}}_q + \widetilde{\mathcal{E}}_g
\end{aligned} \tag{2.61}$$

and $\mathcal{H}_{g,T},\ \widetilde{\mathcal{H}}_{g,T},\ \mathcal{E}_{g,T},\ \widetilde{\mathcal{E}}_{g,T}$ are each individually invariant under running of μ.

2.5 Projections of the parent CF in d dimensions

Let us discuss the modifications to Eqs. (2.44) and (2.54) in d dimensions. First of all notice that CF is of course scheme dependent. Indeed, choosing a minimal subtraction-like scheme, we still retain the freedom to multiply each of the eqs. in (2.44) and (2.54) by an overall factor $f(d)$ such that $f(4) = 1$. Because of the IR divergences in the CF, this factor will lead to different fixed order results. Demanding that the hadronic tensor, and thus the observable, be independent of this scheme, implies that the GPD is also scheme dependent. This is of course already true, since the GPD depends on the factorization scale.

Some modifications for the continuation to d dimensions are natural. First of all, note that while $g_\perp^{\mu\nu}, \varepsilon_\perp^{\mu\nu}$ can be taken to have identical expressions for arbitrary d, in order to preserve

$$g_{\mu\nu}\tau_\perp^{\mu\nu\rho\sigma} = g_{\mu\nu}\tau_\perp^{\rho\sigma\mu\nu} = 0 \tag{2.62}$$

we need to define

$$\tau_\perp^{\mu\nu\rho\sigma} = \frac{d-2}{4} g_\perp^{\mu\rho} g_\perp^{\nu\sigma} + \frac{d-2}{4} g_\perp^{\mu\sigma} g_\perp^{\nu\rho} - \frac{1}{2} g_\perp^{\mu\nu} g_\perp^{\rho\sigma}. \tag{2.63}$$

Secondly, in order to obtain a "canonical" choice of scheme, it is natural to make modifications that take into account the modified traces of the Lorentz structures, i.e.

$$\begin{aligned} g_\perp^{\mu\nu} g_{\perp,\mu\nu} &= d-2, \\ \epsilon_\perp^{\mu\nu} \epsilon_{\perp,\mu\nu} &= (d-2)(d-3), \\ \tau_\perp^{\mu\nu\rho\sigma} \tau_{\perp,\mu\nu\rho\sigma} &= \frac{1}{8} d(d-2)^2(d-3). \end{aligned} \tag{2.64}$$

This is because the projection onto these structures should give exactly the coefficients, so we have to take this normalization into account.

Furthermore, there are numerous possibilities to define γ_5 in d dimensions. A convenient choice is Larin's scheme [73], which can be implemented by the exchange

$$\gamma^\mu \gamma_5 \to \frac{i}{3!} \varepsilon^{\mu\mu_1\mu_2\mu_3} \gamma_{\mu_1}\gamma_{\mu_2}\gamma_{\mu_3}. \tag{2.65}$$

It is customary to introduce an additional finite "renormalization" that can be fixed by the requirement that evolution kernels for the vector and axial-vector case coincide [74]. We discuss this issue in Sec. 2.10. We denote the axial-vector CF in Larin's scheme by $\widetilde{C}_{q,\mathrm{La}}$.

This motivates the following definitions

$$\begin{aligned} C_q(x/\xi, Q) &= -\frac{\xi}{4} \frac{g_{\perp,\mu\nu}}{(d-2)} \mathrm{tr}(\gamma^- \mathcal{C}_q^{\mu\nu}), \\ \widetilde{C}_{q,\mathrm{La}}(x/\xi, Q) &= \frac{\xi}{4} \frac{\varepsilon_{\perp,\mu\nu}}{(d-3)(d-2)} \frac{i}{3!} \varepsilon^{-\mu_1\mu_2\mu_3} \mathrm{tr}(\gamma_{\mu_1}\gamma_{\mu_2}\gamma_{\mu_3}\mathcal{C}_q^{\mu\nu}) \\ C_g(x/\xi, Q) &= -\frac{\xi^2}{4} \frac{g_{\perp,\mu\nu} g_{\perp,\rho\sigma}}{(d-2)^2} \mathcal{C}_g^{\mu\nu,\rho\sigma}, \\ \widetilde{C}_g(x/\xi, Q) &= \frac{\xi^2}{4} \frac{\varepsilon_{\perp,\mu\nu}\varepsilon_{\perp,\rho\sigma}}{(d-2)^2(d-3)^2} \mathcal{C}_g^{\mu\nu,\rho\sigma}, \\ C_{g,T}(x/\xi, Q) &= \frac{\xi^2}{4} \frac{8\,\tau_{\perp,\mu\nu\rho\sigma}}{d(d-2)^2(d-3)} \mathcal{C}_g^{\mu\nu,\rho\sigma}. \end{aligned} \tag{2.66}$$

It is to be repeated that these definitions are subject to additional subtractions of IR divergences. This issue is discussed in the following Sec. 2.6.

2.6 Infrared subtractions

The factorization theorem Eq. (2.25) can be written symbolically as

$$T = C * F, \tag{2.67}$$

where $*$ denotes a general convolution product. This notation will be frequently used throughout. We formalize it to some degree in App. A.

Note that Eq. (2.67) strictly applies in terms of renormalized quantities T, C and F, while in the corresponding formulas in terms of correlation functions (or hadronic matrix elements), Eqs. (2.7), (2.40), (2.35), (2.40), (2.35), the renormalization is tacitly implied.

It is often considered a "bare" factorization theorem

$$T = C^{\text{bare}} * F^{\text{bare}}. \tag{2.68}$$

While T is IR finite when evaluated with hadronic states, it does contain UV divergences when defined in terms of renormalized quark fields. On the other hand, T in terms of bare quark fields is finite, by the well-known fact that the electromagnetic current is UV finite, or equivalently, its renormalization factor Z_j, where $j = Z_j j^{(\text{bare})}$, is equal to the quark wave-function renormalization constant Z_2, where $q^{\text{bare}} = \sqrt{Z_2} q$. This follows from standard arguments using the gauge symmetry Ward identity. Consequently T is exactly given by (2.7) but in terms of bare quark fields. In particular, it is finite, and so should be the right-hand-side of Eq. (2.68).

However, F^{bare} is UV divergent and the renormalized GPD F can be written symbolically as

$$F = Z * F^{\text{bare}}, \tag{2.69}$$

where $*$ denotes a convolution product similar to that of Eq. (2.25). Moreover, the renormalization mixes the quark and gluon GPDs, so there is a vector space structure implicit in Eq. (2.69).

Consequently, in order for Eq. (2.68) to be true, we must have

$$C = C^{\text{bare}} * Z^{-1}, \tag{2.70}$$

where Z^{-1} is the inverse operator to Z. Note that Z^{-1} in Eq. (2.70) does formally subtract the IR divergences in C^{bare}, which motivates the name "IR subtractions" for the corresponding counterterm subtractions. Those same subtractions arise in the graphical proof of the factorization, in which case they correspond to subtractions of the double counting of regions. Furthermore the bare CF C^{bare} is given by the amputated bare correlations functions in Eqs. (2.40) and (2.52) for the quark and gluon cases, respectively.

The proper subtraction of divergences in Eq. (2.70) provides a highly non-trivial check of the calculation of fixed order calculations of C and moreover, there are finite subdivergence subtractions that arise beyond one-loop. The expressions for the integration kernels Z in momentum fraction space are complicated due to their non-analyticity inside the integration regions. For analytical computations, it is more convenient to use the light-ray position space formulation. For this we

consider the renormalization of the light-ray operators

$$\begin{aligned}
\mathcal{O}_{\rm ns}(z_1,z_2) &= \frac{1}{2}\sum_{q=u,d,s,\dots}\Big(\bar q(z_1 n)\gamma^+ W_n(z_1 n,z_2 n) q_\alpha(z_2 n) + (z_1 \leftrightarrow z_2)\Big),\\
\mathcal{O}_{\rm s}(z_1,z_2) &= \frac{1}{2}\sum_{q=u,d,s,\dots}\Big(\bar q(z_1 n)\gamma^+ W_n(z_1 n,z_2 n) q_\alpha(z_2 n) - (z_1 \leftrightarrow z_2)\Big),\\
\mathcal{O}_g(z_1,z_2) &= G^{\mu+}(z_1 n) W_{n,A}(z_1 n,z_2 n) G^+{}_\mu(z_2 n).
\end{aligned} \tag{2.71}$$

The renormalization equations take the form

$$\begin{aligned}
\mathcal{O}_{\rm ns} &= \mathcal{Z}_{\rm ns} * \mathcal{O}^{\rm bare}_{\rm ns},\\
\begin{pmatrix}\mathcal{O}_{\rm s}\\ \mathcal{O}_g\end{pmatrix} &= \begin{pmatrix}\mathcal{Z}_{\rm ss} & \mathcal{Z}_{sg}\\ \mathcal{Z}_{g\rm s} & \mathcal{Z}_{gg}\end{pmatrix} * \begin{pmatrix}\mathcal{O}^{\rm bare}_{\rm s}\\ \mathcal{O}^{\rm bare}_g\end{pmatrix},
\end{aligned} \tag{2.72}$$

where the operators $\mathcal{Z}_{\chi\chi'}$ act on functions f of two positions $z_1 n, z_2 n$ on the light-ray spanned by n as [20]

$$(\mathcal{Z}_{\chi\chi'} * f)(z_1,z_2) = [i(z_1-z_2)]^{\eta_{\chi\chi'}}\int_{\Delta_2} d(\alpha,\beta)\ \mathcal{Z}_{\chi\chi'}(\alpha,\beta) f(\bar\alpha z_1 + \alpha z_2, z_2\bar\beta + z_1\beta), \tag{2.73}$$

where $\bar x = 1-x$ and $\Delta_2 = \{0\le\beta\le 1-\alpha\le 1\}$ is a two-dimensional simplex and $\eta = \begin{pmatrix}0 & 1\\ -1 & 0\end{pmatrix}$. The renormalized GPDs are then defined as in Eqs. (2.37) and (2.51), but in terms of the renormalized light-ray operators like in Eq. (2.72). Explicit expressions for the $\mathcal{Z}$ factors are gathered in App. B.

In order to compute the IR subtractions for the vector contribution we consider Eq. (2.25) in terms of renormalized quantities with partonic external states with light-like momenta

$$\hat p = (1+\xi)P^+\bar n, \qquad \hat p' = (1-\xi)P^+\bar n, \tag{2.74}$$

averaged over spin and color. We denote by $\hat F_{i/j}$ for $i,j\in\{u,d,s,...,g\}$ the renormalized GPDs of parton i evaluated with partonic external states of parton species j, normalized such that

$$\begin{aligned}
\hat F_{q/q'}(x,\xi) &= \delta_{qq'}\delta(1-x) + O(\alpha_s),\\
\hat F_{g/g}(x,\xi) &= (1-\xi^2)\Big(\delta(1-x)+\delta(1+x)\Big) + O(\alpha_s).
\end{aligned} \tag{2.75}$$

Note that for the corresponding bare versions $\hat F^{\rm bare}_{q/q}, \hat F^{\rm bare}_{g/g}$ the $O(\alpha_s)$ terms vanish exactly in dim. reg., since they involve only scaleless integrals. For the same reason $\hat F^{\rm bare}_{q/g} = \hat F^{\rm bare}_{g/q} = 0$. In fact $\hat F_{i,j}$ are determined entirely by $\mathcal{Z}_{\chi\chi'}$. More precisely, the quark in quark partonic GPD is given by

$$\begin{aligned}
\hat F_{q/q'}(x,\xi) &= \frac{1}{2}\int\frac{dz}{2\pi}e^{ixzP^+}\,\langle q'(\hat p')|\,\mathcal{O}_q(-z/2,z/2)\,|q'(\hat p)\rangle\\
&= \frac{1}{2}\int\frac{dz}{2\pi}e^{ixzP^+}\,\langle q'(\hat p')|\,\Big[(\mathcal{Z}_{\rm ns}*\mathcal{O}^{\rm bare}_q)(-z/2,z/2) + \frac{1}{n_f}(\mathcal{Z}_{\rm ps}*\mathcal{O}^{\rm bare}_{q'})(-z/2,z/2)\Big]\,|q'(\hat p)\rangle\\
&= \int_{\Delta_2} d(\alpha,\beta)\,\Big[\delta_{qq'}\mathcal{Z}_{\rm ns}(\alpha,\beta) + \frac{1}{n_f}\mathcal{Z}_{\rm ps}(\alpha,\beta)\Big]\delta\Big(x-(1/2-\alpha)(1-\xi)-(1/2-\beta)(1+\xi)\Big),
\end{aligned} \tag{2.76}$$

where $\mathcal{Z}_{\rm ps} = \mathcal{Z}_{\rm ss} - \mathcal{Z}_{\rm ns}$ is the pure-singlet contribution. Furthermore

$$\begin{aligned}
\hat{F}_{q/g} &= \frac{1}{2n_f}\int \frac{dz}{2\pi} e^{ixzP^+} \langle g(\hat{p}')| \left(\mathcal{Z}_{\rm sg} * \mathcal{O}_g^{\rm bare}\right)(-z/2, z/2) |g(\hat{p})\rangle \,, \\
\hat{F}_{g/q} &= \frac{1}{P^+}\int \frac{dz^-}{2\pi} e^{ixP^+z^-} \langle q(\hat{p}')| \left(\mathcal{Z}_{\rm gs} * \mathcal{O}_s^{\rm bare}\right)(-z/2, z/2) |q(\hat{p})\rangle \,, \\
\hat{F}_{g/g} &= \frac{1}{P^+}\int \frac{dz^-}{2\pi} e^{ixP^+z^-} \langle g(\hat{p}')| \left(\mathcal{Z}_{gg} * \mathcal{O}_g^{\rm bare}\right)(-z/2, z/2) |g(\hat{p})\rangle \,.
\end{aligned} \tag{2.77}$$

The one-loop subtractions also get a contribution from $\hat{F}_{q/g}$. It reads

$$\begin{aligned}
\hat{F}_{q/g}(x,\xi) = -\frac{(1-\xi^2)}{2n_f}\int_{\Delta_2} d(\alpha,\beta)\ \mathcal{Z}_{\rm sg}(\alpha,\beta)\Big[\delta'\Big(x-(1/2-\alpha)(1-\xi)-(1/2-\beta)(1+\xi)\Big) \\
+\delta'\Big(x+(1/2-\alpha)(1-\xi)+(1/2-\beta)(1+\xi)\Big)\Big],
\end{aligned} \tag{2.78}$$

where δ' is the derivative of the δ function.

To determine the IR subtractions, one can proceed to consider the hadronic tensor, here only the vector case for simplicity, in terms of the same partonic states, denoted by $\hat{\mathcal{V}}_q(\xi)$ and $\hat{\mathcal{V}}_g(\xi)$ for quarks and gluons, respectively. The CF can be obtained by matching the two sides in Eq. (2.67), i.e.

$$\begin{aligned}
\hat{\mathcal{V}}_q(\xi) &= \int \frac{dx}{\xi} C_q(x/\xi)\hat{F}_{q/q}(x,\xi) + \int \frac{dx}{\xi^2} C_g(x/\xi)\hat{F}_{g/q}(x,\xi), \\
\hat{\mathcal{V}}_g(\xi) &= \int \frac{dx}{\xi} C_q(x/\xi)\hat{F}_{q/g}(x,\xi) + \int \frac{dx}{\xi^2} C_g(x/\xi)\hat{F}_{g/g}(x,\xi).
\end{aligned} \tag{2.79}$$

This gives the CFs C_j in terms of $\hat{\mathcal{V}}_j$ and $\hat{F}_{i/j}$, where the divergences in $\hat{\mathcal{V}}_j$ and $\hat{F}_{i/j}$ have to cancel such that C_j is finite.

For example, at one-loop we have

$$\begin{aligned}
C_q^{(1)}(y) &= \frac{\hat{\mathcal{V}}_q^{(1)}(1/y)}{y} - \int_{-1}^{1} dx\ C_q^{(0)}(xy)\hat{F}_{q/q}^{(1)}(x,1/y), \\
C_g^{(1)}(y) &= \frac{\hat{\mathcal{V}}_g^{(1)}(1/y)}{2(y^2-1)} - \frac{y}{2(y^2-1)}\sum_q \int_{-1}^{1} dx\ C_q^{(0)}(xy)\hat{F}_{q/g}^{(1)}(x,1/y).
\end{aligned} \tag{2.80}$$

The first terms of the right-hand-sides are that bare CFs $C_j^{\rm bare,(1)}$, while the second terms are pure IR poles, which subtract the IR singularity of $C_j^{\rm bare,(1)}$. However, beyond one-loop also finite terms $\sim \epsilon^0$ can arise, when the beyond-tree-level CF in d dimensions multiplies the beyond-tree-level partonic GPD.

The resulting integrals can be readily calculated in terms of harmonic polylogarithms [50]. In the two-loop calculation of the vector CF, the program `HyperInt` [75] was used. More details on the IR subtractions for the vector case are discussed in App. B.

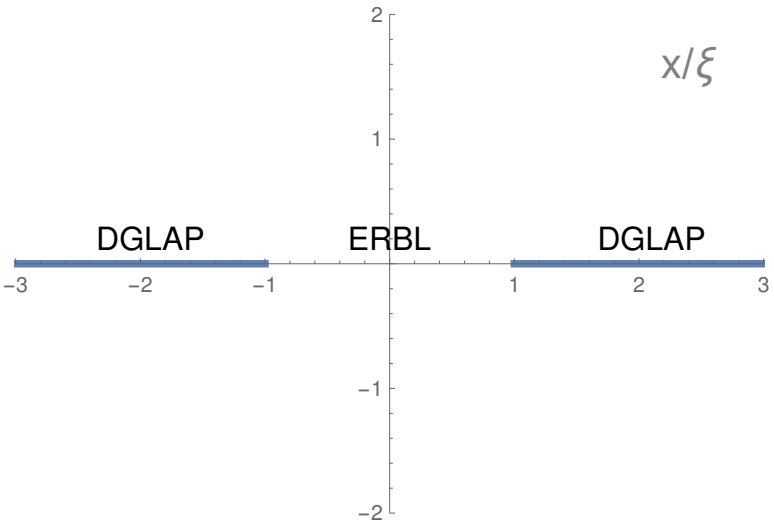

Figure 2.3: The analytic structure of the DVCS CF as a function of x/ξ. Shown in blue are branch cuts that continue to $\pm\infty$ for the left and right cut, respectively. At the branch points $x/\xi = \pm 1$ there are simple poles.

2.7 Analytic structure of the CFs

Let us consider the analytic structure of the CFs. For this, we introduce the partonic Mandelstam variables of the photon-parton subprocess

$$\hat{s} = (\hat{q} + \hat{k})^2 = \frac{1}{2}(1 - x/\xi)Q^2, \qquad \hat{u} = (\hat{q}' - \hat{k})^2 = \frac{1}{2}(1 + x/\xi)Q^2. \tag{2.81}$$

Furthermore $\hat{t} = (\hat{q} - \hat{q}')^2 = 0$ and $\hat{s} + \hat{u} + \hat{t} = Q^2$. The customary assumption that singularities in the scattering amplitudes are related to particle creation thresholds (and bound state poles) implies that we have poles at the breakpoints $\hat{s}, \hat{u} = 0$ (all particles are massless) with protruding branch cuts. We choose the $\hat{s}$-channel cut to go from $x/\xi = 1$ to $+\infty$ on the real axis and the $\hat{u}$-channel cut to go from $x/\xi = -1$ to $-\infty$ on the real axis. Everywhere else, the CFs are analytic functions of x/ξ, so they have the analytic structure shown in Fig. 2.3. According to the $\xi \to \xi - i0$ prescription, the physical values in the DGLAP region $|x/\xi| > 1$ are obtained by approaching the $\hat{s}$-channel cut from the upper half plane and the $\hat{u}$-channel cut from the lower half plane.

We have mentioned in the previous two sections that C_q is odd under $\hat{s} \leftrightarrow \hat{u}$ crossing, i.e. $x/\xi \to -x/\xi$, while $\widetilde{C}_q$ is even. On the other hand, one similarly shows that $C_g, C_{g,T}$ are even under $\hat{s} \leftrightarrow \hat{u}$ crossing, while $\widetilde{C}_g$ is odd. This means that one only has to calculate half of the diagrams, since the sum of $\hat{s}$-channel diagrams is obtained from the sum over the $\hat{u}$-channel diagrams by $x/\xi \to -x/\xi$ and an overall sign.

Throughout this work we will frequently consider the CFs as analytic functions of the variable

$$z = \frac{1}{2}(1 - x/\xi). \tag{2.82}$$

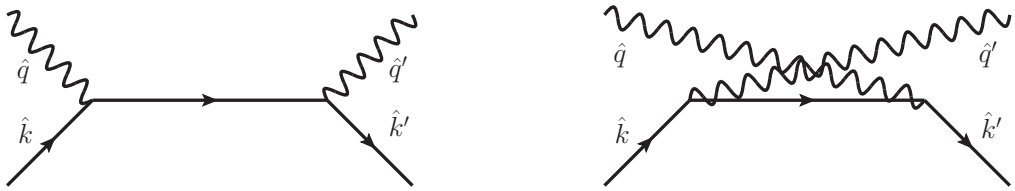

Figure 2.4: Tree-level diagrams for the quark CF.

The $\hat{s} \leftrightarrow \hat{u}$-channel crossing then corresponds to $z \to 1 - z = \bar{z}$. It is clear that we can calculate the CF in the ERBL region $|x/\xi| < 1$ or equivalently $0 < z < 1$, where it is real, and then continue uniquely to the complex plane, given that we do not cross the branch cuts seen in Fig. 2.3.

2.8 The CFs at NLO

At LO there are no subtractions and the CFs are given by the tree-level contribution in Eqs. (2.44) and (2.54). For the quark CF we get the diagrams in Fig. 2.4, while the gluon CF clearly vanishes at LO. We have

$$C_q^{(0)} = \frac{e_q^2}{2}\Big(\frac{1}{z} - \frac{1}{\bar{z}}\Big), \qquad \widetilde{C}_q^{(0)} = \frac{e_q^2}{2}\Big(\frac{1}{z} + \frac{1}{\bar{z}}\Big). \tag{2.83}$$

At one-loop there are a total of eight quark diagrams contributing to $\hat{\mathcal{V}}_q^{(1)}$. However, due to the crossing symmetry $\hat{s} \leftrightarrow \hat{u}$ only four of them need to be calculated. These diagrams, denoted by $D_{q,i}$, are shown in the upper row of Fig. 2.5. In order to get the CF $C_q^{(1)}$, the IR divergences need to be subtracted according to Eq. (2.80). The resulting contributions, denoted by $D_{q,i}^{\text{sub}}$, can be represented diagrammatically as the graphs in the lowest row of Fig. 2.5. It is clear that the lower parts of these graphs are precisely the contributions to $\hat{F}_{q/q}$, while the upper parts of the graphs are the one-loop CF $C_q^{(0)}$.

For $\hat{\mathcal{V}}_g^{(1)}$ there are a total of six diagrams. On the one hand, we have $D_{g,1}$, $D_{g,1}$ with crossed photon lines, and those two with reversed fermion lines. On the other hand we have $D_{g,2}$ and $D_{g,2}$ with reversed fermion lines, for a total of six. Since reversing the fermion lines does not change the value of the diagrams and crossing the photon lines simply corresponds to changing $\hat{s} \leftrightarrow \hat{u}$ and possibly an overall sign, there are effectively two diagrams that need to be calculated, namely $D_{g,1}$ and $D_{g,2}$. There is a single IR subtraction diagram for the one-loop gluon CF $D_{g,1}^{\text{sub}}$, since $\hat{F}_{q/g}^{(1)}$ is also given by a single diagram.

The diagrams in Fig. 2.5 can be easily evaluated, using the methods discussed in Cha. 3. The subtraction diagrams together with their photon-crossed partners give

$$\begin{aligned}
&\int_{-1}^{1} dx\; C_q^{(0)}(xy)\hat{F}_{q/q}^{(1)}(x,1/y) = -\frac{1}{\epsilon}a_s C_F \frac{e_q^2}{2z}(3 + 2\log z) - (z \leftrightarrow \bar{z}) \\
&\frac{y}{2(y^2-1)}\int_{-1}^{1} dx\; C_q^{(0)}(xy)\hat{F}_{q/g}^{(1)}(x,1/y) = \frac{1}{\epsilon}a_s 2T_F \sum_q e_q^2 \frac{1}{z^2}\log\bar{z} + (z \leftrightarrow \bar{z}),
\end{aligned} \tag{2.84}$$

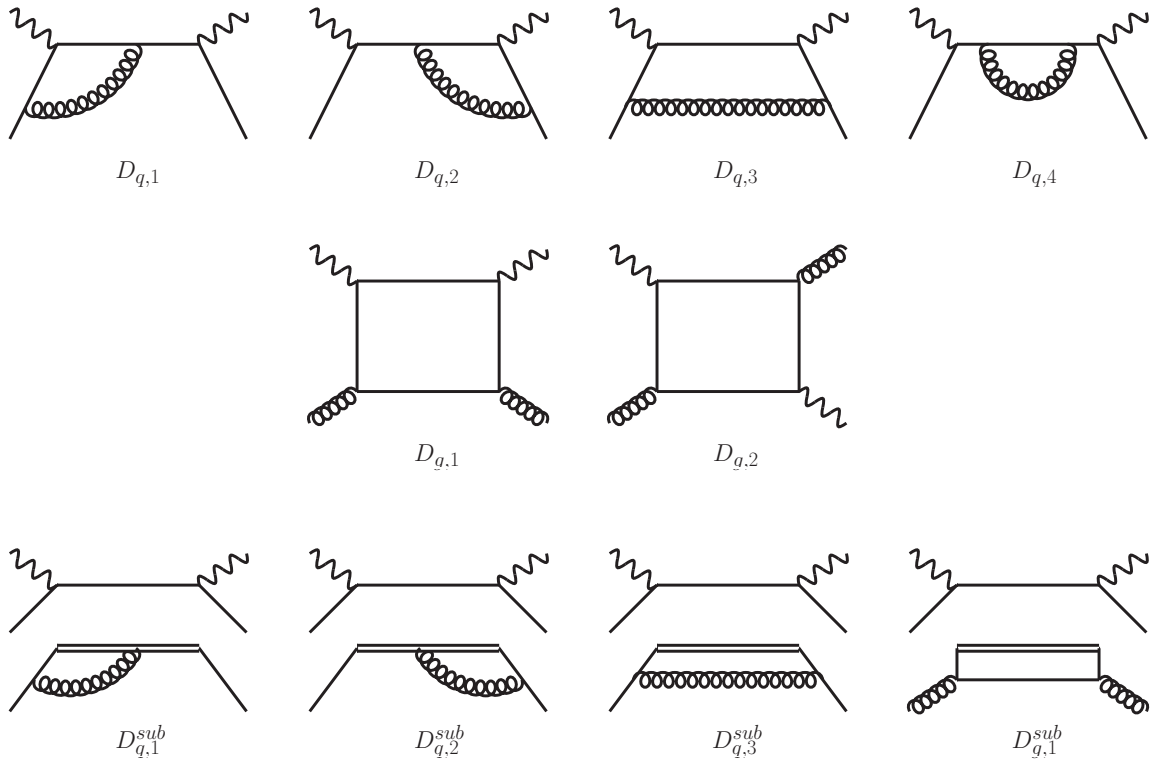

Figure 2.5: Upper row: One-loop diagrams for the quark CF, Middle row: One-loop diagrams for the gluon CF, Lower row: Graphical representation of the IR subtractions in Eq. (2.80).

where $y = x/\xi = 1 - 2z$. Similar expressions hold for the axial-vector case, but with the opposite sign of the $(z \leftrightarrow \bar{z})$ term. Subtracting these results from the corresponding bare expressions, as in Eq. (2.80), gives a finite result for the CF at $d = 4$. Note that the transversity amplitude is finite, so there is no subtraction for $C_{g,T}$.

One obtains the NLO expressions for the CFs [64, 76–80]

$$\begin{aligned}
C_q &= \frac{e_q^2}{2z}\Big[1 + a_s C_F\Big[-L(3 + 2\log z) + \log^2 z - 3\frac{z}{\bar{z}}\log z - 9\Big]\Big] - (z \leftrightarrow \bar{z}),\\
\widetilde{C}_{q,\mathrm{La}} &= \frac{e_q^2}{2z}\Big\{1 + a_s C_F\Big[-L(3 + 2\log z) + \log^2 z + 7\frac{z}{\bar{z}}\log z - 9\Big]\Big] + (z \leftrightarrow \bar{z}),\\
C_g &= \sum_q e_q^2 a_s T_F \frac{1}{2\bar{z}z}\Big[L\frac{z}{\bar{z}}\log z - \frac{z}{2\bar{z}}\log^2 z + \frac{1+z}{\bar{z}}\log z\Big] + (z \leftrightarrow \bar{z}),\\
\widetilde{C}_g &= \sum_q e_q^2 a_s T_F \frac{1}{2\bar{z}z}\Big[L\frac{z}{\bar{z}}\log z - \frac{z}{2\bar{z}}\log^2 z + \Big(\frac{5z}{\bar{z}} - 1\Big)\log z + 1\Big] - (z \leftrightarrow \bar{z}),\\
C_{g,T} &= \sum_q e_q^2 a_s T_F \frac{1}{z\bar{z}},
\end{aligned} \tag{2.85}$$

which hold up to terms $O(a_s^2)$ and $L = \log\frac{\mu^2}{Q^2}$.

We have plotted the CFs on the real x/ξ axis in Fig. 2.6, where we have included the NNLO CF, for which the explicit formulas can be found in App. C. A remarkable property that can be noticed from these plots is that quark and gluon CFs have opposite signs.

2.9 Evolution equations for GPDs

So far we have so far largely ignored the discussion of the dependence on the factorization scale μ. The CF and GPD depend on this scale, with the dependence cancelling order by order in T, i.e.

$$0 = \frac{d}{d\mu}\Big(C(\mu) * F(\mu)\Big). \tag{2.86}$$

The dependence on μ expresses the arbitrariness of separating the small scales $-t, m^2$ from the hard scale Q^2. This is illustrated by the simple example

$$\log\frac{m^2}{Q^2} = \log\frac{\mu^2}{Q^2} - \log\frac{\mu^2}{m^2},$$

where terms like $\log\mu^2/Q^2$ are factored into the CF and terms like $\log\mu^2/m^2$ are factored into the GPD.

The μ-dependence of C is, at fixed order given through $a_s(\mu)$ and $L = \log\mu^2/Q^2$. The GPD F is usually modeled at an input scale $\mu_0 \sim -t, m^2 \sim 1\,\mathrm{GeV}$, but evaluating

$$T = C(\mu_0) * F(\mu_0)$$

is not ideal, since one wants to minimize the combination $a_s(\mu)\log\frac{\mu^2}{Q^2}$ to get a decent convergence of the perturbative series in which C is expanded, which is not the case for $\mu = \mu_0$.

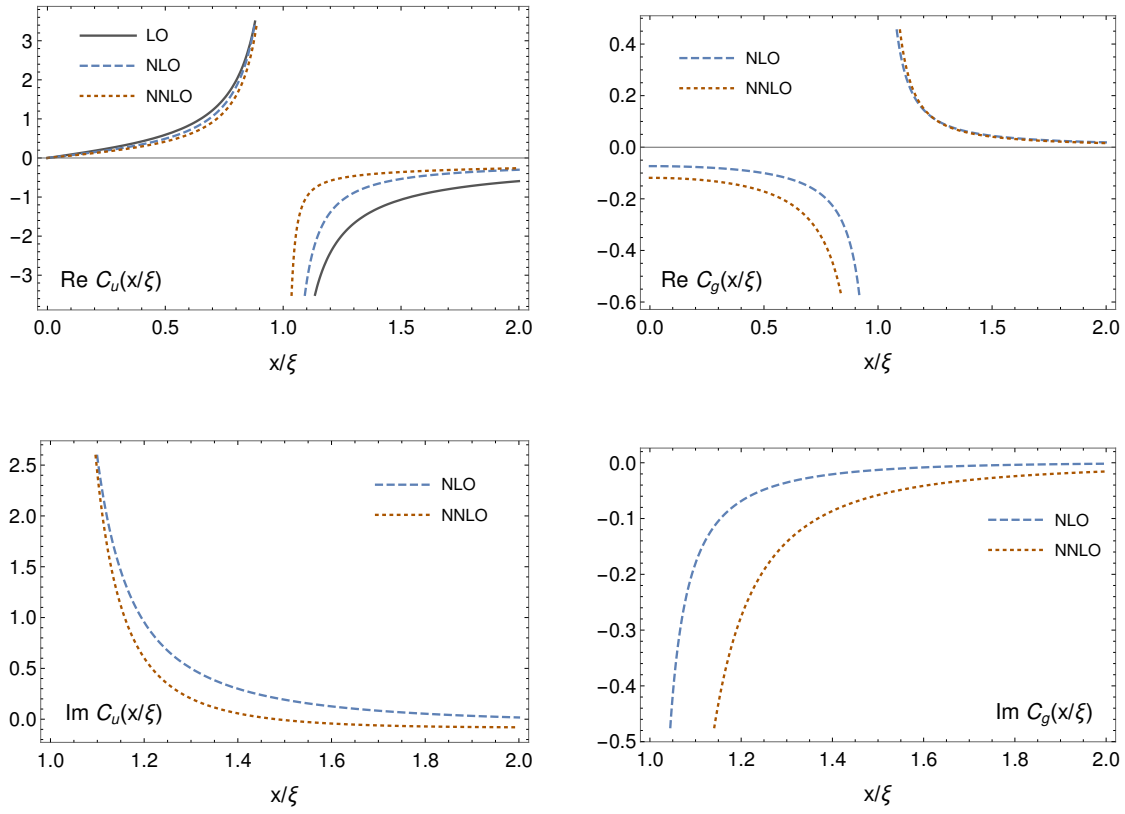

Figure 2.6: Real and imaginary parts of the vector u-quark CF C_u and the gluon CF C_g for real x/ξ. We have used the value $\alpha_s(2\text{ GeV}) = 0.3$.

Thus, since $Q \gg \mu_0$, one should resum terms of the form $a_s^j L^{j-k}$. This can be done by solving perturbatively the evolution equation

$$\mu \frac{d}{d\mu} F = -K * F, \tag{2.87}$$

where the evolution kernel K is given by

$$K = -\mu \frac{dZ}{d\mu} * Z^{-1} = \beta(a_s) \frac{dZ}{da_s} * Z^{-1}, \tag{2.88}$$

where we used that Z does depend on μ only through its dependence on a_s in the $\overline{\text{MS}}$-scheme. The evolution equation (2.87) can be used to evolve the initial input model $F(\mu_0)$ to some large scale $\mu_1 \sim Q$, so that the perturbative series for $C(\mu_1)$ exhibits decent convergence. Effectively this resums terms of the form $a_s^j L^{j-k}$ to all orders in C, where $k+1$ is the order in a_s to which K is expanded.

The two-loop evolution equations, i.e. K expanded to a_s^2 accuracy, are known for the vector case in momentum fraction space [81] and light-ray position space [82]. The three-loop equations for the vector case are known in the non-singlet sector [83] while for the singlet sector only the first eight moments are known [84].

We denote by $\mathcal{K}$ the evolution kernel in light-ray position space. For the non-singlet case there is no mixing, so we have a single kernel $\mathcal{K}_{\text{ns}}$. The singlet sector has an additional matrix structure $\mathcal{K}_{\chi\chi'}$ in position space, where $\chi, \chi' \in \{\text{s}, \text{g}\}$. The kernels are directly related to $\mathcal{Z}_{\text{ns}}$ and $\mathcal{Z}_{\chi\chi'}$ in Eq. (2.73), by the light-ray position space version of Eq. (2.88)

$$\mathcal{K} = -\mu \frac{d\mathcal{Z}}{d\mu} * \mathcal{Z}^{-1} = -\beta(a_s) \frac{d\mathcal{Z}}{da_s} * \mathcal{Z}^{-1}. \tag{2.89}$$

We write

$$\begin{aligned}
(\mathcal{K}_{\text{ns}} * f)(z_1, z_2) &= \int_{\Delta_2} d(\alpha, \beta)\ \mathcal{K}_{\text{ns}}(\alpha, \beta) f(\bar{\alpha} z_1 + \alpha z_2, z_2 \bar{\beta} + z_1 \beta), \\
(\mathcal{K}_{\chi\chi'} * f)(z_1, z_2) &= [i(z_1 - z_2)]^{\eta_{\chi\chi'}} \int_{\Delta_2} d(\alpha, \beta)\ \mathcal{K}_{\chi\chi'}(\alpha, \beta) f(\bar{\alpha} z_1 + \alpha z_2, z_2 \bar{\beta} + z_1 \beta).
\end{aligned} \tag{2.90}$$

The leading, one-loop contribution reads [15, 17, 70, 85, 86]

$$\begin{aligned}
\mathcal{K}_{\text{ns}}(\alpha, \beta) &= \mathcal{K}_{\text{ss}}(\alpha, \beta) = -4 a_s C_F \Big\{ 1 + \Big[\frac{\bar{\alpha}}{\alpha}\Big]_+ \delta(\beta) + \Big[\frac{\bar{\beta}}{\beta}\Big]_+ \delta(\alpha) - \frac{1}{2} \delta(\alpha)\delta(\beta) \Big\}, \\
\mathcal{K}_{\text{sg}}(\alpha, \beta) &= -8 a_s n_f T_F (\bar{\alpha}\bar{\beta} + 3\alpha\beta), \\
\mathcal{K}_{gs}(\alpha, \beta) &= -4 a_s C_F \Big[2 + \delta(\alpha)\delta(\beta) \Big], \\
\mathcal{K}_{gg}(\alpha, \beta) &= -4 a_s C_A \Big\{ 4(\bar{\alpha}\bar{\beta} + 2\alpha\beta) \\
&\qquad + \Big[\frac{\bar{\alpha}^2}{\alpha}\Big]_+ \delta(\beta) + \Big[\frac{\bar{\beta}^2}{\beta}\Big]_+ \delta(\alpha) + \frac{1}{2}(\beta_0 - 6C_A)\delta(\alpha)\delta(\beta) \Big\},
\end{aligned} \tag{2.91}$$

where the delta functions are defined such that $\int_0^1 d\alpha\ \delta(\alpha) = 1$ and the plus distribution is defined by $[f(\alpha)]_+ = f(\alpha) - \delta(\alpha) \int_0^1 d\beta\ f(\beta)$.

For practical calculations it is necessary to have a representation of the momentum fraction space kernel Z which acts directly on the GPDs. For this, we have to perform the "Fourier transform" from light-ray position space. Using the translation property

$$\langle p'|\,\mathcal{O}_{\rm ns}(z_1,z_2)\,|p\rangle = e^{-iy\cdot\Delta}\,\langle p'|\,\mathcal{O}_{\rm ns}(z_1+y,z_2+y)\,|p\rangle \tag{2.92}$$

it is easy to show that

$$\langle p'|\,\mathcal{O}_{\rm ns}(z_1,z_2)\,|p\rangle = 2P^+\int_{-\infty}^{\infty} dx\; e^{iP^+[(\xi+x)z_1+(\xi-x)z_2]}F_{\rm ns}(x,\xi). \tag{2.93}$$

Hence

$$\begin{aligned}\mu\frac{d}{d\mu}F_{\rm ns}(x,\xi) &= -\frac{1}{2}\int\frac{dz}{2\pi}e^{ixzP^+}\,\langle p'|\,(\mathcal{K}_{\rm ns}*\mathcal{O}_{\rm ns})(-z/2,z/2)\,|p\rangle\\ &= -\int_{\Delta_2} d(\alpha,\beta)\frac{\mathcal{K}_{\rm ns}(\alpha,\beta)}{1-\alpha-\beta}F_{\rm ns}\Big(\frac{x+(\alpha-\beta)\xi}{1-\alpha-\beta},\xi\Big).\end{aligned} \tag{2.94}$$

However, because of the double integral, this form is not well-suited for numerical evaluation. In fact, one can do one of the two integrals without loss of generality.

We demonstrate this in the following, setting $P^+=1$ for simplicity. It is more elegant to consider the Fourier transform of a function $f(z_1,z_2)$ of two light-ray positions

$$\begin{aligned}\mathcal{F}(f)(x_1,x_2) &= \int_{-\infty}^{\infty}\frac{dz_1}{2\pi}\int_{-\infty}^{\infty}\frac{dz_2}{2\pi}e^{-ix_1z_1-ix_2z_2}f(z_1,z_2),\\ f(z_1,z_2) &= \int_{-\infty}^{\infty}dx_1\int_{-\infty}^{\infty}dx_2\; e^{ix_1z_1+ix_2z_2}\mathcal{F}(f)(x_1,x_2).\end{aligned} \tag{2.95}$$

Let

$$f_{\rm ns}(z_1,z_2) = \frac{1}{2}\,\langle p'|\,\mathcal{O}_{\rm ns}(z_1,z_2)\,|p\rangle\,. \tag{2.96}$$

Then the GPD and $\mathcal{F}(f_{\rm ns})$ can be written in terms of each other as the projective integrals

$$\begin{aligned}F_{\rm ns}(x,\xi) &= \int_{-\infty}^{\infty}dx_1\int_{-\infty}^{\infty}dx_2\;\delta\Big(x-\frac{x_1-x_2}{2}\Big)\mathcal{F}(f_{\rm ns})(x_1,x_2)\\ \mathcal{F}(f_{\rm ns})(x_1,x_2) &= \int_{-1}^{1}dx\;\delta(x_1-\xi-x)\delta(x_2-\xi+x)F_{\rm ns}(x,\xi).\end{aligned} \tag{2.97}$$

The action of a momentum fraction space kernel K is given by

$$\begin{aligned}(K*\mathcal{F}(f))(x_1,x_2) &= \int_{-\infty}^{\infty}dx_1\int_{-\infty}^{\infty}e^{-ix_1z_1-ix_2z_2}(\mathcal{K}*f)(z_1,z_2)\\ &= \int_{-\infty}^{\infty}dy_1\int_{-\infty}^{\infty}dy_2\;\delta(x_1+x_2-y_1-y_2)\mathcal{F}(f)(x_1,x_2)\mathrm{K}(x_1,x_2|y_1,y_2),\end{aligned} \tag{2.98}$$

where

$$\mathrm{K}(x_1,x_2|y_1,y_2) = \int_{\Delta_2} d(\alpha,\beta)\;\mathcal{K}(\alpha,\beta)\delta(x_1-\bar\alpha y_1-\beta y_2), \tag{2.99}$$

subject to the constraint $x_1 + x_2 = y_1 + y_2$. Applying this to the evolution equation for the GPD gives

$$\begin{aligned}\mu\frac{d}{d\mu}F_{\rm ns}(x,\xi) &= -\int_{-\infty}^{\infty} dx_1 \int_{-\infty}^{\infty} dx_2\ \delta\Big(x - \frac{x_1+x_2}{2}\Big)(K_{\rm ns} * \mathcal{F}(f_{\rm ns}))(x_1,x_2) \\ &= -\int_{-1}^{1} dy\ \mathrm{K}_{\rm ns}(\xi+x,\xi-x|\xi+y,\xi-y)F_{\rm ns}(y,\xi). \end{aligned} \tag{2.100}$$

We have written the evolution equation for the GPDs in terms of a single integral with the kernel K. It is straightforward to apply the same manipulations in the singlet sector. Explicit formulas for those kernels in terms of generalized step functions can be found in Ref. [20].

2.10 Finite renormalization of the axial-vector GPD

In Eq. (2.66) we have defined the axial-vector CF $\widetilde{C}_{q,\rm La}$ in Larin's scheme. Typically, one applies additional subtractions to this CF to get what is called "$\overline{\rm MS}$-scheme". For the forward case these subtractions are known to three loops [87].

In the following, we consider how these subtractions can be implemented, following [74]. The axial-vector light-ray operator in Larin's scheme can be defined as

$$\widetilde{\mathcal{O}}_{q,\rm La}(z_1,z_2) = \frac{i}{3!}\varepsilon^{+\mu_1\mu_2\mu_3}\bar{q}(z_1 n)\gamma_{\mu_1}\gamma_{\mu_2}\gamma_{\mu_3}W_n(z_1,z_2)q(z_2 n). \tag{2.101}$$

Let $\mathcal{K}_{\rm La}$ denote its evolution kernel in light-ray position space, i.e.

$$\mu\frac{d}{d\mu}\widetilde{\mathcal{O}}_{q,\rm La} = -\mathcal{K}_{\rm La} * \widetilde{\mathcal{O}}_{q,\rm La}. \tag{2.102}$$

We write the light-ray operator in the $\overline{\rm MS}$-scheme by

$$\widetilde{\mathcal{O}}_q = \mathcal{U} * \widetilde{\mathcal{O}}_{q,\rm La}. \tag{2.103}$$

The light-ray position space operator $\mathcal{U}(a_s) = 1 + O(a_s)$ is defined by the requirement that

$$\mathcal{K} = \mathcal{U} * \mathcal{K}_{\rm La} * \mathcal{U}^{-1} - \beta(a_s)\frac{d\mathcal{U}}{da_s} * \mathcal{U}^{-1}, \tag{2.104}$$

where $\mathcal{K}$ is the evolution kernel for the vector case, defined in Sec. 2.9. $\mathcal{U}$ is determined in Ref. [74] to a_s^3 accuracy. For example, to a_s^1 accuracy it is given by

$$(\mathcal{U} * f)(z_1,z_2) = f(z_1,z_2) - 8a_s C_F \int_{\Delta_2} d(\alpha,\beta)\ f(\bar{\alpha}z_1 + \alpha z_2, \bar{\beta}z_2 + \beta z_1) + O(a_s^2). \tag{2.105}$$

The scheme rotation given by the operator $\mathcal{U}$ must be compensated in the axial-vector CF, such that $\mathcal{A}$ is invariant, i.e.

$$\widetilde{C}_q = \widetilde{C}_{q,\rm La} * U^{-1}, \tag{2.106}$$

where U is the momentum fraction space representation of $\mathcal{U}$. As usual, we can circumvent the tedious transformation to momentum fraction space and determine $\widetilde{C}_q$ entirely in terms of the light-ray position space representation $\mathcal{U}$. The derivation is analogous to the one for the IR subtractions in Sec. 2.6. We obtain that the one-loop axial-vector CF in the $\overline{\text{MS}}$-scheme is given by

$$\begin{aligned}\widetilde{C}_q^{(1)}(y) &= \widetilde{C}_{q,\text{La}}^{(1)}(y) + 8C_F \int_{\Delta_2} d(\alpha,\beta)\, \widetilde{C}_q^{(0)}\Big((1/2-\alpha)(y-1) + (1/2-\beta)(y+1)\Big) \\ &= \widetilde{C}_{q,\text{La}}^{(1)}(y) - \Big[4e_q^2 a_s C_F \frac{\log z}{\bar{z}} + (z \leftrightarrow \bar{z})\Big] \\ &= \frac{e_q^2}{2z}\Big\{1 + a_s C_F\Big[-L(3+2\log z) + \log^2 z - \frac{z}{\bar{z}}\log z - 9\Big]\Big]\Big\} + (z \leftrightarrow \bar{z}),\end{aligned} \tag{2.107}$$

where $y = x/\xi$ and $z = \frac{1}{2}(1-y)$.

In Ref. [88] the two-loop axial-vector CF in the $\overline{\text{MS}}$ was computed using the approach in terms of the $\mathcal{U}$ operator considered here, but the CF in Larin's scheme was computed from conformal algebra, using the techniques discussed in Sec. 3.3. On the other hand in Ref. [89] the CF was calculated using Feynman diagrams and the authors used a different – but equivalent – approach to determine the subtractions.

3 Computation of the coefficient function

3.1 Computational methods for calculating Feynman diagrams

Methods using computer algebra have become a key part of Feynman diagram calculations, allowing for efficient computations of multiloop diagrams. These methods involve using computer programs that can perform algebraic manipulations and symbolic computations, enabling the manipulation of large mathematical expressions that arise in Feynman diagram calculations.

The first step in the standard workflow is to generate the diagrams, using for example `qgraf` [90]. The resulting output are then usually converted to expressions in `FORM` [91]. This step can be omitted in the calculation of the two-loop CF, since there are only about 70 non-related diagrams that need to be calculated.

In `FORM` one then needs to apply projections on the free indices. In the present case the projection relations are given by Eq. (2.66). Consequently one obtains a set of scalar integrals. One can find linear relations between these integrals by the means of integration-by-parts (IBP) identities [46]

$$\int \frac{d^d k}{(2\pi)^d} \frac{\partial}{\partial k^\mu} \Big[K^\mu f(k) \Big] = 0,$$

where K^μ can be any linear combination of external and loop momenta and $f(k)$ is a generic Feynman integrand.

For the computation of the two-loop CF [52] the program `FIRE6` [92] was used to perform the IBP reduction. This results in a set of master integrals (MIs) in which the complete amplitude can be expressed. For the case of the DVCS CF the MIs are discussed in Sec. 3.2.

The integrals in our case are effectively functions of a single variable, which can be taken to be z defined in Eq. (2.82). To summarize, we are considering a $2 \to 2$ process

$$q(\hat{k}) + \gamma^*(\hat{q}) \to q(\hat{k}') + \gamma(\hat{q}') \tag{3.1}$$

with momenta

$$\hat{k} = \bar{z}\widetilde{P}^+ \bar{n}, \qquad \hat{k}' = -z\widetilde{P}^+ \bar{n}, \qquad \hat{q} = -\widetilde{P}^+ \bar{n} + \frac{Q^2}{2\widetilde{P}^+} n, \qquad \hat{q}' = \frac{Q^2}{2\widetilde{P}^+} n. \tag{3.2}$$

Furthermore, it is convenient to define $\hat{P} = \hat{k} - \hat{k}' = \widetilde{P}^+ \bar{n}$. We can set $\widetilde{P}^+ = 2\xi P^+ = 1$, since no scalar product depends on it. The hard scale Q^2 can also be set to one. The scale dependence can be easily reintroduced later by multiplying with a factor of $e^{\epsilon L}$ for each loop and possibly factors Q^2 raised to integer powers from dimensional analysis.

Note that it is necessary to implement by hand the restriction that $\hat{k}$ and $\hat{k}'$ are linearly dependent, since it is not assumed automatically in `FIRE6`. This can be done by applying the IBP reduction to the right-hand side of the equation

$$0 = \int d^d l \; (z\hat{k}^\mu - \bar{z}\hat{k}'^\mu) l_\mu f(l),$$

for a generic integrand $f(l)$ and using the resulting identity to find further relations between integrals.

3.2 Master integrals

At one-loop there is only a single master integral

$$M_0(z) = \int \frac{d^d l}{i\pi^{d/2}} \frac{e^{\epsilon\gamma_E}}{l^2(l+\hat{q}+\hat{k})^2} = \frac{e^{\epsilon\gamma_E}\Gamma(\epsilon)\Gamma(1-\epsilon)^2}{\Gamma(2-2\epsilon)} z^{-\epsilon}. \tag{3.3}$$

Note that $M_0(1-z)$ and $M_0(1)$ also appear, but they can clearly be obtained from this result. M_0 is easily evaluated using standard methods.

All MIs appearing in the two-loop calculation of the DVCS CF are shown in Fig. 3.1. We used the notation $M_{i,j}$, where the first index i refers to the number internal lines, while j enumerates the different MIs with the same number of internal lines. These graphs in their entirety were first evaluated in Ref. [89]. The results are unpublished at this point.

A powerful method to evaluate MIs is the method of differential equations [47]. We illustrate how this can be applied to the present case. We use the strategy of bringing the differential equation for a Feynman integral into the so-called canonical form [93].

Here we use a simplified version of this argument where we consider a single integral $I(\epsilon, z)$, which is one of the above two-loop MIs. Then one can determine by trial and error a factor z^j (or $\bar{z}^j$) for some power $j \in \mathbb{Z}$, such that for $J(\epsilon, z) = z^j I(\epsilon, z)$, we get, after taking a derivative ∂_z and applying IBP reduction to the result, a differential equation of the form

$$\partial_z J(\epsilon, z) = f(\epsilon, z) + \epsilon g(z) J(\epsilon, z), \tag{3.4}$$

where $f(\epsilon, z)$ is a function that depends on MIs that have a lower number of internal lines than $I(z)$ and $g(z)$ is a rational function of z. In this way, one can calculate the MIs inductively in the number of internal lines. We write

$$J(\epsilon, z) = \frac{1}{\epsilon^4} \sum_{k=0}^{\infty} \epsilon^k J_k(z), \qquad f(\epsilon, z) = \frac{1}{\epsilon^2} \sum_{k=0}^{\infty} \epsilon^k f_k(z), \tag{3.5}$$

where we have used that f should have at most a ϵ^{-2} divergence (this is found by explicit calculation). Clearly, this implies that J_0 must be a constant. Further terms in the ϵ expansion of J can be readily calculated iteratively by integrating Eq. (3.4) and comparing coefficients of ϵ^{k-4}, giving

$$J_k(z) = \int^z dz' \, \Big(f_{k-2}(z') + g(z') J_{k-1}(z') \Big). \tag{3.6}$$

The most difficult part in the computation is usually the determination of the integration constants in Eq. (3.6). For this one must choose a value z_0, usually 0 or 1, and evaluate explicitly $J_k(z_0)$. This is particularly difficult if an analytical expression is required. A possible strategy is to use the Mellin-Barnes representation [94], which relies on the identity

$$\frac{1}{(A+B)^\lambda} = \frac{1}{\Gamma(\lambda)} \frac{1}{2\pi i} \int_{c-i\infty}^{c+i\infty} dz \, \frac{B^z}{A^{\lambda z}} \Gamma(\lambda+z)\Gamma(-z), \tag{3.7}$$

where the position of the contour on the real axis c is to be choosen such that the poles from $\Gamma(\lambda+z)$ are to the left and the poles of $\Gamma(-z)$ are to the right of the contour. Formula (3.7) can be applied to the Feynman integral in the Feynman parameter representation and the integral over the now factored Feynman parameter dependent A, B can be taken more easily. The remaining task is to evaluate the contour integral in Eq. (3.7). For some of the integrations constants the program `MB tools` [95] was used in the calculation of the diagrams in Fig. 3.1.

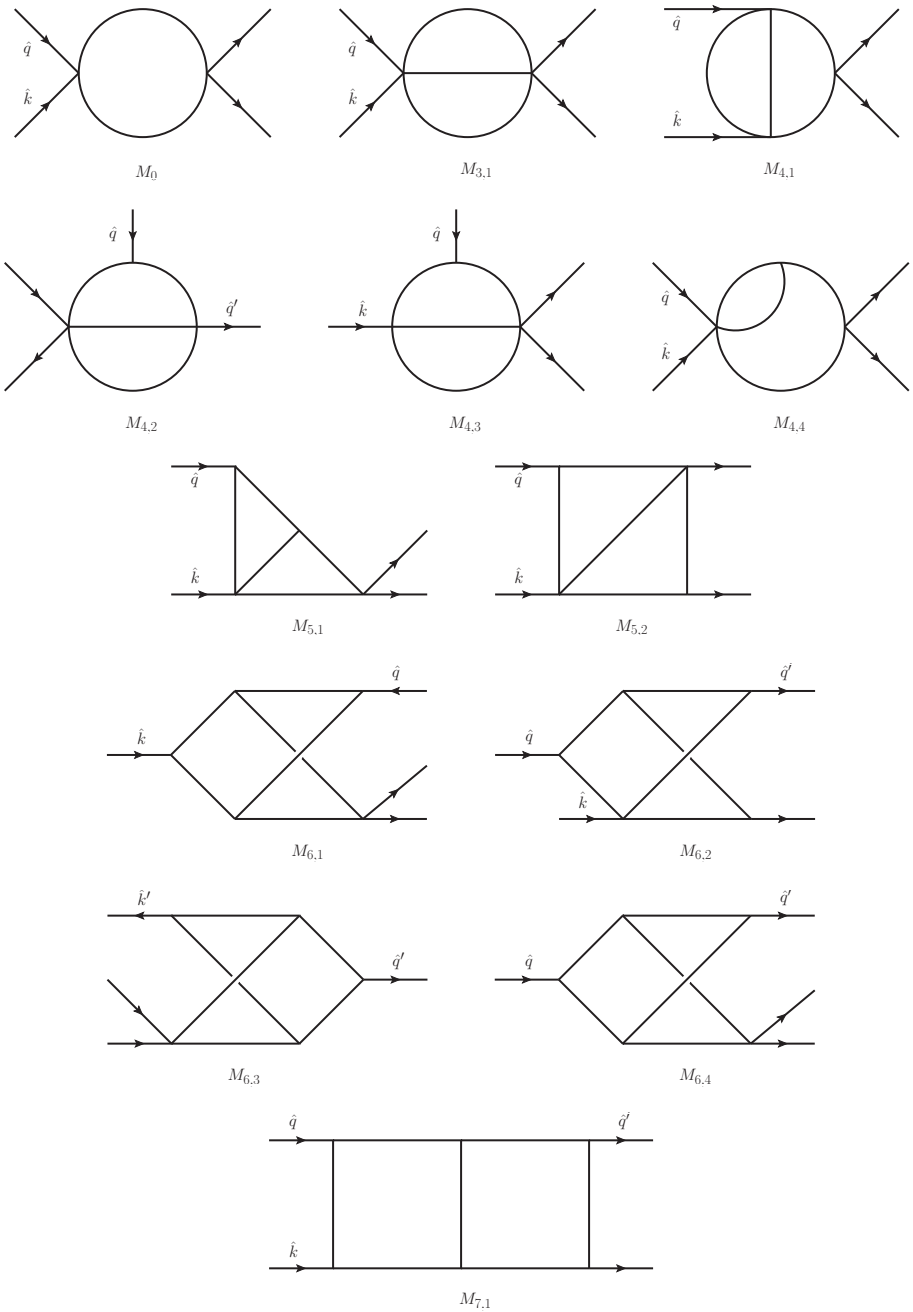

Figure 3.1: Master integrals for the two-loop DVCS CF, i.e. for the scattering amplitude in Eq. (3.1).

3.3 The CF from conformal symmetry

The DVCS CF can also be obtained without calculating any Feynman diagrams, by considering a group of space-time transformations called conformal transformations. These include the usual space-time transformations, i.e. Lorentz transformations and translations, and furthermore dilation and space-time inversion. It is beyond the scope of this thesis to introduce this formalism from scratch. See for example Ref. [96] for a comprehensive review in the context of QCD.

Techniques using conformal symmetry in QCD can, for example, be used to obtain the evolution kernels. This method was developed in Refs. [97, 98] and it was used to calculate the complete two-loop mixing matrix for twist-two operators in QCD [77, 99, 100]. Moreover, it was used to calculate the two-loop evolution kernel $\mathcal{K}^{(2)}$ of the GPDs [81, 82, 101, 102] and the three-loop non-singlet evolution kernel [83].

In a similar way, one can also obtain the CF of DVCS, as was first shown in Ref. [77]. The non-singlet CF at NNLO was first calculated using this method [82] and it was also used to compute the axial-vector non-singlet CF at NNLO [88]. The results were reproduced in Ref. [48] and [89], respectively by calculation of the Feynman diagrams. The singlet case is significantly more involved however, in particular because one ingredient is missing in the two-loop singlet conformal anomaly.

In this section we present a review of this method, based on [103]. The essential statement is the conformal symmetry of QCD in (possibly non-integer) d dimensions at the critical point where the QCD β vanishes [104]

$$0 = \beta(a_s) = 2a_s\Big(\epsilon + \sum_{j=0}^{\infty} \beta_j (a_s)^j\Big). \tag{3.8}$$

This equation can be understood in the way that for a given non-integer ϵ we can tune the value of $a_s = a_{s*}$ such that Eq. (3.8) holds, or equivalently, for a given value of the coupling a_s, we tune the value of $\epsilon = \epsilon_*$ such that Eq. (3.8) holds. We will adopt the latter viewpoint in the following. Also we consider only the non-singlet piece of the quark CF $C_{\rm ns}$, defined by

$$C_q = e_q^2 C_{\rm ns} + \Big(\sum_{q'} e_{q'}\Big) C_{\rm ps}. \tag{3.9}$$

The CF in $d_* = 4 - 2\epsilon_*$ dimensions can be written as

$$C_{\rm ns*} = C_{\rm ns}|_{\epsilon=\epsilon^*(a_s)} = \sum_{j,k=0}^{\infty} a_s^j \epsilon_*^k C_{\rm ns}^{(j,k)} = \sum_{j}^{\infty} a_s^j C_{\rm ns*}^{(j)}. \tag{3.10}$$

The coefficients $C_{\rm ns*}^{(j)}$ can be easily determined in terms of $C_{\rm ns}^{(j,k)}$ and β function coefficients, e.g.

$$C_{\rm ns*}^{(0)} = C_{\rm ns}^{(0)}, \qquad C_{\rm ns*}^{(1)} = C_{\rm ns}^{(1,0)}, \qquad C_{\rm ns*}^{(2)} = C_{\rm ns}^{(2)} - \beta_0 C_{\rm ns}^{(1,1)}. \tag{3.11}$$

For the rest of this section we drop the "ns" index and tacitly omit any flavor-singlet contributions. Furthermore, we frequently use the notation for integral operators, which was already used in Cha. 2, and is summarized in App. A.

3.3.1 Conformal operator product expansion

Retaining the contributions of vector operators only, the most general expression for the operator product expansion (OPE) of two electromagnetic currents to the twist-two accuracy has the form

$$T\{j^\mu(x_1)j^\nu(x_2)\} = \sum_{N,\text{even}} \frac{\mu^{\gamma_N}}{(-x_{12}^2+i0)^{t_N}} \int_0^1 du \Bigg\{ -\frac{1}{2}A_N(u)\left(g^{\mu\nu} - \frac{2x_{12}^\mu x_{12}^\nu}{x_{12}^2}\right) + B_N(u) g^{\mu\nu} + C_N(u) x_{12}^\nu \partial_1^\mu - C_N(\bar u) x_{12}^\mu \partial_2^\nu + D_N(u) x_{12}^2 \partial_1^\mu \partial_2^\nu \Bigg\} \mathcal{O}_N^{x_{12}\dots x_{12}}(x_{21}^u)\,, \qquad (3.12)$$

where

$$\partial_k^\mu = \frac{\partial}{\partial x_k^\mu}, \qquad x_{12} = x_1 - x_2\,, \qquad \bar u = 1-u\,, \qquad x_{21}^u = \bar u x_2 + u x_1\,, \qquad (3.13)$$

and

$$\mathcal{O}_N^{x\dots x}(y) = x_{\mu_1}\dots x_{\mu_N}\mathcal{O}_N^{\mu_1\dots\mu_N}(y)\,. \qquad (3.14)$$

Here $\mathcal{O}_N^{\mu_1\dots\mu_N}(y)$ are the leading twist conformal operators that transform in the proper way under conformal transformations. That is, given that $\mathbb{K}_\mu$ is the quantum Hilbert space representation of the generator of special conformal transformations, we have

$$[\mathbb{K}_\mu, \mathcal{O}_N^{x\dots x}(y)] = \left(2y_\mu y^\nu \frac{\partial}{\partial y^\nu} - y^2\frac{\partial}{\partial y^\mu} + 2\Delta_N y_\mu + 2y^\nu\left(x_\mu\frac{\partial}{\partial x^\nu} - x_\nu\frac{\partial}{\partial x^\mu}\right)\right)\mathcal{O}_N^{x\dots x}(y). \qquad (3.15)$$

Here and below N is the operator spin, Δ_N is its scaling dimension, $\Delta_N = d_* + N - 2 + \gamma_N$ where $d_* = 4-2\epsilon_*$, $\gamma_N = \gamma_N(a_s)$ is the anomalous dimension, $t_N = 2 - \epsilon_* - \frac{1}{2}\gamma_N(a_s)$ is the twist and $j_N = N + 1 - \epsilon_* + \frac{1}{2}\gamma_N(a_s)$ is the conformal spin. We have separated in Eq. (3.12) the scale factor μ^{γ_N} to make the functions $A_N(u),\dots,D_N(u)$ dimensionless. Note that only vector operators with even spin N contribute to the expansion.

The conditions of conformal invariance and current conservation $\partial^\mu j_\mu = 0$ lead to constraints on the functional form and also certain relations between the invariant functions $A_N(u),\dots,D_N(u)$ in Eq. (3.12). One obtains

$$A_N(u) = a_N\, u^{j_N-1}\bar u^{j_N-1}, \qquad B_N(u) = b_N\, u^{j_N-1}\bar u^{j_N-1}. \qquad (3.16)$$

The remaining functions $C_N(u)$ and $D_N(u)$ are given by the following expressions:

$$C_N(u) = u^{N-1}\int_u^1 \frac{dv}{v^N} v^{j_N}\bar v^{j_N-2}\left(c_N - \frac{b_N}{v}\right), \qquad (3.17)$$

$$D_N(u) = -\frac{1}{N-1}\int_0^1 dv (v\bar v)^{j_N-1}\left[\theta(v-u)\left(\frac{u}{v}\right)^{N-1} + \theta(\bar v - \bar u)\left(\frac{\bar u}{\bar v}\right)^{N-1}\right]\left(d_N - \frac{c_N - b_N}{2v\bar v}\right).$$

The coefficients c_N and d_N are not independent and are given in terms of a_N and b_N by linear relations

$$\begin{aligned}(j_N-1)\; a_N &= 2\,t_N\,(c_N - b_N)\,,\\ 2\,(t_N-1)\,d_N &= -\frac{1}{2}a_N(N-j_N) - \gamma_N b_N + \big(j_N - 2 + 2t_N\big)(c_N - b_N).\end{aligned} \qquad (3.18)$$

Thus the form of the OPE of the product of two conserved spin-one currents in a conformal theory is fixed up to two constants, $a_N(a_s)$ and $b_N(a_s)$, for each (even) spin N. In QCD the expansion of $a_N(a_s)$ starts at order $O(a_s)$, so that also $c_N - b_N = O(a_s)$ and $d_N = O(a_s)$.

3.3.2 Relating DIS and DVCS

It is convenient to fix the normalization of the leading twist conformal operators such that

$$\mathcal{O}_N^{\mu_1\dots\mu_N}(0) = i^{N-1}\bar{q}(0)\gamma^{\{\mu_1}D^{\mu_2}\dots D^{\mu_N\}}q(0) + \text{ total derivatives}\,, \tag{3.19}$$

where D^μ are covariant derivatives and $\{\dots\}$ denotes the symmetrization of all enclosed Lorentz indices and the subtraction of traces. In this way, the forward matrix elements of these operators are related to moments $f_N^{(\mathrm{DIS})}$ of quark PDFs.

$$\langle p|\mathcal{O}_N^{\mu_1\dots\mu_N}(0)|p\rangle = p^{\{\mu_1}\dots p^{\mu_N\}}f_N^{(\mathrm{DIS})}\,. \tag{3.20}$$

Note that the CF does not depend on the external states so we can use unpolarized nucleon states. Using this parametrization and taking the Fourier transform of the forward matrix element of Eq. (3.12) one obtains the OPE for the forward Compton tensor in a generic conformal theory

$$\begin{aligned} T_{\mu\nu}^{(\mathrm{DIS})} &= i\int d^dx\, e^{-iqx}\langle p|T\{j_\mu(x)j_\nu(0)\}|p\rangle \\ &= \sum_{N,\text{even}} f_N^{(\mathrm{DIS})}\left(\frac{2p\cdot q}{Q^2}\right)^N\left(\frac{\mu}{Q}\right)^{\gamma_N} \\ &\qquad\times\left[\left(-g_{\mu\nu}+\frac{q_\mu q_\nu}{q^2}\right)\mathrm{c}_{1,N}(a_*) + \frac{(q_\mu+2x_Bp_\mu)(q_\nu+2x_Bp_\nu)}{Q^2}\mathrm{c}_{2,N}(a_*)\right], \end{aligned} \tag{3.21}$$

where

$$\begin{aligned} \mathrm{c}_{1,N} &= i^N\pi^{d/2}2^{\gamma_N}B(j_N,j_N)\frac{\Gamma(N+\gamma_N/2)}{\Gamma(t_N)}\left(\frac{t_N-1}{2t_N}a_N - b_N\right), \\ \mathrm{c}_{2,N} &= i^N\pi^{d/2}2^{\gamma_N}B(j_N,j_N)\frac{\Gamma(N+\gamma_N/2)}{\Gamma(t_N)}\left(-b_N + \frac{2N+d-t_N-1}{2t_N}a_N\right). \end{aligned} \tag{3.22}$$

Here and below $B(j_N, j_N)$ is the Euler Beta function.

The same expansion in QCD is usually written as [105]

$$\begin{aligned} T_{\mu\nu}^{(\mathrm{DIS})} = \sum_{N,\text{even}} f_N^{(\mathrm{DIS})}\left(\frac{2p\cdot q}{Q^2}\right)^N &\left[\left(g_{\mu\nu}-\frac{q_\mu q_\nu}{q^2}\right)c_L\left(N,\frac{Q^2}{\mu^2},a_s\right)\right. \\ &\left.-\left(g_{\mu\nu}-p_\mu p_\nu\frac{4x_B^2}{Q^2}-(p_\mu q_\nu+p_\nu q_\mu)\frac{2x_B}{Q^2}\right)c_2\left(N,\frac{Q^2}{\mu^2},a_s\right)\right], \end{aligned} \tag{3.23}$$

where we dropped electromagnetic charges and the sum over flavors. Thus we can identify

$$\begin{aligned} \mathrm{c}_{2,N}(a_s)\left(\frac{\mu}{Q}\right)^{\gamma_N} &= c_2\left(N,\frac{Q^2}{\mu^2},a_s,\epsilon_*\right), \\ \mathrm{c}_{1,N}(a_s)\left(\frac{\mu}{Q}\right)^{\gamma_N} &= c_2\left(N,\frac{Q^2}{\mu^2},a_s,\epsilon_*\right) - c_L\left(N,\frac{Q^2}{\mu^2},a_s,\epsilon_*\right) = c_1\left(N,\frac{Q^2}{\mu^2},a_s,\epsilon_*\right). \end{aligned} \tag{3.24}$$

The OPE coefficient functions c_2 and c_L contribute to the OPE for the well-known DIS structure functions F_2 and F_L, respectively, and are known to NNNLO.

Let us now consider the off-forward case of DVCS. In comparison to forward scattering there are two modifications. Firstly, the position of the operator $\mathcal{O}_N(ux)$ in Eq. (3.12) (we take $x_1 \to x$, $x_2 \to 0$) becomes relevant since

$$\langle p'|\mathcal{O}_N(ux)|p\rangle = e^{iu(x\cdot\Delta)}\langle p'|\mathcal{O}_N(0)|p\rangle. \tag{3.25}$$

This effectively results in a shift of the momentum in the Fourier integral $q \to q - u\Delta$. Secondly, the matrix element becomes more complicated and can be parameterized as

$$\begin{aligned}\langle p'|n^{\mu_1}\dots n^{\mu_N}\mathcal{O}_{\mu_1\dots\mu_N}(0)|p\rangle &= \sum_k \left(-\frac{1}{2}\right)^k f_N^{(k)}(P^+)^{N-k}(\Delta^+)^k = (P^+)^N f_N(\xi)\,,\\ f_N(\xi) &= \sum_k f_N^{(k)}\xi^k\,, \qquad f_N^{(0)} = f_N^{(\mathrm{DIS})}\,.\end{aligned} \tag{3.26}$$

Hence one needs the more general Fourier integral

$$\begin{aligned}\sum_{k=0}^{N}\left(-\frac{1}{2}\right)^k f_N^{(k)}\int d^dx\, e^{-i(q-u\Delta)x}\frac{\Gamma(t_N)}{(-x^2+i\epsilon)^{t_N}}(x\cdot P)^{N-k}(x\cdot\Delta)^k =\\ = \; i^{N-1}2^{\gamma_N}\pi^{\frac{d}{2}}\frac{\Gamma(\frac{1}{2}\gamma_N+N)}{\bar u^{N+\frac{1}{2}\gamma_N}Q^{\gamma_N}}\left(\frac{2P\cdot q}{Q^2}\right)^N\sum_{k=0}^{N}f_N^{(k)}\xi^k,\end{aligned} \tag{3.27}$$

where we neglected all power suppressed corrections $O(-t/Q^2)$ and also used that to this accuracy $(q-u\Delta)^2 = -\bar u Q^2$.

Up to the obvious replacement $p \mapsto P$ there are two differences to the forward case (DIS): an extra factor $\bar u^{-N-\frac{1}{2}\gamma_N}$, and the matrix element $f_N \to f_N(\xi)$. In Eq. (2.33) we have defined the vector amplitude $\mathcal{V}$ as the projection on the Lorentz structure $g_\perp^{\mu\nu}$ in the Compton tensor. Therefore, it can be traced by contributions $\propto g^{\mu\nu}$ (in momentum space). Starting from the position space expression in Eq. (3.12), such terms can only originate from structures $\propto g^{\mu\nu}$ and $\propto x^\mu x^\nu$ which involve the functions $A_N(u)$ and $B_N(u)$, which have the same u-dependence. The extra factor $\bar u^{-N-\frac{1}{2}\gamma_N}$, therefore, results in both cases in the following modification

$$B(j_N, j_N) = \int du\,(u\bar u)^{j_N-1} \mapsto \int du (u\bar u)^{j_N-1}\bar u^{-N-\frac{1}{2}\gamma_N} = B(j_N, \tfrac{d}{2}-1)\,. \tag{3.28}$$

Since this modification affects the contribution of $A_N(u)$ and $B_N(u)$ structures in the same way, we actually do not need to consider them separately. Thus the OPE for the vector non-singlet amplitude in conformal QCD in d_* dimensions can be written as

$$\begin{aligned}\mathcal{V} &= \sum_{N,\mathrm{even}} f_N(\xi)\left(\frac{2P\cdot q}{Q^2}\right)^N c_1\left(N, \frac{Q^2}{\mu^2}, a_s, \epsilon_*\right)\frac{\Gamma(\frac{d_*}{2}-1)\Gamma(2j_N)}{\Gamma(j_N)\Gamma(j_N+\frac{d_*}{2}-1)}\\ &= \sum_{N,\mathrm{even}} f_N(\xi)\left(\frac{1}{2\xi}\right)^N c_1\left(N, \frac{Q^2}{\mu^2}, a_s, \epsilon_*\right)\frac{\Gamma(\frac{d_*}{2}-1)\Gamma(2j_N)}{\Gamma(j_N)\Gamma(j_N+\frac{d_*}{2}-1)}.\end{aligned} \tag{3.29}$$

Note that it is completely determined by the forward-scattering coefficients $c_1(N)$ (in d_* dimensions). For $d = 4$ the above expression agrees with [77, Eq. (22)].

3.3.3 Coefficient function in momentum fraction space

In Eq. (2.46) we have defined the vector quark GPD as a matrix element of the non-local light-ray operator $\mathcal{O}_q = \mathrm{tr}(\gamma^+\mathcal{O}_q)$. As before, we omit the q index and flavor-singlet contributions. Furthermore, we consider all operators as renormalized. In order to relate the CF to the OPE coefficients, one needs an expansion of the type

$$\mathcal{O}(z_1, z_2) = \sum_{N,k} \Psi_{N,k}(z_1, z_2)\, (\partial^+)^k \mathcal{O}_N(0)\,, \tag{3.30}$$

where $\mathcal{O}_N = n_{\mu_1} \dots n_{\mu_N} \mathcal{O}_N^{\mu_1 \cdots \mu_N}$ are renormalized conformal operators that satisfy the renormalization group equation (RGE)

$$\Big(\mu \frac{d}{d\mu} + \gamma_N(a_s)\Big)\mathcal{O}_N = 0\,. \tag{3.31}$$

We will tacitly assume that conformal operators are normalized as in Eq. (3.19). The light-ray operator $\mathcal{O}(z_1, z_2)$, in turn, satisfies an RGE of the form

$$\mu \frac{d}{d\mu}\mathcal{O}(z_1, z_2) = -(\mathcal{K}(a_s) * \mathcal{O})(z_1, z_2)\,, \tag{3.32}$$

where $\mathcal{K}$ is the vector non-singlet evolution kernel in position space, introduced in Sec. 2.9. Conformal symmetry ensures that $\mathcal{K}$ commutes with the three generators $S_{\pm,0}$ of $\mathrm{SL}(2,\mathbb{R})$ subgroup of the conformal group. Translation-invariant polynomials $z_{12}^N = (z_1 - z_2)^N$ are eigenfunctions of the evolution kernel and corresponding eigenvalues define the anomalous dimensions

$$\mathcal{K}(a_s) * z_{12}^{N-1} = \gamma_N(a_s) z_{12}^{N-1}. \tag{3.33}$$

The expansion coefficients $\Psi_{N,k}$ in Eq. (3.30) are homogeneous polynomials in z_1, z_2 of degree $N+k-1$ and are given by a repeated application of the generator of special conformal transformation S_+ to the coefficient of the conformal operator, $\Psi_{N,k}(z_1, z_2) \propto S_+^k * z_{12}^N$. The problem is that S_+ in the interacting theory in the $\overline{\mathrm{MS}}$-scheme contains a rather complicated conformal anomaly term $z_{12}\mathbf{\Delta}_+$ [106], so that finding an explicit expression for $S_+^k z_{12}^N$ is difficult.

The way out is to do a rotation to the "conformal scheme" at the intermediate step using a similarity transformation defined in Ref. [83]

$$\mathbf{O}(z_1, z_2) = \mathrm{U} * \mathcal{O}_q(z_1, z_2)\,, \qquad \mathcal{K} = \mathrm{U}^{-1} * \mathbf{K} * \mathrm{U}\,, \qquad S_{\pm,0} = \mathrm{U}^{-1} * \mathbf{S}_{\pm,0} * \mathrm{U}\,. \tag{3.34}$$

Note that $\mathcal{K}$ and $\mathbf{K}$ obviously have the same eigenvalues (anomalous dimensions). Going over to the "boldface" operators can be thought of as a change of the renormalization scheme. The GPD in conformal scheme, $\mathbf{F}$, is related to the GPD F in the $\overline{\mathrm{MS}}$ scheme by the U-"rotation"[1]

$$\mathbf{F}(x, \xi) = (\mathrm{U} * F)(x, \xi) = \int_{-1}^{1} \frac{dx'}{\xi} \mathrm{U}(x, x', \xi) F(x', \xi)\,, \tag{3.35}$$

[1]Note that the kernel $\mathrm{U}(x, x', \xi)$ in Eqs. (3.35), (3.36) has to be taken in the momentum fraction representation. The corresponding expressions can be derived from the results in [83], given in light-ray position space, but in fact are not needed as we will find a possibility to avoid this step.

and, similarly, for the CF

$$C(x/\xi,\mu^2/Q^2) = (\mathbf{C}*\mathrm{U})(x/\xi,\mu^2/Q^2) = \int_{-1}^{1}\frac{dx'}{\xi}\mathbf{C}(x'/\xi,\mu^2/Q^2)\mathrm{U}(x',x,\xi)\,. \tag{3.36}$$

The "rotated" light-ray operator $\mathbf{O}(z_1,z_2)$ at $d=4$ satisfies the RGE

$$\mu\frac{d}{d\mu}\mathbf{O} = -\mathbf{K}*\mathbf{O}\,. \tag{3.37}$$

Looking for the operator U in the form

$$\mathrm{U} = e^X\,, \qquad X(a_s) = a_s X^{(1)} + a_s^2 X^{(2)} + \dots\,, \tag{3.38}$$

we require that the "boldface" generators do not include conformal anomaly terms,

$$\begin{aligned}\mathbf{S}_- &= S_-^{(0)}\,,\\ \mathbf{S}_0 &= S_0^{(0)} - \epsilon_* + \frac{1}{2}\mathbf{K}\,,\\ \mathbf{S}_+ &= S_+^{(0)} + (z_1+z_2)\left(-\epsilon_* + \frac{1}{2}\mathbf{K}\right),\end{aligned} \tag{3.39}$$

where

$$S_-^{(0)} = -\partial_{z_1} - \partial_{z_2}\,, \qquad S_0^{(0)} = z_1\partial_{z_1} + z_2\partial_{z_2} + 2\,, \qquad S_+^{(0)} = z_1^2\partial_{z_1} + z_2^2\partial_{z_2} + 2(z_1+z_2)\,, \tag{3.40}$$

are the canonical (free, i.e. $a_s=0$) generators. Explicit expressions for $X^{(1)}$ and $X^{(2)}$ are given in [83].

With this choice, the generators $\mathbf{S}_\alpha$ on the subspace of the eigenfunctions of the operator $\mathbf{K}$ with a given anomalous dimension γ_N take the canonical form with shifted conformal spin

$$S_+ = S_+^{(0)} + (z_1+z_2)\left(-\epsilon_* + \frac{1}{2}\gamma_N\right) \tag{3.41}$$

and the eigenfunctions of the rotated kernel, $\mathbf{K}*\mathbf{\Psi}_{N,k} = \gamma_N\mathbf{\Psi}_{N,k}$, can be constructed explicitly [107]:

$$\mathbf{\Psi}_{N,k} = \mathrm{U}*\,\Psi_{N,k} \propto (S_+)^k * z_{12}^{N-1} = z_{12}^{N-1}\frac{\Gamma(2j_N+k)}{\Gamma(j_N)^2}\int_0^1 du\,(u\bar u)^{j_N-1}\,(z_{21}^u)^k. \tag{3.42}$$

For the forward matrix element of the light-ray operator one obtains, in our normalization,

$$\langle p|\mathcal{O}(z_1,z_2)|p\rangle = \sum_N \frac{i^{N-1}}{(N-1)!}z_{12}^{N-1}\,\langle p|\mathcal{O}_N|p\rangle, \tag{3.43}$$

and for the rotated light-ray operator

$$\langle p|\mathbf{O}(z_1,z_2)|p\rangle = \sum_N \frac{i^{N-1}}{(N-1)!}z_{12}^{N-1}\,\sigma_N\,\langle p|\mathcal{O}_N|p\rangle\,, \tag{3.44}$$

where σ_N are the eigenvalues of U:

$$\mathrm{U} * z_{12}^{N-1} = \sigma_N z_{12}^{N-1}\,, \qquad \sigma_N = \sigma_N(a_s)\,. \tag{3.45}$$

The generalization of this expansion to include off-forward matrix elements is completely fixed by conformal algebra and effectively amounts to the operator relation

$$\mathbf{O}(z_1,z_2) = \sum_{N,k} \frac{i^{N-1}}{(N-1)!}\sigma_N\, a_{N,k}\Big[(S_+)^k * z_{12}^{N-1}\Big](\partial^+)^k\mathcal{O}_N(0)\,, \tag{3.46}$$

where

$$a_{N,k} = \frac{\Gamma(2j_N)}{k!\Gamma(2j_N+k)}\,. \tag{3.47}$$

This expression can be derived applying ∂^+ to Eq. (3.44). On the one hand, taking a derivative amounts to a shift $k\to k-1$. On the other hand, it corresponds to an application of $-S_-$ and using the commutation relation $S_-S_+^k z_{12}^{N-1} = -k(2j_N+k-1)S_+^{k-1}z_{12}^{N-1}$, one gets a recurrence relation $a_{N,k-1} = k(2j_N+k-1)a_{N,k}$. The overall normalization (function of N) is fixed by the condition $a_{N,0}=1$.

Taking a matrix element of Eq. (3.46) between states with fixed momenta and using that $\langle p'|(\partial^+)^k\mathcal{O}(0)|p\rangle = (i\Delta^+)^k\langle p'|\mathcal{O}(0)|p\rangle$, one obtains

$$\langle p'|\mathbf{O}(z_1,z_2)|p\rangle = \sum_N \frac{i^{N-1}}{(N-1)!}\sigma_N\,\langle p'|\mathcal{O}_N(0)|p\rangle\sum_{k=0}^{\infty} a_{N,k}(i\Delta^+)^k S_+^k(\gamma_N) * z_{12}^{N-1}\,. \tag{3.48}$$

The sum over k can be evaluated with the help of Eq. (B.10) in Ref. [108] (for the special case $n=2$):

$$\sum_{k=0}^{\infty}(i\Delta^+)^{N-1+k}\,a_{N,k}S_+^k(\gamma_N) * z_{12}^{N-1} = \frac{1}{2}\omega_N\,(-1)^{N-1}\int_{-1}^{1}dx\,e^{-i\xi P^+(z_1+z_2-xz_{12})}\,P_{N-1}^{(\lambda_N)}(x)\,, \tag{3.49}$$

where

$$P_{N-1}^{(\lambda_N)}(x) = \left(\frac{1-x^2}{4}\right)^{\lambda_N-\frac{1}{2}}\mathrm{C}_{N-1}^{(\lambda_N)}(x)\,, \qquad\qquad \lambda_N = \frac{3}{2}-\epsilon_* + \frac{1}{2}\gamma_N(a_s)\,, \tag{3.50}$$

$\mathrm{C}_N^{(\lambda)}$ are Gegenbauer polynomials, and

$$\omega_N = \frac{(N-1)!\,\Gamma(2j_N)\Gamma(2\lambda_N)}{\Gamma(\lambda_N+\frac{1}{2})\Gamma(j_N)\Gamma(N-1+2\lambda_N)}\,. \tag{3.51}$$

Using this representation and the parametrization of the matrix element in Eq. (3.26), we obtain

$$\langle p'|\mathbf{O}(z_1,z_2)|p\rangle = P^+\sum_N \frac{\sigma_N f_N(\xi)}{(N-1)!}\left(\frac{1}{2\xi}\right)^{N-1}\frac{\omega_N}{2}\int_{-1}^{1}dx\,e^{-i\xi P_+(z_1+z_2-xz_{12})}\,P_{N-1}^{(\lambda_N)}(x)\,. \tag{3.52}$$

This expression should be matched to the definition of the GPD in the rotated scheme

$$\langle p'|\mathbf{O}(z_1,z_2)|p\rangle = 2P^+\int_{-1}^{1} dx\, e^{-iP_+[z_1(\xi-x)+z_2(x+\xi)]}\mathbf{F}(x,\xi,t)\,. \tag{3.53}$$

Changing variables $x \to x/\xi$, one can bring the exponential factor in Eq. (3.52) to the same form as in Eq. (3.53) and try to interchange the order of summation and integration to obtain the answer for the GPD as a series in contributions of local conformal operators. Attempting this one would find, however, that $\mathbf{F}(x,\xi,t)$ vanishes outside the ERBL region $|x| \le \xi$ that is certainly wrong. This problem is well known and is caused by non-uniform convergence of a sum representation for GPDs in the DGLAP region $\xi < |x|$. It can be avoided, however, because the CF in DVCS only depends on the ratio x/ξ so that for our purposes we can set $\xi = 1$ and eliminate the DGLAP region completely. In this way we obtain

$$\mathbf{F}(x,\xi=1) = \frac{1}{4}\sum_N \frac{\sigma_N\,\omega_N}{2^{N-1}(N-1)!}\, f_N(\xi=1) P_{N-1}^{(\lambda_N)}(x) \tag{3.54}$$

and the vector non-singlet amplitude is then given by

$$\begin{aligned}\mathcal{V}(\xi=1,Q^2) &= \int_{-1}^{1} dx\, C(x,Q^2)F(x,\xi=1) = \int_{-1}^{1} dx\, \mathbf{C}(x,Q^2)\mathbf{F}(x,\xi=1)\\ &= \frac{1}{4}\sum_N \frac{\sigma_N\,\omega_N}{2^{N-1}(N-1)!}\, f_N(\xi=1)\int_{-1}^{1} dx\, \mathbf{C}(x,Q^2)P_{N-1}^{(\lambda_N)}(x)\,.\end{aligned} \tag{3.55}$$

On the other hand, from the conformal OPE, Eq. (3.29), we have

$$\mathcal{V}(\xi=1,Q^2) = \sum_N f_N(\xi=1)\left(\frac{1}{2}\right)^N c_1\left(N,\frac{Q^2}{\mu^2},a_s,\epsilon_*\right)\frac{\Gamma(\frac{d}{2}-1)\Gamma(2j_N)}{\Gamma(j_N)\Gamma(j_N+\frac{d}{2}-1)}. \tag{3.56}$$

Comparing the coefficients in front of $f_N(\xi=1)$ for these two expressions we obtain

$$\int_{-1}^{1} dx\, \mathbf{C}(x,Q^2,a_s)P_{N-1}^{(\lambda_N)}(x) = c_1\left(N,\frac{Q^2}{\mu^2},a_s,\epsilon_*\right)\frac{2\Gamma(\frac{d_*}{2}-1)\Gamma(\lambda_N+\frac{1}{2})\Gamma(N-1+2\lambda_N)}{\sigma_N\,\Gamma(2\lambda_N)\Gamma(j_N+\frac{d_*}{2}-1)}\,. \tag{3.57}$$

It remains to solve this equation to obtain an explicit expression for the CF in momentum fraction space and, in the last step, to go over from the "rotated" to the $\overline{\rm MS}$ scheme. In the remaining part of this section we outline the general procedure for this calculation.

To leading order (tree level) everything is simple. To this accuracy $\gamma_N = 0$, $\lambda_N = 3/2$, $j_N = N+1$ and $c_1^{(0)}(N) = 1$ for even N and zero otherwise. Eq. (3.57) reduces to

$$\int_{-1}^{1} dx\, \mathbf{C}^{(0)}(x)\left(\frac{1-x^2}{4}\right)C_{N-1}^{(3/2)}(x) = 1 \tag{3.58}$$

for all even integers N. This has the unique analytical solution

$$C^{(0)}(x) = \mathbf{C}^{(0)}(x) = \frac{1}{1-x} - \frac{1}{1+x}\,, \tag{3.59}$$

as expected. A remaining technicality is that beyond the leading order λ_N depends on N in a nontrivial way and the functions $P_{N-1}^{(\lambda_N)}(x)$ are not orthogonal for different N with some simple weight function. Note, however, that they are eigenfunctions of the (exact) "rotated" evolution kernel

$$(\mathbf{K} * P_{N-1}^{(\lambda_N)})(x) = \int_{-1}^{1} dx'\, \mathbf{K}(x,x')\, P_{N-1}^{(\lambda_N)}(x') = \gamma_N P_{N-1}^{(\lambda_N)}(x) \tag{3.60}$$

and they are also eigenfunctions of the "rotated" $SL(2)$ Casimir operator.

This property suggests the following ansatz for the CF:

$$\mathbf{C}(x) = (C^{(0)} * Y)(x) = \int_{-1}^{1} dx'\, C^{(0)}(x') Y(x',x)\,, \tag{3.61}$$

where Y is an SL(2)-invariant operator, i.e. $[Y, \mathbf{S}_{\pm,0}] = 0$. Since the polynomials $P_{N-1}^{(\lambda_N)}(x)$ are eigenfunctions of the quadratic Casimir operator, they are also eigenfunctions of any SL(2)-invariant operator, in particular

$$(Y * P_{N-1}^{(\lambda_N)})(x) = \int_{-1}^{1} dx'\, Y(x,x')\, P_{N-1}^{(\lambda_N)}(x') = Y(N)\, P_{N-1}^{(\lambda_N)}(x)\,. \tag{3.62}$$

Using the above ansatz one obtains

$$\begin{aligned} \mathbf{C} * P_{N-1}^{(\lambda_N)} &= \int_{-1}^{1} dx\, \mathbf{C}(x)\, P_{N-1}^{(\lambda_N)}(x) \\ &= \int_{-1}^{1} dx \int_{-1}^{1} dx'\, C^{(0)}(x') Y(x',x)\, P_{N-1}^{(\lambda_N)}(x) \\ &= Y(N) \int_{-1}^{1} dx\, C^{(0)}(x) P_{N-1}^{(\lambda_N)}(x) = 2Y(N) B(\lambda_N + \tfrac{1}{2}, \lambda_N - \tfrac{1}{2})\,. \end{aligned} \tag{3.63}$$

Comparing this expression with Eq. (3.57) gives

$$Y(N) = c_1\left(N, \frac{Q^2}{\mu^2}, a_s, \epsilon_*\right) \sigma_N^{-1} \frac{\Gamma(\frac{d_*}{2} - 1)\Gamma(j_N + \lambda_N - \frac{1}{2})}{\Gamma(\lambda_N - \frac{1}{2})\Gamma(j_N + \frac{d_*}{2} - 1)}\,, \tag{3.64}$$

i.e. the spectrum of Y is given directly in terms of moments of the DIS CF and the spectrum of the rotation operator U.

An $\mathrm{SL}(2,\mathbb{R})$-invariant operator, i.e., an operator that commutes with the generators $\mathbf{S}_{\pm,0}$ in Eq. (3.39), is fixed uniquely by its spectrum. Therefore Eq. (3.64) uniquely defines the operator Y and, by virtue of Eqs. (3.61), (3.36), also the CF $\mathbf{C}(x)$. In the next two subsections we describe this calculation for the one-loop and the two-loop CFs, respectively.

3.3.4 One-loop

In this section we set $\mu = Q$, as logarithmic terms L^j in the CF can easily be restored from the evolution equation. To one-loop accuracy one needs to expand Eq. (3.64) to order $O(a_s)$, taking into account that $\epsilon_* = -\beta_0 a_s + \ldots$. Since the tree-level CF does not depend on the space-time

dimension, the ϵ-dependence in $c_1\left(N, \frac{Q^2}{\mu^2}, a_s, \epsilon_*\right)$ starts at order $O(a_s)$ and can be neglected here. Thus we only need the one-loop result for $c_1(N)$ in $d = 4$ dimensions, which can be taken from [105]:

$$\begin{aligned} c_1(N) &= 1 + a_s c_1^{(1)}(N) + \dots \\ c_1^{(1)}(N) &= C_F\Big[9(S_1 - 1) + 2(N_+ + N_-)(S_{11} - S_2 + 2S_1) - 7(N_- + 1)S_1 - 4(N_+ - 1)S_1\Big], \end{aligned} \tag{3.65}$$

where $S_{k_1 \dots k_n} = S_{k_1 \dots k_n}(N)$ are harmonic sums and $N_\pm$ are shift operators that change the argument of harmonic sums by unity: $N_\pm\, S_{k_1 \dots k_n}(N) = S_{k_1 \dots k_n}(N \pm 1)$. We also need the one-loop flavor-nonsinglet anomalous dimension

$$\gamma_N^{(1)} = 4C_F\Big[2S_1(N) - \frac{1}{N(N+1)} - \frac{3}{2}\Big] \tag{3.66}$$

and the (one-loop) eigenvalues $\sigma_N = 1 + a_s \sigma_N^{(1)} + \dots$ of the rotation matrix Eq. (3.38) $\mathrm{U} = 1 + a_s X^{(1)} + \dots$. This is the only new element that requires a calculation. From Ref. [83]

$$(\mathcal{X}^{(1)} * f)(z_1, z_2) = 2C_F \int_0^1 d\alpha\, \frac{\log \alpha}{\alpha} [2f(z_1, z_2) - f(z_{12}^\alpha, z_2) - f(z_1, z_{21}^\alpha)], \tag{3.67}$$

where $\mathcal{X}$ denotes the light-ray position space representation of X. In order to calculate σ_N we take $f(z_1, z_2) = z_{12}^{N-1}$ and get

$$\mathcal{X}^{(1)} * z_{12}^{N-1} = 4C_F \int_0^1 d\alpha \frac{\log \alpha}{\alpha} (1 - \bar{\alpha}^{N-1}) z_{12}^{N-1} = \sigma_N^{(1)}\, z_{12}^{N-1}, \tag{3.68}$$

where

$$\sigma_N^{(1)} = -2C_F\Big[S_1^2(N-1) + S_2(N-1)\Big]. \tag{3.69}$$

Collecting everything, we obtain

$$\begin{aligned} Y(N) &= 1 + a_s Y^{(1)}(N) + \dots, \\ Y^{(1)}(N) &= c_1^{(1)}(N) - \sigma_N^{(1)} + \frac{1}{2}\gamma_N^{(1)}\, S_1(N+1) \\ &= 8C_F\left\{S_1^2(N) - \frac{S_1(N)}{N(N+1)} + \frac{5}{8}\frac{1}{N(N+1)} + \frac{1}{4}\frac{1}{N^2(N+1)^2} - \frac{9}{8}\right\} \\ &= 2C_F\left\{\left(\bar{\gamma}_N^{(1)} + \frac{3}{2}\right)^2 + \frac{5}{2}\frac{1}{N(N+1)} - \frac{9}{2}\right\}, \end{aligned} \tag{3.70}$$

where $\bar{\gamma}_N^{(1)}$ in the last line is the one-loop anomalous dimension Eq. (3.66) stripped of the color factor, $\gamma_N^{(1)} = 4C_F \bar{\gamma}_N^{(1)}$. Note that the asymptotic expansion of the anomalous dimension $\bar{\gamma}_N^{(1)}$ and therefore also $Y^{(1)}(N)$ at large j_N is symmetric under the substitution $j_N \to 1 - j_N$, alias $N \to -N - 1$ (reciprocity relation). We will find that this relation holds to two-loops as well, in agreement with the general argumentation [109–111].

As already mentioned, a $\mathrm{SL}(2, \mathbb{R})$-invariant operator is completely determined by its spectrum. This is easy to do in the case under consideration, because an invariant operator with eigenvalues

$\bar{\gamma}_N^{(1)}$ is the one-loop evolution kernel, and $\frac{1}{N(N+1)}$ is nothing else but the inverse Casimir operator. The corresponding explicit expressions in position space are well known:

$$\begin{aligned}\bar{\mathcal{K}}^{(1)} * z_{12}^{N-1} &= \Big[\widehat{\mathcal{K}} - \mathcal{K}_+ - \frac{3}{2}\Big] * z_{12}^{N-1} = \bar{\gamma}_N^{(1)} z_{12}^{N-1}\,,\\ \mathcal{K}_+ * z_{12}^{N-1} &= \frac{1}{N(N+1)} z_{12}^{N-1},\end{aligned} \tag{3.71}$$

where

$$\begin{aligned}(\mathcal{K}_+ * f)(z_1,z_2) &= \int_{\Delta_2} d(\alpha,\beta)\, f(z_{12}^\alpha, z_{21}^\beta)\,,\\ (\widehat{\mathcal{K}} * f)(z_1,z_2) &= \int_0^1 \frac{d\alpha}{\alpha}\Big[2f(z_1,z_2) - \bar{\alpha}\big(f(z_{12}^\alpha,z_2) + f(z_1,z_{21}^\alpha)\big)\Big].\end{aligned} \tag{3.72}$$

These kernels commute with the canonical generators $S_{\pm,0}^{(0)}$.

Let $\mathcal{Y}$ denote the light-ray position space representation of Y. We obtain

$$\mathcal{Y}^{(1)} = 2C_F\bigg[\Big(\bar{\mathcal{K}}^{(1)} + \frac{3}{2}\Big)^2 + \frac{5}{2}\mathcal{K}_+ - \frac{9}{2}\bigg]. \tag{3.73}$$

The same expression holds in momentum fraction space.

For the one-loop example considered here, the transformation from position to momentum fraction space is not difficult to do and the results are available from Ref. [112]:

$$K_+(\omega',\omega) = \theta(\omega-\omega')\frac{\omega'}{\omega} + \theta(\omega'-\omega)\frac{1-\omega'}{1-\omega}, \tag{3.74}$$

$$\widehat{K}(\omega',\omega) = -\theta(\omega-\omega')\frac{\omega'}{\omega}\left[\frac{1}{\omega-\omega'}\right]_+ + \theta(\omega'-\omega)\frac{1-\omega'}{1-\omega}\left[\frac{1}{\omega-\omega'}\right]_+ - \delta(\omega-\omega')\Big(\log\omega + \log\bar{\omega}\Big),$$

where ω, ω' are rescaled momentum fractions, $\omega = (1-x)/2$, and the plus distribution is defined as

$$\left[\frac{1}{\omega-\omega'}\right]_+ f(\omega) = \frac{f(\omega)-f(\omega')}{\omega-\omega'}.$$

It remains to calculate the convolution of $Y^{(1)}(x,x')$ with the leading-order CF Eq. (3.61) and "rotate" the result to the $\overline{\text{MS}}$ scheme:

$$C^{(1)}(x) = \mathbf{C}^{(1)}(x) + (C^{(0)} * X^{(1)})(x). \tag{3.75}$$

The one-loop rotation kernel in momentum fraction space $X^{(1)}(x,x')$ can also be found explicitly,

$$\begin{aligned}(X^{(1)} * f)(\omega') = \int_0^1 d\omega\, X^{(1)}(\omega',\omega) f(\omega) \;&=\; 2C_F\bigg[\int_{\omega'}^1 \frac{d\omega}{\omega}\log\Big(1-\frac{\omega'}{\omega}\Big)\frac{\omega' f(\omega') - \omega f(\omega)}{\omega-\omega'}\\ &+ \int_0^{\omega'}\frac{d\omega}{\bar{\omega}}\log\Big(1-\frac{\bar{\omega}'}{\bar{\omega}}\Big)\frac{\bar{\omega}' f(\omega') - \bar{\omega} f(\omega)}{\bar{\omega}-\bar{\omega}'} - \frac{1}{2}(\log^2\omega' + \log^2\bar{\omega}')f(\omega')\bigg].\end{aligned} \tag{3.76}$$

Here, as above, $\omega = \frac{1}{2}(1-x)$, $\omega' = \frac{1}{2}(1-x')$ are rescaled momentum fractions. Collecting all terms, one reproduces after some algebra the well-known expression for the one-loop quark CF in Eq. (2.86).

Beyond one-loop, the last part of this strategy – restoration of momentum fraction kernels from the known position space results and taking the remaining convolution integrals – becomes impractical because of very complicated expressions. It can be avoided, however, using the formulas derived in the following.

Let $\widetilde{f}(x)$ be a function of the momentum fraction x so that its light-ray position space analogue is

$$f(z_1, z_2) = \int_{-1}^{1} dx\, e^{-iz_1(1-x)-iz_2(1+x)}\, \widetilde{f}(x)\,. \tag{3.77}$$

The convolution of $\widetilde{f}(x)$ with the leading order CF $C^{(0)}(x)$ can be rewritten as a position space integral

$$C^{(0)} * f = \int_{-1}^{1} dx\, C^{(0)}(x)\, \widetilde{f}(x) = \int_{0}^{\infty} dz \Big[f(-iz, 0) - f(0, -iz) \Big]. \tag{3.78}$$

As usual, the operator $\mathcal{Y}$ can be written in the following form

$$(\mathcal{Y} * f)(z_1, z_2) = \int_{\Delta_2} d(\alpha, \beta)\, \mathcal{Y}(\alpha, \beta) f(z_{12}^{\alpha}, z_{21}^{\beta})\,. \tag{3.79}$$

Then

$$C^{(0)} * Y * \widetilde{f} = \int_{-1}^{1} dx\, \widetilde{f}(x) \int_{\Delta_2} d(\alpha, \beta) \left(\frac{\mathcal{Y}(\alpha, \beta)}{\bar{\alpha}(1-x) + \beta(1+x)} - (x \leftrightarrow -x) \right). \tag{3.80}$$

Since this has to hold for arbitrary function $\widetilde{f}$ we conclude that

$$(C^{(0)} * Y)(x) = \int_{\Delta_2} d(\alpha, \beta) \left(\frac{\mathcal{Y}(\alpha, \beta)}{\bar{\alpha}(1-x) + \beta(1+x)} - (x \leftrightarrow -x) \right). \tag{3.81}$$

If Y is given by a product of operators of the type in Eq. (3.79), then the r.h.s. of Eq. (3.81) can be written as a manyfold integral of the same type, e.g., for $Y_1 * Y_2$ one gets

$$\begin{aligned} &(C^{(0)} * Y_1 * Y_2)(x) \\ &\quad = \int_{\Delta_2} d(\alpha, \beta) \int_{\Delta_2} d(\alpha', \beta') \left(\frac{\mathcal{Y}_1(\alpha', \beta') \mathcal{Y}_2(\alpha, \beta)}{(\bar{\alpha}\bar{\alpha}' + \alpha\beta')(1-x) + (\beta\bar{\alpha}' + \bar{\beta}\beta')(1+x)} - (x \leftrightarrow -x) \right). \end{aligned} \tag{3.82}$$

Integrals of this kind can be evaluated with the help of `HyperInt` [75] in terms of harmonic polylogarithms, which are discussed in Sec. 3.4. In this way a very time consuming transformation of beyond-one-loop kernels to the momentum fraction representation can be avoided.

For instance, instead of using the momentum fraction expression for $X^{(1)}$ in Eq. (3.76), its convolution with $C^{(0)}(x)$ can be calculated using eq. (3.81) directly from the position space

representation in Eq. (3.67). This leads to simple integrals

$$\begin{aligned}(C^{(0)} * X^{(1)})(x) &= C_F \int_0^1 d\alpha \frac{\log\alpha}{\alpha}\left(\frac{1}{\omega} - \frac{1}{\bar\alpha\omega} + \frac{1}{\omega} - \frac{1}{\omega+\bar\omega\alpha}\right) - (\omega\to\bar\omega)\\ &= C_F \frac{1}{\omega}\int_0^1 d\alpha\left(-\frac{\log\alpha}{\bar\alpha} + \frac{\bar\omega}{\omega}\frac{\log\alpha}{1+\alpha\bar\omega/\omega}\right) - (\omega\to\bar\omega)\\ &= \frac{1}{\omega}\Big(\mathrm{Li}_2(1) + \mathrm{Li}_2(-\bar\omega/\omega)\Big) - (\omega\to\bar\omega),\end{aligned} \tag{3.83}$$

where $\omega = (1-x)/2$. Beyond one loop, this simplification proves to be crucial.

3.3.5 Two-loop

The spectrum of the invariant operator $Y(N)$ to two-loop accuracy is obtained by expanding Eq. (3.64) to second order in a_s. Since $\epsilon_* = O(a_s)$, one needs the two-loop CF in DIS in $d = 4$ and moreover, terms of $O(\epsilon)$ in the one-loop DIS CF as ingredients. The corresponding expressions are available from [105]. In addition we need to calculate the spectrum of eigenvalues $\sigma_N = 1 + a_s\sigma_N^{(1)} + a_s^2\sigma_N^{(2)} + \ldots$ of the rotation operator in Eq. (3.38) to the two-loop accuracy. Explicit expressions for the corresponding kernels X are collected in Appendix B in Ref. [83][2]. The necessary integrals can be done analytically in terms of harmonic sums up to fourth order using computer algebra packages [113–115]. The resulting expressions are rather cumbersome and we do not present them here. Final expressions for the CFs turn out to be considerably shorter thanks to many cancellations.

The next step is to restore the invariant operator Y from its spectrum. This is not as simple as at one-loop because the invariant kernel has to commute with the deformed $\mathrm{SL}(2,\mathbb{R})$ generators in Eq. (3.39) (including $O(a_s)$ terms) rather than the canonical generators Eq. (3.40). In other words, we are now looking for the integral operator (with the given spectrum) with eigenfunctions $P_{N-1}^{(\lambda_N)}(x)$ where $\lambda_N = \frac{3}{2} + a_s(\beta_0 + \frac{1}{2}\gamma_N^{(1)}) + \ldots$ rather than $\lambda_N = 3/2$. All expressions can of course be truncated at order a_s^2 so that for the second-order contributions to the spectrum, $Y(N) = \ldots + a_s^2 Y^{(2)}(N)$, it is sufficient to require canonical conformal invariance. However, we need to modify the first-order operator $Y^{(1)} \to \widehat{Y}^{(1)} = Y^{(1)} + \delta Y^{(1)}$ in such a way that $\widehat{Y}^{(1)}$ has eigenfunctions $P_{N-1}^{(\lambda_N)}(x)$, i.e. it commutes with deformed generators $\mathbf{S}_\alpha$ in Eq. (3.39) (up to terms $O(a_s^2)$). This can be achieved by replacing

$$\mathcal{Y}^{(1)} = 2C_F\left[\left(\bar{\mathcal{K}}^{(1)} + \frac{3}{2}\right)^2 + \frac{5}{2}\mathcal{K}_+ - \frac{9}{2}\right] \quad\to\quad \widehat{\mathcal{Y}}^{(1)} = 2C_F\left(\left(\widetilde{\mathcal{K}} + \frac{3}{2}\right)^2 + \frac{5}{2}\widetilde{\mathcal{K}}_+ - \frac{9}{2}\right), \tag{3.84}$$

where $\widetilde{\mathcal{K}} = \bar{\mathcal{K}}^{(1)} + O(a_s)$ is the complete two-loop evolution kernel (up to normalization and some terms discussed below) and $\widetilde{\mathcal{K}}_+ = \mathcal{K}_+ + \mathcal{O}(a_s)$ is the inverse to the deformed Casimir operator, $\widetilde{\mathcal{K}}_+ \sim [\mathbf{J} * (\mathbf{J}-1)]^{-1}$ (to the required one-loop accuracy). The spectrum of eigenvalues of $\widehat{Y}^{(1)}$ will of course differ from the spectrum of $Y^{(1)}$, $\widehat{Y}^{(1)}(N) = Y^{(1)}(N) + O(a_s)$ and this difference will have to be compensated by the corresponding change in $Y^{(2)} \to \widehat{Y}^{(2)}$, which is, however, straightforward.

[2] In [83, Eq. (B.9)] there is a typo, the second term in the first equation, $\sim \mathbb{T}^{(1)}$, has to be omitted.

The non-singlet two-loop evolution kernel in light-ray position space can be written as [83],

$$\mathcal{K}^{(2)} = \mathcal{K}^{(2,\text{inv})} + \mathbb{T}^{(1)} * \Big(\beta_0 + \frac{1}{2}\mathcal{K}^{(1)}\Big), \tag{3.85}$$

where $\mathbb{T}^{(1)}$ is an integral operator defined in [83, Eq. (C.2)], and $\mathcal{K}^{(2,\text{inv})}$ is a certain canonically SL(2)-invariant operator, i.e. $[\mathcal{K}^{(2,\text{inv})}, S^{(0)}_{\pm,0}]$ =0. It is easy to see that

$$\Big[\mathcal{K}(a_s), \mathcal{K}^{(1)} + a_s\mathbb{T}^{(1)} * \Big(\beta_0 + \frac{1}{2}\mathcal{K}^{(1)}\Big)\Big] = O(a_s^2) \tag{3.86}$$

so that they have the same eigenfunctions up to $O(a_s^2)$. In other words, by dropping the canonically invariant part $\mathcal{K}^{(2,\text{inv})}$ of the two-loop evolution kernel, the eigenfunctions remain the same up to terms of $O(a_s^2)$ that are not relevant to our accuracy. Thus we can replace the full evolution kernel in the expression for $\widehat{Y}^{(1)}$ in Eq. (3.84) by its (canonically) non-invariant part

$$\widetilde{\mathcal{K}} = \bar{\mathcal{K}}^{(1)} + a_s\bar{\mathbb{T}}^{(1)} * \left(\beta_0 + \frac{1}{2}\mathcal{K}^{(1)}\right), \qquad \widetilde{\mathcal{K}} * P^{(\lambda_N)}_{N-1} = \widetilde{\mathcal{K}}(N)\, P^{(\lambda_N)}_{N-1} + O(a_s^2), \tag{3.87}$$

where $\mathbb{T}^{(1)} = 4C_F\bar{\mathbb{T}}^{(1)}$ and

$$\widetilde{\mathcal{K}}(N) = \bar{\mathcal{K}}^{(1)}(N) + a_s\bar{\mathbb{T}}^{(1)}(N)\left(\beta_0 + \frac{1}{2}\mathcal{K}^{(1)}(N)\right) = \bar{\gamma}^{(1)}_N + a_s\left(\beta_0 + 2C_F\bar{\gamma}^{(1)}_N\right)\frac{d}{dN}\bar{\gamma}^{(1)}_N. \tag{3.88}$$

In addition we need to find the inverse of the Casimir operator

$$\begin{aligned}\mathbf{J} * (\mathbf{J}-1) &= \mathbf{S}_+ * \mathbf{S}_- + \mathbf{S}_0 * (\mathbf{S}_0 - 1)\\ &= J_0 * (J_0 - 1) + \big(\partial_1 z_{12} + \partial_2 z_{21} + 1\big) * \Big(-\epsilon_* + \frac{1}{2}\mathcal{K}\Big) + \Big(-\epsilon_* + \frac{1}{2}\mathcal{K}\Big)^2,\end{aligned} \tag{3.89}$$

where

$$J_0 * (J_0 - 1) = S^{(0)}_+ * S^{(0)}_- + S^{(0)}_0 * (S^{(0)}_0 - 1) = \partial_1 z_{12} * (\partial_2 z_{21} + 1) = \partial_2 z_{21} * (\partial_1 z_{12} + 1)\,. \tag{3.90}$$

One can show that to the required accuracy

$$[\mathbf{J} * (\mathbf{J}-1)]^{-1} = \Big[1 - a_s\Big(R_1 + R_2 + \mathcal{K}_+\Big) * \Big(\beta_0 + \frac{1}{2}\mathcal{K}^{(1)}\Big) + \mathcal{O}(a_s^2)\Big] * \mathcal{K}_+\,, \tag{3.91}$$

where $\mathcal{K}_+$ is defined in eq. (3.72) and

$$\begin{aligned}(R_1 * f)(z_1, z_2) &= ((\partial_1 z_{12} + 1)^{-1} * f)(z_1, z_2) = \int_0^1 d\alpha\, \bar{\alpha} f(z^\alpha_{12}, z_2),\\ (R_2 * f)(z_1, z_2) &= ((\partial_2 z_{21} + 1)^{-1} * f)(z_1, z_2) = \int_0^1 d\alpha\, \bar{\alpha} f(z_1, z^\alpha_{21}).\end{aligned} \tag{3.92}$$

The term $\propto \mathcal{K}_+^2$ is a canonically invariant operator and can be dropped for the same reasons as $\mathcal{K}^{(2,\text{inv})}$ in the evolution kernel. Thus we can choose

$$\begin{aligned}\widetilde{\mathcal{K}}_+ &= \mathcal{K}_+ - a_s\Big(R_1 + R_2\Big) * \left(\beta_0 + \frac{1}{2}\mathcal{K}^{(1)}\right) * \mathcal{K}_+\,,\\ \mathcal{K}_+ * P^{(\lambda_N)}_{N-1} &= \widetilde{\mathcal{K}}_+(N)\, P^{(\lambda_N)}_{N-1} + O(a_s^2)\,,\end{aligned} \tag{3.93}$$

where

$$\widetilde{\mathcal{K}}_+(N) = \frac{1}{N(N+1)} a_s \left[1 - \frac{2}{N+1}\Big(\beta_0 + 2C_F \bar{\gamma}_N^{(1)}\Big)\right]. \tag{3.94}$$

The terms of $O(a_s)$ in (3.88) and (3.94) modify the spectrum of eigenvalues of $\widehat{Y}^{(1)}$ as compared to $Y^{(1)}$ and have to be subtracted from $Y^{(2)}(N)$. The two-loop kernel has three color structures

$$\widehat{Y}^{(2)}(N) = \beta_0 C_F \widehat{Y}_\beta^{(2)}(N) + C_F^2 \widehat{Y}_P^{(2)}(N) + \frac{C_F}{N_c} \widehat{Y}_A^{(2)}(N). \tag{3.95}$$

and only the $\propto C_F^2$ term is affected by this subtraction. We obtain

$$\begin{aligned}
\widehat{Y}_\beta^{(2)}(N) &= 2\zeta_2 \bar{\gamma}_N^{(1)} + \frac{10}{3}\left(\bar{\gamma}_N^{(1)} + \frac{3}{2}\right)^2 - \left(\frac{2}{9} + 7\zeta_2 + \frac{8}{N(N+1)} + \frac{2}{N^2(N+1)^2}\right)\left(\bar{\gamma}_N^{(1)} + \frac{3}{2}\right) \\
&\quad + 2\zeta_3 - \frac{29}{6}\zeta_2 + \frac{45}{8} - \frac{2}{N^2(N+1)^2} + \frac{31}{6}\frac{1}{N(N+1)}, \\
\widehat{Y}_P^{(2)}(N) &= \frac{1}{2}(Y^{(1)}(N))^2 + 4\zeta_2(\bar{\gamma}_N^{(1)})^2 + 4\zeta_3\left(11 + \frac{12}{N(N+1)}\right) - 64\zeta_3 S_1 + \frac{2}{9}\pi^4 - \frac{28}{3}\pi^2 S_1^2 \\
&\quad + 2\pi^2\left(3 + \frac{14}{3N(N+1)}\right) S_1 - 2\pi^2\left(\frac{4}{9} + \frac{2}{N(N+1)} + \frac{1}{N^2(N+1)^2}\right) \\
&\quad + \frac{6}{N(N+1)} S_{-2} + \left(\frac{64}{3} - \frac{14}{N(N+1)} - \frac{8}{N^2(N+1)^2}\right) S_1^2 \\
&\quad + \left(\frac{86}{9} - \frac{64}{3N(N+1)} + \frac{2}{N^2(N+1)^2} + \frac{8}{N^3(N+1)^3}\right) S_1 \\
&\quad + \left(\frac{11}{8} - \frac{137}{18N(N+1)} - \frac{25}{6N^2(N+1)^2} - \frac{2}{N^4(N+1)^4}\right),
\end{aligned}$$

$$\begin{aligned}
\widehat{Y}_A^{(2)}(N) &= 16 S_1\Big(2S_{1,-2} - S_{-3}\Big) - 12 S_{-2}^2 - 8 S_{-4} + 16 S_1 S_3 + 4\Big(2S_{1,3} - S_4\Big) - \frac{20 S_3}{N(N+1)} \\
&\quad + \frac{32\,(S_{-3} - 2S_{1,-2})}{N(N+1)} + \left(\frac{44}{N^2(N+1)^2} + \frac{24}{(N-2)(N+3)} + \frac{52}{N(N+1)} + 8\right) S_{-2} \\
&\quad + \frac{32}{3} S_1^2 + \left(-\frac{8}{N^3(N+1)^3} - \frac{8}{N^2(N+1)^2} - \frac{86}{3N(N+1)} + \frac{52}{9}\right) S_1 \\
&\quad + \frac{20}{3N^2(N+1)^2} - \frac{59}{9N(N+1)} + \frac{18}{(N-2)(N+3)} - \frac{35}{4} + \left(\frac{50}{N(N+1)} + 54\right)\zeta_3 \\
&\quad - \frac{\pi^4}{9} - 36\zeta_3 S_1 - \frac{2\pi^2 S_1}{N(N+1)} + \pi^2\left(\frac{4}{3N^2(N+1)^2} + \frac{2}{3N(N+1)} - \frac{10}{9}\right),
\end{aligned} \tag{3.96}$$

where $S_{\vec{m}} = S_{\vec{m}}(N)$. It can be checked that these expressions satisfy the reciprocity relation [109–111]: their asymptotic expansion at $N \to \infty$ is symmetric under the substitution $N \to -N-1$.

It remains to find an invariant operator $\widehat{Y}^{(2)}$ with the spectrum $\widehat{Y}^{(2)}(N)$. This is not very hard to do since we only need canonical SL(2)-invariance, i.e. the operators in question have to be diagonal in the basis of $P_{N-1}^{(3/2)}(x)$. The SL(2)-invariant kernels with eigenvalues given by the

required harmonic sums are collected in Appendix A of [103]. Note that in contrast to anomalous dimensions which grow logarithmically at large N to all orders in perturbation theory, $\gamma_N^{(k)} \sim \log N$, the spectrum $Y(N)$ contains higher powers on the logarithm, up to $\log^{2\ell} N \sim S_1^{2\ell}(N)$, where ℓ is the number of loops.

With the invariant operators at hand, the DVCS coefficient function in the rotated scheme is obtained by the convolution with the leading-order CF

$$\mathbf{C}(x) = \int_{-1}^{1} dx'\, C^{(0)}(x') \left[\delta(x-x') + a_s Y^{(1)}(x',x) + a_s^2 Y^{(2)}(x',x) + O(a_s^3)\right] \tag{3.97}$$

and the CF in the $\overline{\rm MS}$ scheme (so far still in conformal QCD at the critical point) recovered as

$$C(x) = \int_{-1}^{1} dx'\, \mathbf{C}(x') \left[\delta(x-x') + a_s X^{(1)}(x',x) + a_s^2 \Big(\frac{1}{2}(X^{(1)})^2 + X^{(2)}\Big)(x',x) + O(a_s^3)\Big)\right]. \tag{3.98}$$

In both cases one can use the formulas in Eqs. (3.81) and (3.82) to avoid Fourier transformation of the kernels to the momentum fraction space. All necessary integrals can be computed using `HyperInt` in terms of the harmonic polylogarithms.

3.4 Harmonic polylogarithms

For multiloop scattering amplitudes one needs to simplify huge expressions, which typically are written in terms of complicated integrals of Feynman parameters.

In many cases, including the present case of the DVCS CF, the integrals can be expressed in terms of classical polylogarithms defined by recursively in $n \in \mathbb{N}$ by

$$\mathrm{Li}_n(z) = \int_0^z \frac{dt}{t}\, \mathrm{Li}_{n-1}(t), \tag{3.99}$$

where the recursion begins with $\mathrm{Li}_1(z) = -\log(1-z)$. A more general class of functions, which covers a wider class of Feynman integrals is given by Goncharov polylogarithms (GPLs) [49], defined in terms of iterated integrals

$$\mathrm{G}(a_1,...,a_n;z) = \int_0^z \frac{dt}{t-a_1} \mathrm{G}(a_2,...,a_n;t), \tag{3.100}$$

where $a_j, z \in \mathbb{C}$ and the recursion begins with $\mathrm{G}(z) = 1$. The GPLs are related to the classical polylogarithms by

$$\mathrm{G}(\underbrace{0,...,0}_{n-1 \text{ times}}, a; z) = -\mathrm{Li}_n(z/a). \tag{3.101}$$

A subclass of GPLs are the so-called Harmonic polylogarithms (HPLs) [50].

$$\mathrm{H}_{a_1,...,a_n}(z) = \mathrm{G}(a_1,...,a_n;z) \tag{3.102}$$

for $a_j \in \{1, 0, -1\}$. The amplitude in Eq. (3.1) can be entirely expressed in terms of HPLs. It is customary to use the notation that for $\mathrm{H}_{a_1,...,a_n}$ with $a_n \neq 0$, we drop all indices that are 0, adding

1 to the absolute value of the next right non-zero index for each dropped 0. This notation is used in the results presented in App. B and C.

A great simplification that arises from being able to express amplitudes in terms of GPLs and HPLs is due to the shuffle algebra property [116]

$$\mathrm{G}(a_1,...,a_n;z)\mathrm{G}(a_{n_1+1},...,a_{n_1+n_2};z) = \sum_{\sigma\in\Sigma(n_1,n_2)} \mathrm{G}(a_{\sigma(1)},...,a_{\sigma(n_1+n_2)};z), \tag{3.103}$$

where

$$\Sigma(n_1,n_2) = \Big\{\sigma\in S_{n_1+n_2} \mid \sigma^{-1}(1) < ... < \sigma^{-1}(n_1) \\ \text{and } \sigma^{-1}(n_1+1) < ... < \sigma^{-1}(n_1+n_2)\Big\} \tag{3.104}$$

and S_n is the symmetric group of n elements.

It turns out that the ℓ loop contribution to the DVCS CF can be written in all generality as

$$C^{(\ell)}(z,L) = \frac{1}{z\bar{z}}\sum_{j=0}^{\ell} L^j \sum_{\vec{a}} f_{j,\vec{a}}(z)\mathrm{H}_{\vec{a}}(z), \tag{3.105}$$

where we sum over all $\vec{a} = (a_1,...,a_n) \in \{0,1\}^n$ with $n \leq 2\ell$ and the coefficients $f_{j,\vec{a}}$ are polynomials in z. This relatively simple behavior is mostly due to the fact that all Feynman integrals depend only on a single parameter, namely $z = \frac{1}{2}(1-x/\xi)$. In related processes, such as double deeply virtual Compton scattering or deeply virtual meson production one has a second scale in $q'^2 \neq 0$, which significantly complicates the calculation, in particular the evaluation of the MIs.

There are many publicly available codes that handle GPLs and HPLs. For the evaluation of the integrals involved in the IR subtractions in App. B we have used the `Maple` package `HyperInt` [75]. This program is also very well-suited for the integral in Eq. (3.81), necessary for the computation using conformal algebra and it was used in Ref. [88, 103]. For the numerical evaluation in Sec. 4 we have used the `Mathematica` package `HPL.m` [117].

4 Numerical estimates

4.1 DVCS phenomenology

A detailed review of DVCS phenomenology is beyond the scope of this thesis. In the following we give a very rough overview in order to put the results of this thesis into context.

The differential cross section for leptoproduction of a photon from a nucleon target is given by

$$d\sigma = \frac{\alpha_{\text{em}}^3 x_B}{16\pi^2 Q^4 \sqrt{1+\varepsilon^2}} \left| \frac{\mathcal{M}}{e^3} \right|^2 dx_B dQ^2 d|t| d\phi d\phi_S, \tag{4.1}$$

where $\varepsilon = 2x_B m/Q$ and the azimuthal angles ϕ, ϕ_S are defined in Fig. 4.1. The scattering amplitude $\mathcal{M}$ was defined in Eq. (2.4). It is determined by the elastic nucleon form factors and, at leading twist, by the CFFs $\mathcal{H}, \mathcal{E}, \widetilde{\mathcal{H}}, \widetilde{\mathcal{E}}, \mathcal{H}_T, \mathcal{E}_T, \widetilde{\mathcal{H}}_T, \widetilde{\mathcal{E}}_T$. Deriving the corresponding relations for the various observables is tedious, but straightforward.

The kinematic coverage of existing and planned measurements of DVCS is shown in Fig. 4.2 for various observables. The existing data from JLAB and HERA covers the region of moderately large $\xi \gtrsim 0.01$ and low $Q^2 \lesssim 10\,\text{GeV}^2$. This region is also covered by recent measurements at CERN and JLAB. On the other hand, the EIC will give the complementary information about the very low $\xi \lesssim 0.01$ with Q^2 from about $2\,\text{GeV}^2$ up to about $100\,\text{GeV}^2$. Note that the small ξ region is particularly interesting, since the IPDs are obtained from extrapolating the GPDs to $\xi = 0$.

Although recently there have been efforts to determine GPDs from lattice QCD [10] using the framework of large momentum effective theory [118, 119], the standard method to determine GPDs is to invent models or parametrizations and fit them to experimental data. Numerous ways have been suggested to model GPDs, see Ref. [120] for a comprehensive review. Later we will consider the classic model by Goloskokov and Kroll [51] explicitly. This will enable us to give an estimate of the impact of the α_s corrections to observables and hence to the final extraction of the GPD from experimental data.

As example for an observable, consider the following parametrization of the differential cross section on an unpolarized target [121]

$$d\sigma^{h_l, e_l}(\phi) = d\sigma_{\text{UU}}(\phi)[1 + h_l A_{\text{LU,DVCS}}(\phi) + e_l h_l A_{\text{LU,I}}(\phi) + e_l A_{\text{C}}(\phi)], \tag{4.2}$$

where $d\sigma_{\text{UU}}$ is the differential cross section for an unpolarized beam and target, e_l is the lepton charge in units of the positron charge and $h_l/2$ is the lepton helicity. The so-called beam spin asymmetry is defined as

$$A_{\text{LU}}^{e_l}(\phi) = \frac{d\sigma^{e_l,+}(\phi) - d\sigma^{e_l,-}(\phi)}{d\sigma^{e_l,+}(\phi) + d\sigma^{e_l,-}(\phi)} = \frac{e_l A_{\text{LU,I}}(\phi) + A_{\text{LU,DVCS}}(\phi)}{1 + e_l A_C(\phi)}. \tag{4.3}$$

It can be shown that the first sine harmonic of $A_{\text{LU}}^-(\phi)$ is approximately proportional to the imaginary part of $\mathcal{H}$ [120]

$$\frac{1}{\pi} \int_{-\pi}^{\pi} d\phi \, \sin\phi \, A_{LU}^-(\phi) \propto \text{Im}\, \mathcal{H}. \tag{4.4}$$

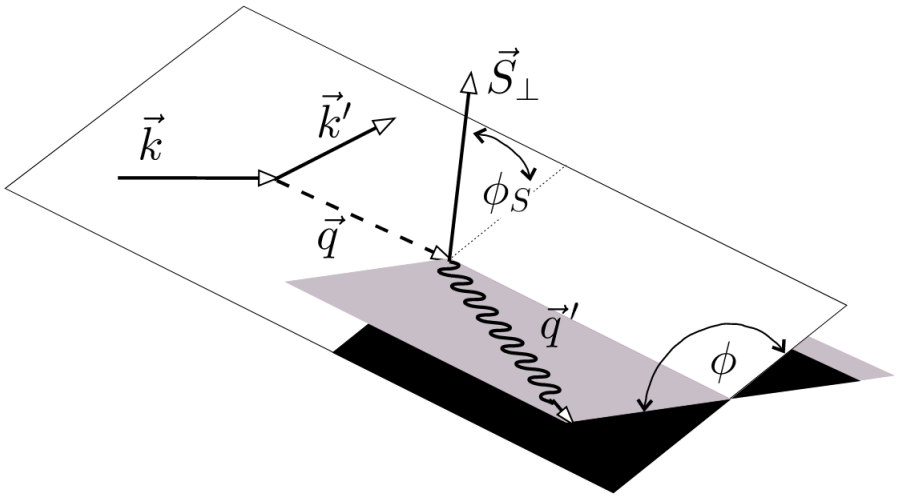

Figure 4.1: Momenta and azimuthal angles for leptoproduction of a photon from a nucleon target. ϕ is the angle between the lepton plane and the plane spanned by $\vec{q}$ and $\vec{q}'$. ϕ_S is the angle between the lepton plane and $\vec{S}_\perp$, the component of the target polarization vector that is orthogonal to $\vec{q}$. Figure taken from [31].

The statistical accuracy of the data is usually around the few percent level. As we will observe later, see Fig. 4.5, the ratio $\mathrm{Im}\,\mathcal{H}^{\mathrm{NLO}}/\mathrm{Im}\,\mathcal{H}^{\mathrm{LO}}$ is about 0.7, i.e. a correction of about 30%, around $\xi = 0.1$ and $Q^2 = 4\,\mathrm{GeV}^2$. Furthermore $\mathrm{Im}\,\mathcal{H}^{\mathrm{NNLO}}/\mathrm{Im}\,\mathcal{H}^{\mathrm{NLO}}$ is about 0.9, implying roughly a 10% correction from including the NNLO result. We will discuss these statements in more detail in Sec. 4.4. Suffice it to say that the NNLO corrections are generally well above the few percent level and hence well above the experimental accuracy. So far, no phenomenological analysis exists that even considers the NLO.

4.2 The Goloskokov-Kroll model

We consider the Goloskokov-Kroll (GK) model [51] for H_q and H_g, defined in Eqs. (2.37), (2.48), (2.53) and (2.56), which is based on the double-distribution ansatz [122]

$$f_i(\beta,\alpha,t') = g_i(\beta,t')h_i(\beta)\frac{\Gamma(2n_i+2)}{2^{2n_i+1}\Gamma(n_i+1)^2}\frac{[(1-|\beta|)^2-\alpha^2]^{n_i}}{(1-|\beta|)^{2n_i+1}}., \tag{4.5}$$

where $i \in \{u_{\mathrm{val}}, d_{\mathrm{val}}, u_{\mathrm{sea}}, d_{\mathrm{sea}}, s_{\mathrm{sea}}, g\}$ and $n_{q_{\mathrm{val}}} = 1, n_g = n_{q_{\mathrm{sea}}} = 2$ and $t' = t + \frac{4m^2\xi^2}{1-\xi^2}$. The form of the t-dependence is inspired by Regge theory [51, 121]

$$g_i(\beta,t) = e^{b_i t}|\beta|^{-\alpha_i' t}\,, \tag{4.6}$$

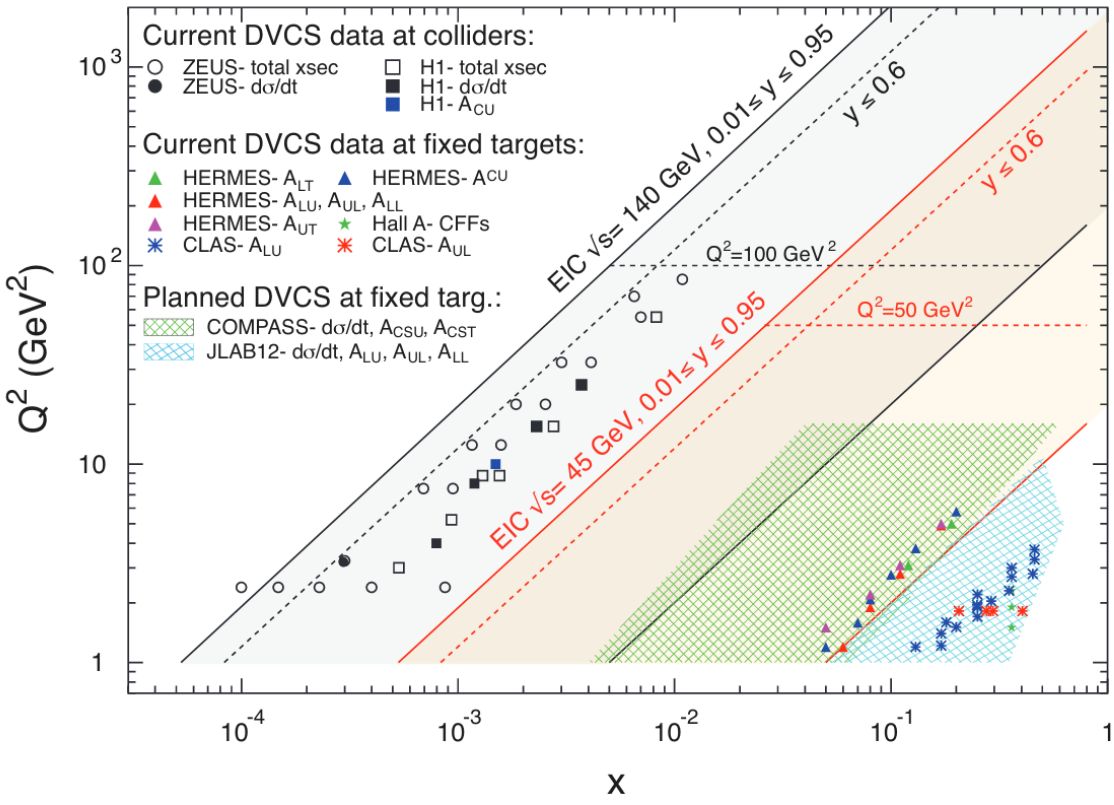

Figure 4.2: An overview of existing and planned measurements of DVCS in the x, Q^2 plane. Taken from [1]

with $\alpha_i' = 0.9,\ b_i = 0$ for valence quarks and $\alpha_i' = 0.15$,

$$b_i = 2.58 + \frac{1}{4}\log\frac{m^2}{\mu^2 + m^2} \tag{4.7}$$

for sea quarks and gluons. The functions $H_i(\beta)$ are related to the corresponding PDFs through the normalization condition

$$H_q(x,0,0) = q(x)\,, \qquad H_g(x,0,0) = xg(x)\,, \tag{4.8}$$

where $q(x)$ and $g(x)$ are proton PDFs. Eq. (4.8) implies that

$$\begin{aligned} h_g(\beta) &= |\beta| g(|\beta|)\,, \\ h_{\rm sea}(\beta) &= q_{\rm sea}(|\beta|)\text{sign}(\beta)\,, \\ h_{\rm val}(\beta) &= q_{\rm val}(\beta)\theta(\beta)\,, \end{aligned} \tag{4.9}$$

where $q_{\rm val}(x) = q(x) - q(-x)$ and $q_{\rm sea}(x) = q(-x)$. Correspondingly we define

$$H_{q_{\rm val}}(x,\xi,t) = H_q(x,\xi,t) - H_q(-x,\xi,t), \qquad H_{q_{\rm sea}}(x,\xi,t) = H_q(-x,\xi,t). \tag{4.10}$$

The GPD is obtained from f_i by the relation

$$H_i(x,\xi,t) = \int_{\Diamond_2} d(\alpha,\beta)\ f_i(\beta,\alpha,t)\delta(x-\beta-\xi\alpha) + D_i(x/\xi,t)\Theta(\xi^2 - x^2), \tag{4.11}$$

where $\Diamond_2 = \{|\alpha| + |\beta| \le 1\}$. The so-called D-term [123] contributes only to the real part of $\mathcal{H}$. It is very poorly known, so we neglect it in the following discussion.

Using the parametrization

$$h_i(\beta) = \beta^{-\delta_i}\bar{\beta}^{2n_i+1}\sum_{j=0}^{3} c_{ij}\beta^{j/2} \tag{4.12}$$

for the PDFs, we can perform the integration over the section of $\Diamond_2$ in Eq. (4.11). The GK model can be written as

$$H_i(x,\xi,t) = \chi(x \ge \xi)H_i^{(DGLAP)}(x,\xi,t) + \chi(0 \le x < \xi)H_i^{(ERBL)}(x,\xi,t) \tag{4.13}$$

for $i \in \{u_{\rm sea}, d_{\rm sea}, s_{\rm sea}, g\}$ and $1 \ge x \ge 0$, where $\chi(P) = 1$ if the proposition P is true and 0 if it is false. For $x < 0$ the sea quark and gluon models are defined by

$$H_g(x,\xi,t) = H_g(-x,\xi,t), \qquad H_{q_{\rm sea}}(x,\xi,t) = -H_{q_{\rm sea}}(-x,\xi,t). \tag{4.14}$$

For $i = q_{\rm val}$ we have

$$H_i(x,\xi,t) = \chi(x \ge \xi)H_i^{(DGLAP)}(x,\xi,t) + \chi(-\xi \le x < \xi)H_i^{(ERBL)}(x,\xi,t) \tag{4.15}$$

and $H_i(x,\xi,t) = 0$ for $x < -\xi$. Explicit expressions for $H_i^{(DGLAP)}, H_i^{(ERBL)}$ are readily derived and are given in Ref. [51].

The PDF parameters δ_i, c_{ij} in Eq. (4.12) should be fixed by fitting it to an up-to-date PDF extraction. We use HERAPDF20 [124] and ABMP16 [125, 126] LO/NLO/NNLO PDFs for the calculation of the CFF $\mathcal{H}$ including LO/NLO/NNLO CFs, respectively. We have used two PDF sets to get a rough idea of the model dependence.

In Fig. 4.3 we have plotted the GPDs using fits to HERAPDF20 NNLO PDFs.

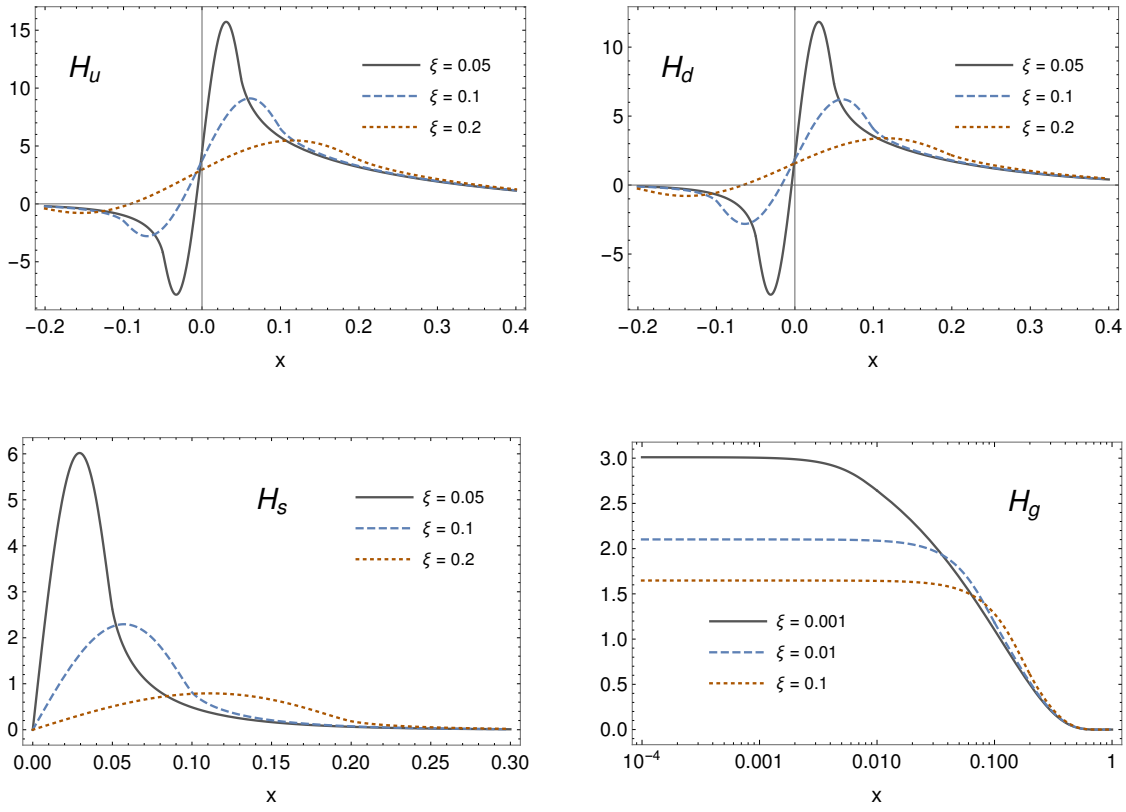

Figure 4.3: Plots of the GK model with PDF parameters fitted to the HERAPDF20 NNLO set [124].

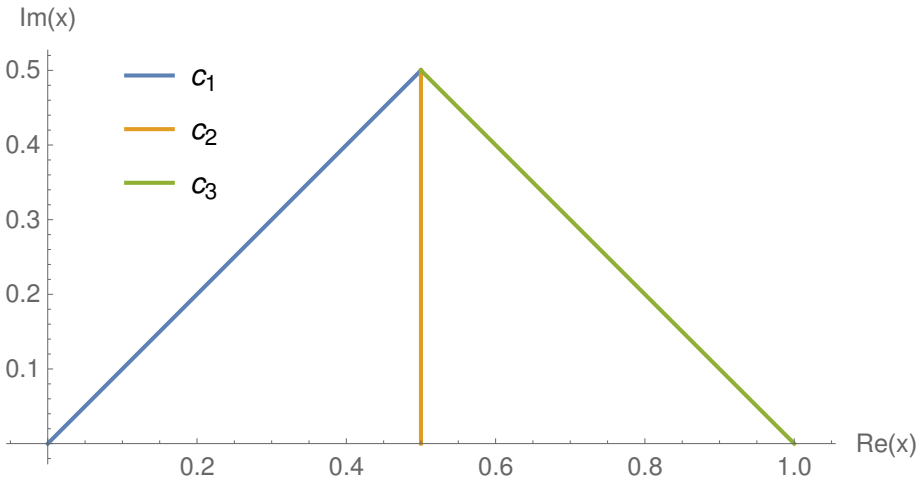

Figure 4.4: Sample contour for the evaluation of the integral in Eq. (4.20) for $\xi = 0.5$.

4.3 Evaluation of the convolution integral

The factorization integral for the CFF $\mathcal{H}$ becomes

$$\mathcal{H} = \sum_q \int_{-\xi}^{1} \frac{dx}{\xi} C_q(x/\xi) H_{q_{\text{val}}}(x,\xi,t) + 2\sum_q \int_0^1 \frac{dx}{\xi} C_q(x/\xi) H_{q_{\text{sea}}}(x,\xi,t) + 2\int_0^1 \frac{dx}{\xi^2} C_g(x/\xi) H_g(x,\xi,t). \tag{4.16}$$

To evaluate this integral, as explained in Sec. 2.3, we define for $i \in \{u_{\text{sea}}, d_{\text{sea}}, s_{\text{sea}}, g\}$

$$\begin{aligned} H_i^{\{0<x<1\}}(x,\xi,t) &= H_i^{(ERBL)}(x,\xi,t), \\ H_i^{\{\xi<x<1\}}(x,\xi,t) &= H_i^{(DGLAP)}(x,\xi,t) - H_i^{(ERBL)}(x,\xi,t), \end{aligned} \tag{4.17}$$

extended to negative x by Eq. (4.14). For $i = q_{\text{val}}$ we define

$$\begin{aligned} H_i^{\{-\xi<x<1\}}(x,\xi,t) &= H_i^{(ERBL)}(x,\xi,t), \\ H_i^{\{\xi<x<1\}}(x,\xi,t) &= H_i^{(DGLAP)}(x,\xi,t) - H_i^{(ERBL)}(x,\xi,t). \end{aligned} \tag{4.18}$$

The functions H_{ij}^R can now be analytically continued from $R \subseteq [-1,1]$ into the upper half complex plane for $\operatorname{Re} x > 0$ and into the lower half plane for $\operatorname{Re} x < 0$. In particular, the pole of the CF at $x = \xi$ can be avoided for the $H_i^{\{0<x<1\}}, H_i^{\{-\xi<x<1\}}$ terms. On the other hand

$$H_i^{\{\xi<x<1\}}(x,\xi,t) \xrightarrow{x\to\xi} \text{const.}\ (x-\xi)^{p_i(\xi,t)} \tag{4.19}$$

for some $p_i(\xi,t) > 1$, implying that the integrand in (4.16) goes to zero like $(x-\xi)^{p_i(\xi,t)-1}$.

As an example we consider a possible integration contour for the gluon contribution as shown in Fig. 4.4. The integral reads

$$\frac{1}{2}\mathcal{H}_g = \int_{c_1} \frac{dx}{\xi^2} C_g(x/\xi) H_g^{\{0<x<1\}}(x,\xi,t) + \int_{c_2} \frac{dx}{\xi^2} C_g(x/\xi) H_g^{\{\xi<x<1\}}(x,\xi,t) + \int_{c_3} \frac{dx}{\xi^2} C_g(x/\xi) H_g^{(DGLAP)}(x,\xi,t), \tag{4.20}$$

where we have recombined the integrals on the contour c_3 for better numerical stability. This is necessary, since $H_i^{(ERBL)}$ becomes very large for $\mathrm{Re}\, x > \xi$ and it is better to combine the large cancelling contributions from $H_i^{\{0<x<1\}}$ and $H_i^{\{\xi<x<1\}}$ on the level of the integrand.

4.4 Size of radiative corrections to $\mathcal{H}$

The numerical integration in Eq. (4.16) can be readily performed. We have used `Mathematica` to produce the results shown in Fig. 4.5 and 4.6.

Firstly, we can observe from those plots that the NLO corrections is substantial, in particular in the phenomenologically relevant small ξ region. While this is already the case for the quark contribution, with a negative correction of about 30%, it is exacerbated by the inclusion of the gluon correction, which has opposite sign to the quark contribution. This applies to both real and imaginary parts, with a particular large negative NLO correction, up to about 60%, to the imaginary part.

Going over to NNLO, we observe that the NNLO/NLO correction is quite small, indicating a decent convergence of the perturbative series. The NNLO/NLO correction to $\mathcal{H}_g$ is the leading correction and it can be found to be up to 30%, as expected. For $\mathrm{Re}\,\mathcal{H}_g$ the NNLO/NLO correction is smaller that for imaginary part, even getting positive for $\xi \lesssim 10^{-3}$. As a consequence the NNLO/NLO correction to $\mathrm{Re}\,\mathcal{H}_g$ is quite small. The imaginary part $\mathrm{Im}\,\mathcal{H}$ however receives a substantial NNLO/NLO correction, up to about 50% around $\xi \approx 0.01$. This large ratio is however not a good indicator of the actual size of the correction, since $\mathcal{H}$ gets close to zero. This is particularly apparent for the real part, which even changes sign at $\xi \approx 0.2$ and $\xi \approx 0.01$.

We conclude that at Q of the order of a few GeV, due to the large NLO/LO correction, predictions for observables using only the LO CF are poor. Hence DVCS should be investigated at least at NLO. If one wants to achieve below 10% precision one should also include NNLO corrections, due to its substantial correction to $\mathrm{Im}\,\mathcal{H}$.

In Fig. 4.6 we have also shown the Q^2 dependence of $\mathcal{H}$ using only the fixed order L logarithms in the CF. A more detailed study should involve the solution of the evolution equation as outlined in Sec. 2.9, which resums such logarithms to all orders. However, in order to get an idea of the Q^2 dependence it is sufficient to consider only the fixed order scale evolution. The situation is improved by going to larger hard scales Q in two ways. Firstly, obviously the coupling constant decreases at larger Q, hence reducing the overall size of radiative corrections. Secondly, the L dependent terms in the CF are positive and are therefore give a positive correction to $\mathcal{H}$. More precisely, while the quark contribution varies relative little with Q^2, the gluon contributions varies substantially. At NNLO and NLO it even becomes positive at some value of Q^2 between $10\,\mathrm{GeV}^2$ and $50\,\mathrm{GeV}^2$.

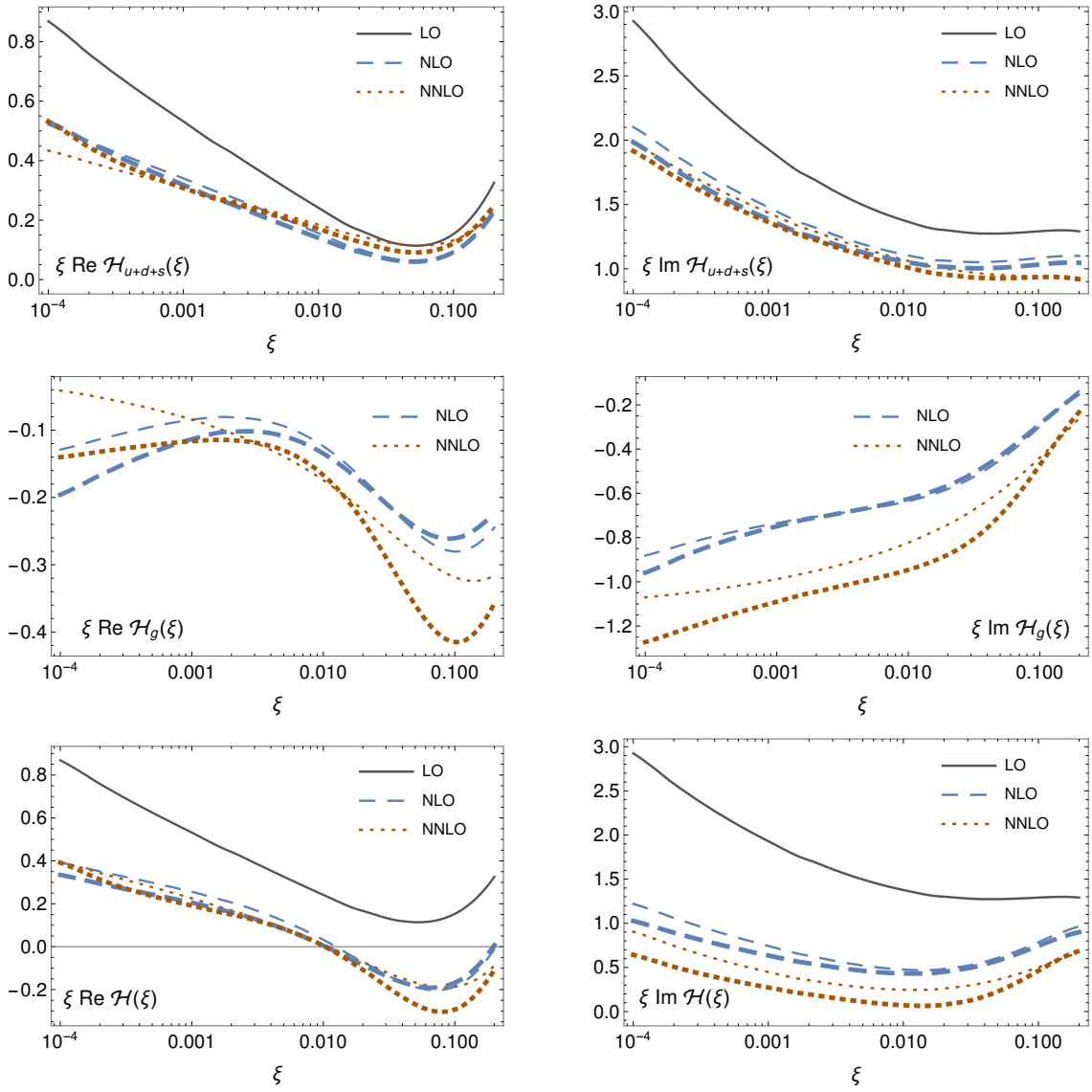

Figure 4.5: Real and imaginary parts of the CFF $\mathcal{H}$ as a function of ξ at $\mu^2 = Q^2 = 4$ GeV^2 and $t = -0.1$ GeV^2 for the GPDs normalized to HERAPDF20 (thin lines) and ABMP16 (thick lines, NLO and NNLO only) PDF sets at the appropriate order in perturbation theory: Solid lines: LO (black), short dashes: NLO (blue), long dashes: NNLO (orange). Upper row: Quark contribution, Middle row: Gluon contribution, Bottom row: Total contribution.

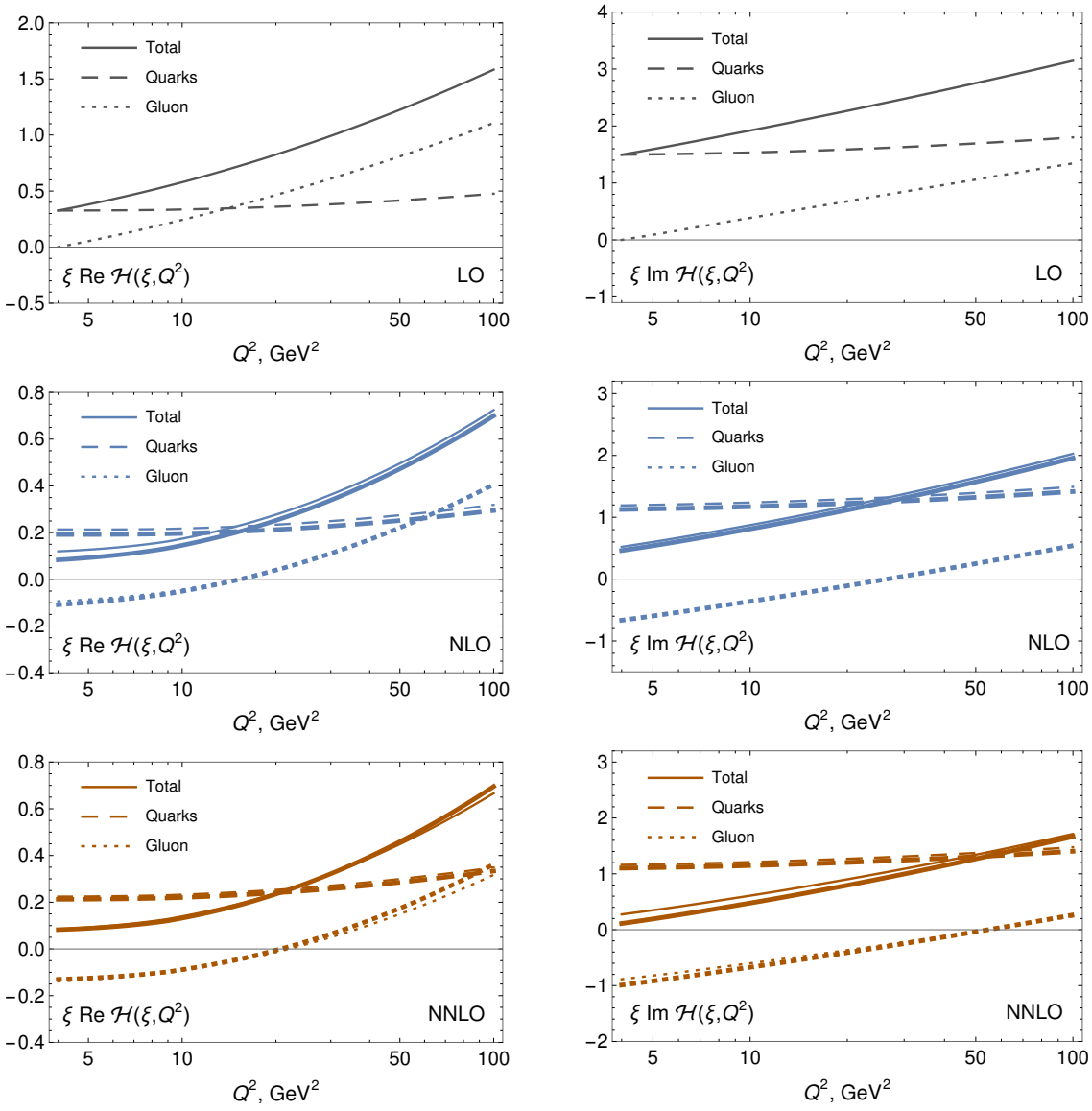

Figure 4.6: The Q^2 dependence from the fixed order L logarithms of the CFF $\mathcal{H}$ for $\xi = 0.005$ and $t = -0.1$ GeV^2 for the GPDs at the input scale $\mu_0^2 = 4$ GeV^2 normalized to HERAPDF20 (thin lines) and ABMP16 (thick lines) PDF sets at the appropriate order in perturbation theory. The quark and gluon contributions are shown by dashed and dotted curves, respectively. Their sum is shown by the solid lines.

5 Threshold resummation

5.1 Quark CF in the $x \to \pm\xi$ limit

The expression in Eq. (3.105) and the asymptotic behavior of $\mathrm{H}_{a_1,\ldots,a_n}(z)$ as $z \to 0$ suggests the following behavior of the CF as $z \to 0$

$$C_q^{(\ell)}(z) = \frac{1}{2z} \sum_{i=0}^{\ell} \sum_{j=0}^{2\ell-i} \hat{c}_{ij} L^i \log^j z + \hat{O}(z^0), \tag{5.1}$$

where $\hat{c}_{ij}$ are constant coefficients and $\hat{O}(z^0)$ means of the order of $z^0 \log^j z$ for some power $j \in \mathbb{N}$. By the $\hat{s} \leftrightarrow \hat{u}$ crossing symmetry the exact same formula holds for the leading term at $\bar{z} \to 0$. This is the behavior of the CF near the $\hat{s} = 0$ and $\hat{u} = 0$ thresholds in Fig. 2.3. Let us denote by

$$\hat{C}_q(-\hat{s}, Q^2, \mu^2) = \sum_{\ell=0}^{\infty} a_s^{\ell}(\mu) \sum_{i=0}^{\ell} \sum_{j=0}^{2\ell-i} \hat{c}_{ij} L^i \log^j \left(\frac{-\hat{s}}{Q^2}\right) \tag{5.2}$$

twice the coefficient of the z^{-1} of C_q. In Ref. [103] it was found that

$$\hat{C}_q = 1 + a_s C_F \log^2 z + \frac{1}{2}(a_s C_F \log^2 z)^2 + \ldots, \tag{5.3}$$

where $\ldots$ denotes terms that do not have the highest power of the $\hat{s}$-threshold logarithms $\log z$ at each order in a_s, which suggests that these leading logarithms exponentiate. This disagreed with an earlier attempt [127] to resum the threshold logarithms, which predicted a different coefficient of the a_s^2 term.

I have proven in Ref. [52] that indeed the leading logarithms exponentiate and I have further found that subleading logarithms can be resummed, with the final result being Eq. (5.34). Remarkably the exact same statements apply to the axial-vector quark CF $\widetilde{C}_q$, since the change in the projection of Dirac indices does not influence the arguments and the finite subtractions discussed in Sec. 2.10 do not contribute to the leading z^{-1} power. In fact, from the results in Refs. [103] and [88] it can be seen that the leading z^{-1} power terms agree for the vector and axial-vector case to NNLO accuracy, which might be true to all orders.

The key observation is that $\hat{C}_q$ factorizes as

$$\hat{C}_q(-\hat{s}, Q^2, \mu^2) = h(Q^2, \mu^2, \nu^2) f(-\hat{s}, \nu^2), \tag{5.4}$$

where ν^2 is a new factorization scale separating the small scale $-\hat{s}$ from the large scale Q^2 and h and f are perturbatively calculable functions. For all purposes we can set $\nu = \mu = Q$, since the μ dependence C_q can be handled by the running of the GPD. Eq. (5.4) allows for the resummation of powers of $\log z = \log \frac{-\hat{s}}{Q^2}$ to all orders. Although the small z or $\bar{z}$ approximation is not valid through the deformed integration region in Eq. (2.25), we still resum terms in the CF to all orders.

To summarize, there are two types of infinite series of terms that can be resummed in the CF. On the one hand, we can resum all terms proportional to $a_s^i L^{i-j}$ from evolution equations in the

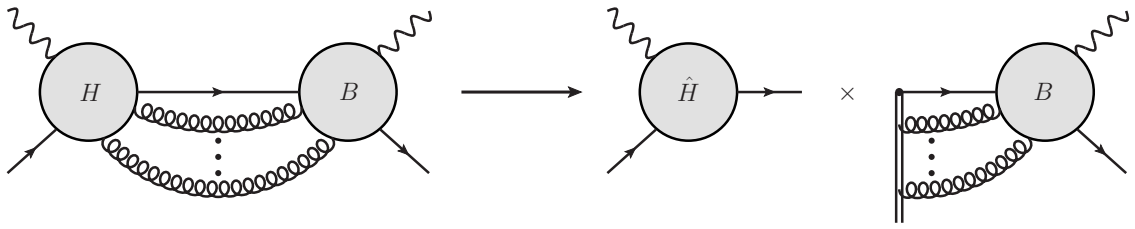

Figure 5.1: Graphical representation of the factorization theorem in Eq. (5.4). Left: Reduced graph for the leading region in the $z \to 0$ limit. Right: Graphical representation of the left-hand-side of Eq. (5.4). Shown is the product of the hard function h, defined in Eq. (5.15), on the left and the n-collinear function f, defined in Eq. (5.14), on the right. The double lines denotes the Wilson line W_n. Note that there are also diagrams with crossed gluons connecting to the Wilson line and a sum over hard subgraphs is implied.

factorization scale μ^2, which was discussed in Sec. 2.9. Thereby j corresponds to the order a_s^{j+1} that $\mathcal{K}$ is expanded in. On the other hand, we can resum terms proportional to $a_s^i \log^{2i-j} z$. In this chapter we will discuss this resummation for the quark CF in detail.

For the rest of this chapter, we omit the q index, always implying that the quark CF is meant.

5.2 Factorization of $\hat{C}$

In this Section we argue that in the $z \to 0$ limit the CF can be written in the factorized form of Eq. (5.4). We start by appealing to the well-known Libby-Sterman analysis [65], of which a review can be found in Ref. [128]. In the same way as in Sec. 2.2, we first must identify the leading regions and associated reduced graphs corresponding to pinch-singular-surfaces, which are determined by the Landau criterion [66–68]. In such reduced graphs one may have subgraphs with its lines being formally considered of the types hard, collinear to n or $\bar{n}$, or soft. The major statement on which our treatment relies is that the $\bar{n}$-collinear and soft regions do not contribute. As is shown later, they are eliminated by setting the external quark momenta on-shell (then the contribution from those regions gives scaleless integrals), as is necessary for calculating hard coefficient functions. In DVCS the separation of the hard scale Q^2 from the small scales $-t, m^2$ has been performed in the factorization formula (2.25). C_q itself corresponds to the hard subgraph from this perspective, but in the limit in region $z \to 0$, which is a region of the convolution integral in (2.25), we find a further hierarchy of scales, namely $-\hat{s} \ll Q^2$.

The argument that we do not have to consider any $\bar{n}$-collinear or soft subgraphs goes as follows. Firstly, any $\bar{n}$-collinear subgraph can depend only on the invariants $\hat{k}^2, \hat{k}'^2, \hat{k} \cdot \hat{k}'$, which are all zero. To demonstrate this, consider the following loop integral with loop momentum in the $\bar{n}$-collinear region

$$\int_{l \sim \hat{P}} \frac{d^d l}{(l^2)^{n_1}[(l+\hat{P})^2]^{n_2}[(l+\hat{q}')]^{n_3}} \sim \int \frac{d^d l}{(l^2)^{n_1}[(l+\hat{P})^2]^{n_1}(2l \cdot \hat{q}')^{n_3}} \propto \int_0^\infty \frac{d\alpha}{\alpha^{n_1+n_2+1-d/2}}. \quad (5.5)$$

The α integral gives zero in dimensional regularization. It is easy to see the same situation occurs for any $\bar{n}$-collinear loop momentum integration after all other integrations have been performed.

Note that we do not have to consider a numerator since it can be written as a sum of the same factors that appear in the denominator, so we get merely a sum of integrals of the same form. Thus any such non-tree-level subgraph gives a scaleless integral and hence vanishes in dimensional regularization. A possible soft subgraph might attach to the n-collinear subgraph B which must be at the outgoing photon vertex (soft lines connecting the hard subgraph give a power-suppression). However, by the same arguments as for example in DIS or DVCS [63] the soft subgraph is not present. Correspondingly, the soft region for a generic loop integral gives scaleless integrals by a similar argument as for the $\bar{n}$-collinear region.

We proceed by using the standard Libby-Sterman power-counting formulas [128] to determine the leading regions. In our case, where only a collinear and hard subgraph are present, the contribution from a given region R is proportional to $\left(\frac{Q^2}{-\hat{s}}\right)^{p(R)}$, where

$$p(R) = 4 - \#(\text{external lines}) - \#(\text{lines } B \text{ to } H) + \#(\text{scalar pol. gluon lines } B \text{ to } H). \tag{5.6}$$

This implies that the leading regions correspond to the reduced diagram shown on the left in Fig. 5.1, where the arbitrary number of collinear gluons connecting the H and B subgraph are scalar-polarized, i.e. the $g^{\mu\nu}$ in the gluon propagator is replaced by $n^\mu \bar{n}^\nu$.

Let us write the amplitude of the generic graph Γ on the left in Fig. 5.1 schematically as follows

$$\Gamma(H,B) = g_{\perp,\mu\nu} \int \prod_{j=1}^{N} d^d l_j \; \frac{1}{N_c} \mathrm{tr}\Big[\hat{\not{P}} B^{\nu\nu_1\ldots\nu_N}_{a_1\ldots a_N}(\hat{k}', l, l_1, ..., l_N) \frac{i(\not{l} + \sum_j \not{l}_j)}{(l + \sum_j l_j)^2 + i0} \times \Big(\prod_j g_{\mu_j\nu_j} \Big) H^{\mu\mu_1\ldots\mu_N}_{a_1\ldots a_N}(\hat{k}, l, l_1, ..., l_N) \Big], \tag{5.7}$$

where $l = \hat{k} + \hat{q}$ and we routed the N loop momenta l_j of the gluon lines as entering the hard subgraph and going back through the single fermion line connecting H to B. Conventional notation would absorb the intermediate fermion line into the B subgraph, but we choose to make it explicit here. To obtain the leading term we need to apply the region approximator $T_{R(H,B)}$, which, when applied to a given graph, corresponds to making the following replacements:

- In the H subgraph, replace $l_j \to \hat{l}_j = l_j^- n$ and $z \to 0$, i.e. $l \to \hat{q}',\ \hat{k} \to \hat{P}$,
- On the fermion line between the H and B subgraph we insert the projector $\frac{1}{2}\not{\bar{n}}\not{n}$,
- Replace $g_{\mu_j\nu_j} \to \frac{\hat{l}_{j,\mu_j}\bar{n}_{\nu_j}}{\hat{l}_j\cdot\bar{n}+i0}$.

Note that the expression for $\Gamma(H,B)$ in Eq. (5.7) has been written in such a way that it corresponds to a region $R(H,B)$ (of loop-momentum space) where the lines in the B subgraph are n-collinear and the lines in the H subgraph are hard. We obtain

$$T_{R(H,B)}\Gamma(H,B) = g_{\perp,\mu\nu} \int \prod_{j=1}^{N} d^d l_j \; \frac{1}{N_c} \mathrm{tr}\Big[\hat{\not{P}} B^{\nu\nu_1\ldots\nu_N}_{a_1\ldots a_N}(\hat{k}', l, l_1, ..., l_N) \frac{i(\not{l} + \sum_j \not{l}_j)}{(l + \sum_j l_j)^2 + i0} \times \frac{1}{2}\not{\bar{n}}\not{n} \Big(\prod_j \frac{\hat{l}_{j,\mu_j}\bar{n}_{\nu_j}}{\hat{l}_j\cdot\bar{n}+i0} \Big) H^{\mu\mu_1\ldots\mu_N}_{a_1\ldots a_N}(\hat{P}, \hat{q}', \hat{l}_1, ..., \hat{l}_N) \Big]. \tag{5.8}$$

The next step is to use graphical Ward identities by taking into account the sum of diagrams with all possible connections of the N gluons to H, in order to show that the collinear gluons decouple from H. This is relatively simple in the case of QED and somewhat more involved in the case of QCD. However, the arguments have become standard, so we do not repeat them here. Note that this step requires to sum over all hard subgraphs of the same order in a_s. This results in the expression

$$\sum_H T_{R(H,B)}\Gamma(H,B) = g_{\perp,\mu\nu}\int\prod_{j=1}^N d^dl_j\ \frac{1}{N_c}\mathrm{tr}\left\{\hat{\not{n}}B^{\nu\nu_1\ldots\nu_N}_{a_1\ldots a_N}(\hat{k}',l,l_1,...,l_N)\hat{\not{n}}\frac{iQ^2}{2\hat{s}}\right.$$
$$\left.\times\left[\sum_{\substack{\text{permutations}\\ \text{of }\{1,\ldots,N\}}}(-g)^N\frac{\bar{n}_{\nu_1}t_{a_1}\ldots\bar{n}_{\nu_N}t_{a_N}}{(l_1^-+i0)\ldots(\sum_{j=1}^N l_j^-+i0)}\right]\sum_{\hat{H}}\hat{H}^\mu(\hat{P},\hat{q}')\right\}, \quad (5.9)$$

where the t_a are color matrices. The remaining sum goes over all possible subgraphs $\hat{H}^\mu(\hat{P},\hat{q}')$, of the given order in a_s, without collinear gluon insertions. The expression in the square brackets can be identified to be a momentum-space Wilson line. In position space and in terms of gluon fields it reads

$$W_{\bar{n}}(x) = \mathrm{P}\exp\left[ig\int_{-\infty}^0 ds\ A^-(x+s\bar{n})\right]. \quad (5.10)$$

Note that $\hat{H}$ is a function of momenta which have zero transverse components. Thus

$$\hat{\not{n}}\hat{H}^\mu(\hat{P},\hat{q}')\hat{\not{n}} = c_{\hat{H}}(Q^2)\hat{\not{n}}\gamma_\perp^\mu\hat{\not{n}}, \quad (5.11)$$

where $c_{\hat{H}}$ is the contribution to the hard function h. Finally we arrive at the factorized form of Γ summed over all possible hard subgraphs. It reads

$$\sum_H T_{R(H,B)}\Gamma(H,B) = -\frac{Q^2}{2\hat{s}}\sum_{\hat{H}} c_{\hat{H}}(Q^2)c_B(-\hat{s}), \quad (5.12)$$

where

$$c_B(-\hat{s}) = -ig_{\perp,\mu\nu}\int\prod_{j=1}^N d^dl_j\ \frac{1}{N_c}\mathrm{tr}\left\{\hat{\not{n}}\gamma^\mu\hat{\not{n}}B^{\nu\nu_1\ldots\nu_N}_{a_1\ldots a_N}(p',k,l_1,...,l_N)[...]\right\} \quad (5.13)$$

is the contribution to the function, which is denoted by f in Eq. (5.4). The above discussion implies that the bare f can be written as a correlation function

$$f^{\mathrm{bare}}(-\hat{s}) = \frac{2\hat{s}}{Q^2}\frac{ig_\perp^{\mu\nu}}{4(d-2)}\int d^dx_1\ e^{i\hat{q}'x_1}\lim_{\hat{k}'\to -z\hat{P}}\int d^dx_2\ e^{i\hat{k}'x_2}$$
$$\times\frac{1}{N_c}\mathrm{tr}\left[\hat{\not{P}}\gamma_\mu(-i\hat{\not{k}}')\,\langle 0|\,T\{\psi(x_2)j_\nu(x_1)\bar{\psi}(0)W_n(0)\}\,|0\rangle_{\mathrm{connected}}\right]. \quad (5.14)$$

A diagrammatic representation of f is shown in Fig. 5.1. Since f describes momentum modes that are collinear to the outgoing photon it is appropriate to call f the n-collinear function in this context. For threshold resummation in the endpoint region of DIS the analogue of f is the jet function, which

is a matrix element of a single quark field and a Wilson line $\bar{\psi}W_n$. f differs markedly from the jet function, since there appears an additional n-collinear electromagnetic current in the correlator.

The hard function h, on the other hand, can be identified as the Sudakov form factor with on-shell massless external legs

$$\langle \hat{q}' | \, \bar{\psi}(0)\gamma^\mu \psi(0) \, | \hat{P} \rangle_{\text{connected, amputated}} = \gamma_\perp^\mu h^{\text{bare}}(Q^2). \tag{5.15}$$

or equivalently, the hard matching coefficient of the Sudakov form factor in momentum space, denoted by $\widetilde{C}_V$ in Ref. [129].

We have shown the factorization of the sum of a set of subgraphs, for a given region. When summing over all graphs Γ and regions R one has to take into account the resulting double counting. On the graphical level one can define a subtraction procedure defined recursively over from smaller to larger regions in the sense of set inclusion. We refer to the standard literature on collinear factorization proofs [128]. In the case presented here it is assumed that the double-counting subtractions can alternatively be formulated by "renormalizing" the corresponding "bare" functions, which is a standard procedure when using factorization theorems. In terms of bare quantities we have the factorization formula

$$\hat{C}^{\text{bare}}(Q^2, -\hat{s}) = h^{\text{bare}}(Q^2) f^{\text{bare}}(-\hat{s}), \tag{5.16}$$

where $C^{\text{bare}} = \frac{1}{2z}\hat{C}^{\text{bare}} + \hat{O}(z^0)$. Note that renormalization of the z^{-1} coefficient of the CF becomes multiplicative, i.e.

$$C = C^{\text{bare}} \otimes Z = \frac{1}{2z}\hat{C}^{\text{bare}}\hat{Z} + O(z^0). \tag{5.17}$$

Note that we can ignore mixing with the gluon CF, since the pure-singlet quark contribution that generates this mixing is suppressed by an additional power of z. This is because such contributions must correspond to reduced graphs that have an additional quark line connecting the hard and collinear subgraph, leading to a suppression according to Eq. (5.6).

On the other hand, h and f can also be renormalized multiplicatively, i.e. $h^{\text{bare}} = hZ_h^{-1}$ and $f^{\text{bare}} = fZ_f$. Note however that $Z_h \neq Z_f$. In fact

$$\hat{C}^{\text{bare}} = \hat{C}\hat{Z}^{-1} = h^{\text{bare}} f^{\text{bare}} = hZ_h^{-1} Z_f f. \tag{5.18}$$

The renormalized quantities are (by definition) finite, so we must have $\hat{Z}Z_h^{-1}Z_f = 1$ in minimal subtraction schemes, i.e. the Z factors cancel, leading to the factorization theorem in terms of the renormalized quantities $\hat{C} = hf$, as stated in Eq. (5.4). The μ-independence of $\hat{C}^{\text{bare}}$ implies

$$\begin{aligned} 0 &= \frac{d}{d\mu}\hat{C}(-\hat{s}, Q^2, \mu^2)\hat{Z}^{-1}(-\hat{s}, Q^2, \mu^2) \\ &= \frac{d}{d\mu}h(Q^2, \mu^2)\hat{Z}^{-1}(-\hat{s}, Q^2, \mu^2) f(-\hat{s}, \mu^2). \end{aligned} \tag{5.19}$$

Thus we are free to set the scale $\mu = Q$ and obtain

$$\hat{C}(-\hat{s}, Q^2, Q^2) = h(Q^2, Q^2) f(-\hat{s}, Q^2). \tag{5.20}$$

We remark that a different approach to proving Eq. (5.4) is to treat the complete DVCS amplitude instead of just the CF itself. For this one must consider the virtuality $-k^2$ as an intermediate scale

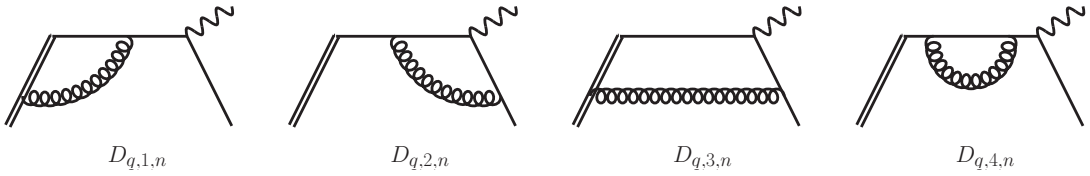

Figure 5.2: One-loop diagrams contributing to f.

between the hard scale Q^2 and the small scales $-t, m^2$, i.e. $-t, m^2 \ll -\hat{s} \ll Q^2$. A proof could proceed in close analogy to [129] using soft-collinear effective theory (SCET), where, in addition to usual hard, collinear and soft degrees of freedom, l would be classified as "semi-hard" and $\hat{k}'$ as "soft-collinear". In the approach of this work, we essentially considered only the separation of the semi-hard scale $-\hat{s}$ from the hard scale Q^2 and we have used that the regions corresponding to the other momentum scalings give scaleless integrals for on-shell partons.

5.3 One-loop example

In this section we verify the general statements of Sec. 5.2 at one-loop accuracy. The unexpanded (in powers of z) diagrams are shown in the upper row of Fig. 2.5. We have

$$\begin{aligned}
D_{q,1} &= \frac{a_s C_F}{2z}\bigg[-\frac{1}{\epsilon}\Big(1+2\log\frac{-\hat{s}}{\mu^2}\Big) - \log^2\frac{Q^2}{\mu^2} + 3\log\frac{Q^2}{\mu^2} \\
&\qquad\qquad + \log^2\frac{-\hat{s}}{\mu^2} - 2\log\frac{-\hat{s}}{\mu^2} - 4\bigg] + \hat{O}(z^0), \\
D_{q,2} &= \frac{a_s C_F}{2z}\bigg[-\frac{1}{\epsilon} + \log\frac{-\hat{s}}{\mu^2} - 4\bigg] + \hat{O}(z^0), \\
D_{q,3} &= \hat{O}(z^0), \\
D_{q,4} &= \frac{a_s C_F}{2z}\bigg[-\frac{1}{\epsilon} + \log\frac{-\hat{s}}{\mu^2} - 1\bigg] + \hat{O}(z^0).
\end{aligned} \tag{5.21}$$

The two relevant regions are R_h and R_n, where the loop momentum is hard and n-collinear, respectively. The corresponding region approximator was defined in Sec. 5.2. We define $D_{q,j,h} = T_{R_h} D_{q,j}$ and $D_{q,j,n} = T_{R_n} D_{q,j}$. As $D_{q,2,n}$ and $D_{q,4,n}$ do not couple to the Wilson line, they are the same as $D_{q,2}$ and $D_{q,4}$, so the corresponding contribution from the hard region is zero. In particular they only depend on $-\hat{s}$ and not on Q^2, as it should be. Diagram $D_{q,3}$ is suppressed by an additional power of z and correspondingly $D_{q,3,n}$ vanishes since the Wilson line connects to the external leg, leading to a factor of $\bar{n}^2 = 0$. Graphical representation of the $D_{q,j,n}$ are shown in Fig. 5.2.

The only one-loop diagram with a non-trivial matching is therefore D_1. We have

$$\begin{aligned} D_{q,1,n} &= -\frac{ig_\perp^{\mu\nu}}{4(d-2)}(ig^2C_F)\Big(\frac{\mu^2e^{\gamma_E}}{4\pi}\Big)^\epsilon\int\frac{d^dl'}{(2\pi)^d}\frac{\mathrm{tr}\Big[\hat{\not{P}}\gamma_\nu\not{l}'\not{\hat{n}}(\not{l}+\not{l}')\gamma_\nu\Big]}{l'^2l^2(l+l')^2l'^-} \\ &= -i\frac{g^2C_F}{2z}\Big(\frac{\mu^2e^{\gamma_E}}{4\pi}\Big)^\epsilon\int\frac{d^dl'}{(2\pi)^d}\frac{2\hat{P}\cdot(l+l')}{l'^2(l+l')^2(2\hat{P}\cdot l')} \\ &= \frac{a_sC_F}{2z}\left[\frac{2}{\epsilon^2}-\frac{1}{\epsilon}\Big(2\log\frac{-\hat{s}}{\mu^2}-2\Big)+\log^2\frac{-\hat{s}}{\mu^2}-2\log\frac{-\hat{s}}{\mu^2}+4-\frac{\pi^2}{6}\right]. \end{aligned} \tag{5.22}$$

The contribution from the hard region, which is obtained by setting $z=0$ in the integrand of $D_{q,1}$, can be found to be

$$D_{q,1,h} = \frac{a_sC_F}{2z}\left[-\frac{2}{\epsilon^2}-\frac{3}{\epsilon}+\frac{2}{\epsilon}\log\frac{Q^2}{\mu^2}-\log^2\frac{Q^2}{\mu^2}+3\log\frac{Q^2}{\mu^2}-8+\frac{\pi^2}{6}\right]. \tag{5.23}$$

As expected, the sum $D_{q,1,n}+D_{q,1,h}$ reproduces the original result in Eq. (5.21).

Eq. (5.20) allows us to resum the logarithms of z. As a simple illustration, I demonstrate how Eq. (5.20) and the one-loop calculation can predict terms $a_s^n\log^{2n-j}z$ for $j=0,1$ in $\hat{C}$ to arbitrary orders. We have shown that

$$f^{\mathrm{bare}}(-\hat{s},\mu^2) = 1+a_sC_F\left[\frac{2}{\epsilon^2}-\frac{2}{\epsilon}\log\frac{-\hat{s}}{\mu^2}+\log^2\frac{-\hat{s}}{\mu^2}-1-\frac{\pi^2}{6}\right]+O(a_s^2), \tag{5.24}$$

which implies that

$$\frac{d}{d\log\mu}f(-\hat{s},\mu^2) = \left[-4a_sC_F\log\frac{-\hat{s}}{\mu^2}+O(a_s^2)\right]f(-\hat{s},\mu^2). \tag{5.25}$$

Solving this differential equation gives

$$f(-\hat{s},Q^2) = \exp\left[a_s(Q)\log^2z+a_s(Q)^2\Big(-\frac{1}{3}\beta_0C_F\log^3z\Big)\right]f(-\hat{s},-\hat{s})+\ldots, \tag{5.26}$$

where the ellipsis denote term that do not contribute to the two highest powers of logarithms. Inserting this expression into Eq. (5.20) gives

$$\hat{C}(z,\mu=Q) = \exp\left[a_s(Q)\log^2z+a_s(Q)^2\Big(-\frac{1}{3}\beta_0C_F\log^3z\Big)\right]+\ldots. \tag{5.27}$$

This result predicts the $a_s^2\log^4z$ and $a_s^2\log^3z$ terms in the two-loop CF and the prediction indeed agrees with the explicit two-loop calculation of C_q [103]. Of course we can resum more logarithms than presented in Eq. (5.27). This is discussed in Sec. 5.4.

5.4 Resummation at NNLL accuracy

By replacing $\log z = \log \frac{-\hat{s}}{\mu^2} - \log \frac{Q^2}{\mu^2}$ in the two-loop result for $\hat{C}$, which can be obtained from the expressions in App. C, we can observe the separation of logarithms verifying Eq. (2.34) at two loops. This also gives the two-loop expressions for f and h up to constants. The one-loop and two-loop expressions are collected in App. D.

In order to carry out the resummation we need the anomalous dimensions.

$$\frac{df}{d\log\mu} = \gamma_f f, \qquad \frac{dh}{d\log\mu} = \gamma_h h, \qquad \frac{d\hat{C}}{d\log\mu} = \gamma_{\hat{C}}\hat{C}. \tag{5.28}$$

We have shown in Sec. 5.2 that h is the hard matching coefficient of the Sudakov form factor. It is well-known that its anomalous dimension has the all-order structure

$$\gamma_h = \Gamma_{\text{cusp}} \log\frac{Q^2}{\mu^2} + \bar{\gamma}_h, \tag{5.29}$$

where the coefficient of the logarithm is the cusp anomalous dimension [130]

$$\Gamma_{\text{cusp}} = 4a_s C_F + a_s^2\Big[\frac{4}{3}(4-\pi^2)C_F C_A + \frac{20}{3}\beta_0 C_F\Big] + O(a_s^3). \tag{5.30}$$

Note that $\gamma_h + \gamma_f = \gamma_{\hat{C}}$ can not depend on μ, since the $\log\frac{Q^2}{\mu^2}$ logarithms in $\hat{C}$ are single logarithms. Hence the dependence on μ has to cancel in $\gamma_{\hat{C}}$, which implies the all-order structure

$$\begin{aligned}\gamma_f &= -\Gamma_{\text{cusp}}\log\frac{-\hat{s}}{\mu^2} + \bar{\gamma}_f,\\ \gamma_{\hat{C}} &= -\Gamma_{\text{cusp}}\log z + \bar{\gamma}_{\hat{C}},\end{aligned} \tag{5.31}$$

where $\bar{\gamma}_{\hat{C}} = \bar{\gamma}_h + \bar{\gamma}_f$. The one- and two-loop expressions for $\bar{\gamma}_f, \bar{\gamma}_h$ are collected in App. D.

Let us turn to the evolution equation for the n-collinear function f, Eq. (5.28), whose solution can be written as

$$f(-\hat{s}, Q^2) = U(z) f(-\hat{s}, -\hat{s}), \tag{5.32}$$

where

$$U(z) = \exp\left\{\frac{1}{2}\int_{\log -\hat{s}}^{\log Q^2} d\log\mu^2\Big[-\Gamma_{\text{cusp}}(a_s(\mu))\log\frac{-\hat{s}}{\mu^2} + \bar{\gamma}_f(a_s(\mu))\Big]\right\}. \tag{5.33}$$

Inserting Eq. (5.32) into Eq. (5.20) gives

$$\hat{C}(z, \mu = Q) = \bar{h}(a_s(Q))U(z)\bar{f}(a_s(\sqrt{z}Q)), \tag{5.34}$$

where $\bar{h}(a_s(\mu)) = h(\mu^2,\mu^2)$, $\bar{f}(a_s(\mu)) = f(\mu^2,\mu^2)$. This implies that the result for the two-loop quark CF can be organized in the following way

$$\begin{aligned}\hat{C}^{(2)}(z,\mu=Q) = \frac{1}{2!}\Big(\frac{\Gamma^{(1)}_{\text{cusp}}}{4}\log^2 z\Big)^2 - \frac{\Gamma^{(1)}_{\text{cusp}}}{12}\beta_0\log^3 z + \frac{1}{4}\Big(\Gamma^{(1)}_{\text{cusp}}\bar{f}^{(1)} + \Gamma^{(1)}_{\text{cusp}}\bar{h}^{(1)} + \Gamma^{(2)}_{\text{cusp}}\Big)\log^2 z\\ - \Big(\frac{\bar{\gamma}_f^{(2)}}{2} + \beta_0\bar{f}^{(1)}\Big)\log z + \text{const.}\end{aligned} \tag{5.35}$$

RG-impr. PT	Log. approx.	$\sim a_s^n \log^k z$ in $\log \hat{C}$	Γ_{cusp}	$\bar{\gamma}_f$	$\bar{h},\ \bar{f}$	β
-	LL	$n+1 \le k \le 2n$	1-loop	-	-	1-loop
LO	NLL	$n \le k \le 2n$	2-loop	1-loop	-	2-loop
NLO	NNLL	$n-1 \le k \le 2n$	3-loop	2-loop	1-loop	3-loop
NNLO	NNNLL	$n-2 \le k \le 2n$	4-loop	3-loop	2-loop	4-loop

Table 5.1: Different approximation schemes. The logarithmic counting agrees with the one from [129].

For applications it can be convenient to rewrite the exponent in Eq. (5.33) using

$$\int_{\log \nu}^{\log \mu} d \log \mu' = \int_{a_s(\nu)}^{a_s(\mu)} \frac{da}{\beta(a)}. \tag{5.36}$$

This gives

$$\begin{aligned} \log \hat{C} &= 2S - A_{\bar{\gamma}_f} + \log \bar{h} + \log \bar{f} \\ &= \frac{1}{a_s(Q)} g_{\text{LL}}(z) + g_{\text{NLL}}(z) + a_s(Q) g_{\text{NNLL}}(z) + O(a_s(Q)^2) \end{aligned} \tag{5.37}$$

where

$$\begin{aligned} S(z) &= \int_{a_s(Q)}^{a_s(\sqrt{z}Q)} d\alpha\ \frac{\Gamma_{\text{cusp}}(a)}{\beta(a)} \int_a^{a_s(\sqrt{z}Q)} \frac{da'}{\beta(a')}, \\ A_{\bar{\gamma}_f}(z) &= \int_{a_s(Q)}^{a_s(\sqrt{z}Q)} da\ \frac{\bar{\gamma}_f(a)}{\beta(a)}. \end{aligned} \tag{5.38}$$

The subscripts of the g-functions correspond to the logarithms that are resummed in it. The corresponding logarithmic counting scheme is defined in Table 5.1. Note that for the NNLL accuracy $\Gamma^{(3)}_{\text{cusp}}$ is required. Though it can not be obtained by methods used in the section, it is readily available in the literature. Hence, at this point in time, the highest accuracy that can be achieved is NNLL. Since $\Gamma^{(4)}_{\text{cusp}}$ and $\bar{h}^{(2)}, \bar{f}^{(2)}$, see Eq. (D.5), are also known, the only missing ingredient for NNNLL is $\bar{\gamma}_f^{(3)}$.

Let us consider how the result can be used in practice. A naive way to implement the resummation corrections is to make the substitution

$$\begin{aligned} C^{(\text{fixed order})}(z) \to C^{(\text{fixed order})}(z) &+ \frac{1}{2z}\Big(\hat{C}^{(\text{resummed})}(z) - \hat{C}^{(\text{fixed order})}(z)\Big) \\ &- \frac{1}{2(1-z)}\Big(\hat{C}^{(\text{resummed})}(1-z) - \hat{C}^{(\text{fixed order})}(1-z)\Big), \end{aligned} \tag{5.39}$$

where $C^{(\text{fixed order})}$ is the CF to fixed order in perturbation theory and

$$\hat{C}^{(\text{resummed})}(z) = \exp\left[\frac{1}{a_s(Q)} g_{\text{LL}}(z) + g_{\text{NLL}}(z) + a_s(Q) g_{\text{NNLL}}(z)\right]. \tag{5.40}$$

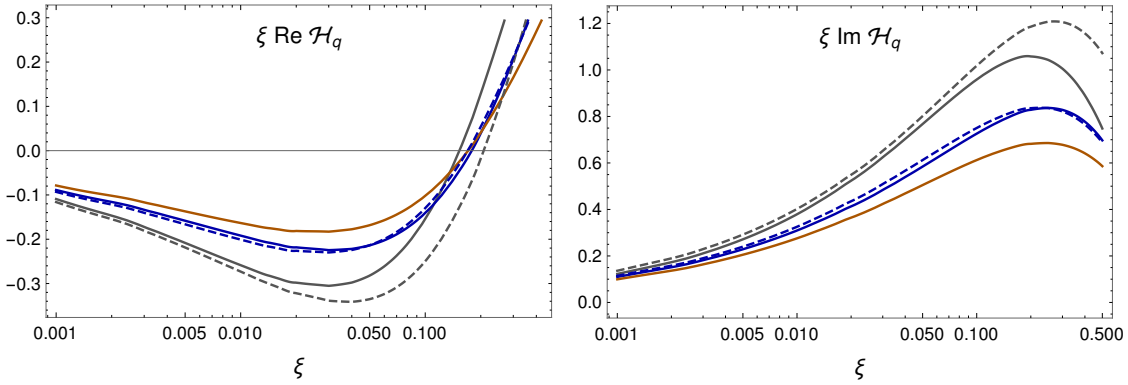

Figure 5.3: Real and imaginary part of the quark CFF $\mathcal{H}_q$, calculated using the model in eq. (3.331) of [20] for $n = 1/2$. The solid lines correspond to the CF at fixed order, gray being LO (fixed order LO and NLL resummation) and blue being NLO (fixed order NLO and NNLL resummation) while the dashed lines include the resummation, with the CF modified according to Eq. (5.39). For reference, the plot of $\mathcal{H}_q$ calculated with the fixed order NNLO non-singlet CF is shown in brown. The resummed NNLO result would require NNNLL resummation and not all the ingredients are known at this point. I have set $\mu = Q$, $n_f = 3$ and used $a_s(Q) = 0.025$.

The function $\hat{C}^{(\text{fixed order})}$ is defined in such a way to subtract the double-counting of the terms of $\hat{C}^{(\text{resummed})}$ that are already contained in $C_q^{(\text{fixed order})}$. It can be obtained by expanding $\hat{C}^{(\text{resummed})}$ in a_s to the desired accuracy.

The integration in Eq. (2.25), when using the resummed CF, can be performed naively by deforming the contour into the complex plane, the same way as was done in Sec. 4.3. In Fig. 5.3 I have used a simple model quark GPD given in Eq. (3.331) of [20] for $n = 1/2$.

For this I used for the analytic form of the running coupling

$$a_s(\sqrt{z}Q) = \frac{a_s(Q)}{r}\Bigg\{1 - \frac{a_s(Q)}{r}\frac{\beta_1}{\beta_0}\log r + \left(\frac{a_s(Q)}{r}\right)^2\left[\frac{\beta_1^2}{\beta_0^2}\Big(\log^2 r - \log r - 1 + r\Big) + \frac{\beta_2}{\beta_0}(1-r)\right]\Bigg] + O(a_s(Q)^4) \tag{5.41}$$

where $r = 1 + a_s(Q)\beta_0 \log z$.

Using the formula Eq. (5.41) we obtain for the g-functions

$$
\begin{aligned}
g_{\mathrm{LL}} &= \frac{\Gamma^{(1)}_{\mathrm{cusp}}}{2\beta_0^2}(1-r+r\log r),\\
g_{\mathrm{NLL}} &= \frac{\Gamma^{(1)}_{\mathrm{cusp}}}{4\beta_0^2}\frac{\beta_1}{\beta_0}\Big(2-2r+2\log r+\log^2 r\Big)-\frac{\Gamma^{(2)}_{\mathrm{cusp}}}{2\beta_0^2}\Big(1-r+\log r\Big),\\
g_{\mathrm{NNLL}} &= \frac{1}{r}\Bigg\{\bar{f}_1+\bar{h}_1 r+\frac{\bar{\gamma}^{(2)}_f}{2\beta_0}(1-r)+\frac{\Gamma^{(1)}_{\mathrm{cusp}}}{4\beta_0^2}\left[\frac{\beta_1^2}{\beta_0^2}\Big(1-r+\log r\Big)^2+\frac{\beta_2}{\beta_0}\Big(1-r^2+2r\log r\Big)\right]\\
&\quad+\frac{\Gamma^{(2)}_{\mathrm{cusp}}}{4\beta_0^2}\frac{\beta_1}{\beta_0}\Big(3-4r+r^2+2\log r\Big)+\frac{\Gamma^{(3)}_{\mathrm{cusp}}}{4\beta_0^2}(1-r)^2\Big].
\end{aligned}
\tag{5.42}
$$

The form in Eq. (5.41) of the running coupling organizes the perturbative expansion in terms of the leading log solution $a_s^{(\mathrm{LL})}(\sqrt{z}Q)=\frac{a_s(Q)}{r}$. Thus the Landau pole is fixed at the point $r=0$, or equivalently $z=e^{-\frac{1}{a_s(Q)\beta_0}}$. It is clear that the points $z=0$ and $z=1$ never coincide with $r=0$, so the contour can be deformed away from the Landau pole, making the numerical evaluation stable. Note that the $\xi\to\xi-i0$ prescription implies a natural direction of the contour deformation that should be performed in order to avoid the Landau pole.

As seen in Fig. 5.3 the correction due to the NNLL resummation appears to be small. This is because, as was discussed in Sec. 2.3, the integration regions where the contour can not be deformed away from $z=0$ or $z=1$, i.e. where threshold logarithms are large, are suppressed by powers of z. This is coherent with the discussion in Ref. [63] which states that there is no leading power contribution from the region where $|x\pm\xi|\lesssim\frac{-t}{Q^2},\frac{m^2}{Q^2},\frac{|p_\perp^2|}{Q^2}$.

6 Conclusion

This dissertation is devoted to the calculation of α_s corrections to DVCS. In Cha. 2 we have reviewed the factorization theorem Eq. (2.25) in detail, which describes the separation of the small scales $-t, m^2$ whose degrees of freedoms are formally described by the GPDs, and the hard scale Q^2, described by the CF. We have then decomposed the leading power contribution to the hadronic tensor $T^{\mu\nu}$ into the form factors $\mathcal{H}, \mathcal{E}, \widetilde{\mathcal{H}}, \widetilde{\mathcal{E}}, \mathcal{H}_T, \mathcal{E}_T, \widetilde{\mathcal{H}}_T, \widetilde{\mathcal{E}}_T$, which encode essentially the complete QCD content of the DVCS process at leading power. These CFFs are given by convolutions of the GPDs with the CFs $C_q, C_g, \widetilde{C}_q, \widetilde{C}_g, C_{g,T}$. We have described how these CFs are related to bare correlation functions, which required the use of dimensional regularization and subtractions of terms corresponding to the renormalization of GPD. We have also taken a look at the NLO calculation of the CFs in all three-sectors: vector, axial-vector and gluon transversity. Furthermore, we have discussed evolution equations for GPDs, which can be used to resum potentially large logarithms $\log \frac{\mu^2}{Q^2}$ in the CFs. Finally, we have discussed a subtlety regarding the use of Larin's scheme for the axial-vector sector, which required additional finite subtractions to $\widetilde{C}_q$.

In Cha. 3, we have discussed computational methods, which become necessary beyond the one-loop order. Firstly we have reviewed the methods of IBP reduction and differential equations for Feynman integrals, which were used in Ref. [48]. We have found that there are a total of 13 MIs that appear in the two-loop calculation. We have explained how these integrals could be calculated using the method of differential equations. Furthermore, we have outlined an entirely different method of calculating the CFs, which is based on the conformal symmetry of QCD in non-integer dimensions at the critical point. This enables one to compute the DVCS CF from the forward case, DIS. Agreement was found when calculating the non-singlet vector CF using both methods, giving further confirmation of the correctness of the computations in Refs. [103] and [48]. We have also introduced the harmonic polylogarithms, in which the CFs can be conveniently expressed in, enabling elegant handling of large expressions and numerical implementation.

In Cha. 4 we discussed how the convolution integral in Eq. (2.25) can be calculated. We have further presented a study of phenomenological impact due to radiative corrections. These corrections were already known to be substantial at NLO and we found that the NNLO correction to the imaginary part of $\mathcal{H}$ is also significant. This can be traced to the cancellation between quark and gluon contributions at moderate Q^2 (that is already present at NLO).

Finally, in Cha. 5 we have reviewed the recent result of the resummation of threshold logarithms in DVCS. This resummation is possible by considering the behaviour of the CF near the partonic threshold poles (branch points). A relatively simple argument shows that the quark CF factorizes near these points, which then enables the resummation by solving RGEs.

We conclude that in order to match the high precision of anticipated experimental data on DVCS in a broad kinematic range from JLAB 12 and the EIC, one should include radiative α_s corrections to NNLO. This includes the three-loop evolution equations and possibly the NNNLL resummation of threshold logarithms. This thesis summarizes essential theoretical foundations that are needed to achieve a good control over perturbation theory. Of course, radiative corrections to DVCS are only part of the theoretical efforts. Further issues that are relevant for GPD physics include power corrections, GPD modeling, data analysis, input from lattice QCD calculations etc.

Furthermore, it will not be enough to consider just the process of electroproduction of a real

photon from the nucleon target. There is a large number of further processes that involve GPDs, see for example Ref. [20] p.226 for a comprehensive list. The set of processes includes, for example, time-like Compton scattering [131, 132], double deeply virtual Compton scattering [133–135] and deeply virtual meson production [136–142]. There are also new processes that are being considered such as the recently proposed single diffractive hard exclusive processes [143]. For these reactions α_s corrections will also be important and they can be calculated using the techniques introduced in Cha. 3. It is apparent that a great deal of theoretical and experimental efforts are needed to deal with the complicated theory of QCD in order to obtain a detailed quantitative knowledge of the most fundamental particles. This applies in particular to the here considered three-dimensional spatial imaging of the nucleon.

To summarize, I state the main results:

1. Calculation of the NNLO (two-loop) flavor-nonsinglet vector CF in DVCS using conformal symmetry [103]; verification of this result by a direct diagrammatic calculation.

2. The same as in 1. for the axial-vector CF starting from Larin's scheme and implementing the necessary additional finite renormalization [88].

3. Calculation of the flavor-singlet vector CF, both for quarks and gluons [48]. Done using a diagrammatic approach and computer algebra methods.

4. Resummation of threshold logarithms in DVCS [52]; a general formalism and implementation to the NNLL accuracy. Phenomenological applications of this result will be studied in future work.

Bibliography

[1] A. Accardi et al. "Electron Ion Collider: The Next QCD Frontier: Understanding the glue that binds us all". In: *Eur. Phys. J. A* 52.9 (2016). Ed. by A. Deshpande, Z. E. Meziani, and J. W. Qiu, p. 268. DOI: 10.1140/epja/i2016-16268-9. arXiv: 1212.1701 [nucl-ex].

[2] Murray Gell-Mann. "Symmetries of baryons and mesons". In: *Phys. Rev.* 125 (1962), pp. 1067–1084. DOI: 10.1103/PhysRev.125.1067.

[3] Yuval Ne'eman. "Derivation of strong interactions from a gauge invariance". In: *Nucl. Phys.* 26 (1961). Ed. by R. Ruffini and Y. Verbin, pp. 222–229. DOI: 10.1016/0029-5582(61)90134-1.

[4] V. E. Barnes et al. "Observation of a Hyperon with Strangeness Minus Three". In: *Phys. Rev. Lett.* 12 (1964), pp. 204–206. DOI: 10.1103/PhysRevLett.12.204.

[5] F. J. Dyson. "Divergence of perturbation theory in quantum electrodynamics". In: *Phys. Rev.* 85 (1952), pp. 631–632. DOI: 10.1103/PhysRev.85.631.

[6] Charles Angas Hurst. "An example of a divergent perturbation expansion in field theory". In: *Proc. Cambridge Phil. Soc.* 48 (1952), p. 625. DOI: 10.1017/S0305004100076416.

[7] Walter E. Thirring. "On the divergence of perturbation theory for quantized fields". In: *Helv. Phys. Acta* 26 (1953), pp. 33–52.

[8] A. Petermann. "Renormalisation dans les séries divergentes". In: *Helv. Phys. Acta* 26.III-IV (1953), pp. 291–299. DOI: 10.5169/seals-112416.

[9] M. Tanabashi et al. "Review of Particle Physics". In: *Phys. Rev. D* 98.3 (2018), p. 030001. DOI: 10.1103/PhysRevD.98.030001.

[10] Huey-Wen Lin. "Nucleon Tomography and Generalized Parton Distribution at Physical Pion Mass from Lattice QCD". In: *Phys. Rev. Lett.* 127.18 (2021), p. 182001. DOI: 10.1103/PhysRevLett.127.182001. arXiv: 2008.12474 [hep-ph].

[11] Andrei V. Belitsky, Xiang-dong Ji, and Feng Yuan. "Quark imaging in the proton via quantum phase space distributions". In: *Phys. Rev. D* 69 (2004), p. 074014. DOI: 10.1103/PhysRevD.69.074014. arXiv: hep-ph/0307383.

[12] Eugene P. Wigner. "On the quantum correction for thermodynamic equilibrium". In: *Phys. Rev.* 40 (1932), pp. 749–760. DOI: 10.1103/PhysRev.40.749.

[13] Dieter Müller et al. "Wave functions, evolution equations and evolution kernels from light ray operators of QCD". In: *Fortsch. Phys.* 42 (1994), pp. 101–141. DOI: 10.1002/prop.2190420202. arXiv: hep-ph/9812448.

[14] Xiang-Dong Ji. "Gauge-Invariant Decomposition of Nucleon Spin". In: *Phys. Rev. Lett.* 78 (1997), pp. 610–613. DOI: 10.1103/PhysRevLett.78.610. arXiv: hep-ph/9603249.

[15] A. V. Radyushkin. "Scaling limit of deeply virtual Compton scattering". In: *Phys. Lett. B* 380 (1996), pp. 417–425. DOI: 10.1016/0370-2693(96)00528-X. arXiv: hep-ph/9604317.

[16] Xiang-Dong Ji. "Deeply virtual Compton scattering". In: *Phys. Rev. D* 55 (1997), pp. 7114–7125. DOI: 10.1103/PhysRevD.55.7114. arXiv: hep-ph/9609381.

[17] A. V. Radyushkin. "Asymmetric gluon distributions and hard diffractive electroproduction". In: *Phys. Lett. B* 385 (1996), pp. 333–342. DOI: 10.1016/0370-2693(96)00844-1. arXiv: hep-ph/9605431.

[18] R. Abdul Khalek et al. "Science Requirements and Detector Concepts for the Electron-Ion Collider: EIC Yellow Report". In: *Nucl. Phys. A* 1026 (2022), p. 122447. DOI: 10.1016/j.nuclphysa.2022.122447. arXiv: 2103.05419 [physics.ins-det].

[19] R. Abdul Khalek et al. "Snowmass 2021 White Paper: Electron Ion Collider for High Energy Physics". In: *2022 Snowmass Summer Study*. Mar. 2022. arXiv: 2203.13199 [hep-ph].

[20] A. V. Belitsky and A. V. Radyushkin. "Unraveling hadron structure with generalized parton distributions". In: *Phys. Rept.* 418 (2005), pp. 1–387. DOI: 10.1016/j.physrep.2005.06.002. arXiv: hep-ph/0504030.

[21] S. Chekanov et al. "Measurement of deeply virtual Compton scattering at HERA". In: *Phys. Lett. B* 573 (2003), pp. 46–62. DOI: 10.1016/j.physletb.2003.08.048. arXiv: hep-ex/0305028.

[22] A. Aktas et al. "Measurement of deeply virtual compton scattering at HERA". In: *Eur. Phys. J. C* 44 (2005), pp. 1–11. DOI: 10.1140/epjc/s2005-02345-3. arXiv: hep-ex/0505061.

[23] A. Airapetian et al. "The Beam-charge azimuthal asymmetry and deeply virtual compton scattering". In: *Phys. Rev. D* 75 (2007), p. 011103. DOI: 10.1103/PhysRevD.75.011103. arXiv: hep-ex/0605108.

[24] F. D. Aaron et al. "Measurement of deeply virtual Compton scattering and its t-dependence at HERA". In: *Phys. Lett. B* 659 (2008), pp. 796–806. DOI: 10.1016/j.physletb.2007.11.093. arXiv: 0709.4114 [hep-ex].

[25] A. Airapetian et al. "Measurement of Azimuthal Asymmetries With Respect To Both Beam Charge and Transverse Target Polarization in Exclusive Electroproduction of Real Photons". In: *JHEP* 06 (2008), p. 066. DOI: 10.1088/1126-6708/2008/06/066. arXiv: 0802.2499 [hep-ex].

[26] S. Chekanov et al. "A Measurement of the Q**2, W and t dependences of deeply virtual Compton scattering at HERA". In: *JHEP* 05 (2009), p. 108. DOI: 10.1088/1126-6708/2009/05/108. arXiv: 0812.2517 [hep-ex].

[27] F. D. Aaron et al. "Deeply Virtual Compton Scattering and its Beam Charge Asymmetry in e+- Collisions at HERA". In: *Phys. Lett. B* 681 (2009), pp. 391–399. DOI: 10.1016/j.physletb.2009.10.035. arXiv: 0907.5289 [hep-ex].

[28] A. Airapetian et al. "Separation of contributions from deeply virtual Compton scattering and its interference with the Bethe-Heitler process in measurements on a hydrogen target". In: *JHEP* 11 (2009), p. 083. DOI: 10.1088/1126-6708/2009/11/083. arXiv: 0909.3587 [hep-ex].

[29] A. Airapetian et al. "Measurement of azimuthal asymmetries associated with deeply virtual Compton scattering on a longitudinally polarized deuterium target". In: *Nucl. Phys. B* 842 (2011), pp. 265–298. DOI: 10.1016/j.nuclphysb.2010.09.010. arXiv: 1008.3996 [hep-ex].

[30] A. Airapetian et al. "Exclusive Leptoproduction of Real Photons on a Longitudinally Polarised Hydrogen Target". In: *JHEP* 06 (2010), p. 019. DOI: 10.1007/JHEP06(2010)019. arXiv: 1004.0177 [hep-ex].

[31] A. Airapetian et al. "Measurement of double-spin asymmetries associated with deeply virtual Compton scattering on a transversely polarized hydrogen target". In: *Phys. Lett. B* 704 (2011), pp. 15–23. DOI: 10.1016/j.physletb.2011.08.067. arXiv: 1106.2990 [hep-ex].

[32] A. Airapetian et al. "Beam-helicity and beam-charge asymmetries associated with deeply virtual Compton scattering on the unpolarised proton". In: *JHEP* 07 (2012), p. 032. DOI: 10.1007/JHEP07(2012)032. arXiv: 1203.6287 [hep-ex].

[33] S. Chen et al. "Measurement of deeply virtual compton scattering with a polarized proton target". In: *Phys. Rev. Lett.* 97 (2006), p. 072002. DOI: 10.1103/PhysRevLett.97.072002. arXiv: hep-ex/0605012.

[34] C. Muñoz Camacho et al. "Scaling tests of the cross-section for deeply virtual compton scattering". In: *Phys. Rev. Lett.* 97 (2006), p. 262002. DOI: 10.1103/PhysRevLett.97.262002. arXiv: nucl-ex/0607029.

[35] M. Mazouz et al. "Deeply virtual compton scattering off the neutron". In: *Phys. Rev. Lett.* 99 (2007), p. 242501. DOI: 10.1103/PhysRevLett.99.242501. arXiv: 0709.0450 [nucl-ex].

[36] F. X. Girod et al. "Measurement of Deeply virtual Compton scattering beam-spin asymmetries". In: *Phys. Rev. Lett.* 100 (2008), p. 162002. DOI: 10.1103/PhysRevLett.100.162002. arXiv: 0711.4805 [hep-ex].

[37] G. Gavalian et al. "Beam spin asymmetries in deeply virtual Compton scattering (DVCS) with CLAS at 4.8 GeV". In: *Phys. Rev. C* 80 (2009), p. 035206. DOI: 10.1103/PhysRevC.80.035206. arXiv: 0812.2950 [hep-ex].

[38] S. Pisano et al. "Single and double spin asymmetries for deeply virtual Compton scattering measured with CLAS and a longitudinally polarized proton target". In: *Phys. Rev. D* 91.5 (2015), p. 052014. DOI: 10.1103/PhysRevD.91.052014. arXiv: 1501.07052 [hep-ex].

[39] H. S. Jo et al. "Cross sections for the exclusive photon electroproduction on the proton and Generalized Parton Distributions". In: *Phys. Rev. Lett.* 115.21 (2015), p. 212003. DOI: 10.1103/PhysRevLett.115.212003. arXiv: 1504.02009 [hep-ex].

[40] M. Defurne et al. "E00-110 experiment at Jefferson Lab Hall A: Deeply virtual Compton scattering off the proton at 6 GeV". In: *Phys. Rev. C* 92.5 (2015), p. 055202. DOI: 10.1103/PhysRevC.92.055202. arXiv: 1504.05453 [nucl-ex].

[41] R. Akhunzyanov et al. "Transverse extension of partons in the proton probed in the sea-quark range by measuring the DVCS cross section". In: *Phys. Lett. B* 793 (2019). [Erratum: Phys.Lett.B 800, 135129 (2020)], pp. 188–194. DOI: 10.1016/j.physletb.2019.04.038. arXiv: 1802.02739 [hep-ex].

[42] M. Vanderhaeghen et al. "QED radiative corrections to virtual Compton scattering". In: *Phys. Rev. C* 62 (2000), p. 025501. DOI: 10.1103/PhysRevC.62.025501. arXiv: hep-ph/0001100.

[43] V. V. Bytev, E. A. Kuraev, and E. Tomasi-Gustafsson. "Radiative corrections to the deeply virtual Compton scattering electron tensor". In: *Phys. Rev. C* 77 (2008), p. 055205. DOI: 10.1103/PhysRevC.77.055205. arXiv: hep-ph/0310226.

[44] Andrei V. Afanasev, M. I. Konchatnij, and N. P. Merenkov. "Single-spin asymmetries in the Bethe-Heitler process e- + p —> e- + gamma + p from QED radiative corrections". In: *J. Exp. Theor. Phys.* 102 (2006), pp. 220–233. DOI: 10.1134/S1063776106020038. arXiv: hep-ph/0507059.

[45] Igor Akushevich and Alexander Ilyichev. "Radiative effects in the processes of exclusive photon electroproduction from polarized protons". In: *Phys. Rev. D* 85 (2012), p. 053008. DOI: 10.1103/PhysRevD.85.053008. arXiv: 1201.4065 [hep-ph].

[46] K. G. Chetyrkin and F. V. Tkachov. "Integration by Parts: The Algorithm to Calculate beta Functions in 4 Loops". In: *Nucl. Phys. B* 192 (1981), pp. 159–204. DOI: 10.1016/0550-3213(81)90199-1.

[47] A. V. Kotikov. "Differential equations method: New technique for massive Feynman diagrams calculation". In: *Phys. Lett. B* 254 (1991), pp. 158–164. DOI: 10.1016/0370-2693(91)90413-K.

[48] V. M. Braun, Yao Ji, and Jakob Schoenleber. "Deeply-virtual Compton scattering at the next-to-next-to-leading order". In: (July 2022). arXiv: 2207.06818 [hep-ph].

[49] Alexander B. Goncharov. "Multiple polylogarithms, cyclotomy and modular complexes". In: *Math. Res. Lett.* 5 (1998), pp. 497–516. DOI: 10.4310/MRL.1998.v5.n4.a7. arXiv: 1105.2076 [math.AG].

[50] E. Remiddi and J. A. M. Vermaseren. "Harmonic polylogarithms". In: *Int. J. Mod. Phys. A* 15 (2000), pp. 725–754. DOI: 10.1142/S0217751X00000367. arXiv: hep-ph/9905237.

[51] S. V. Goloskokov and P. Kroll. "The Longitudinal cross-section of vector meson electroproduction". In: *Eur. Phys. J. C* 50 (2007), pp. 829–842. DOI: 10.1140/epjc/s10052-007-0228-4. arXiv: hep-ph/0611290.

[52] Jakob Schoenleber. "Resummation of threshold logarithms in deeply-virtual Compton scattering". In: *JHEP* 02 (2023), p. 207. DOI: 10.1007/JHEP02(2023)207. arXiv: 2209.09015 [hep-ph].

[53] Markus Diehl et al. "Testing the handbag contribution to exclusive virtual Compton scattering". In: *Phys. Lett. B* 411 (1997), pp. 193–202. DOI: 10.1016/S0370-2693(97)00959-3. arXiv: hep-ph/9706344.

[54] Andreas Freund and Mark Strikman. "Single spin asymmetry in DVCS". In: *Phys. Rev. D* 60 (1999). Ed. by A. De Roeck, D. Barber, and G. Radel, p. 071501. DOI: 10.1103/PhysRevD.60.071501. arXiv: hep-ph/9906205.

[55] Andrei V. Belitsky et al. "Leading twist asymmetries in deeply virtual Compton scattering". In: *Nucl. Phys. B* 593 (2001), pp. 289–310. DOI: 10.1016/S0550-3213(00)00588-5. arXiv: hep-ph/0004059.

[56] Andrei V. Belitsky, Dieter Mueller, and A. Kirchner. "Theory of deeply virtual Compton scattering on the nucleon". In: *Nucl. Phys. B* 629 (2002), pp. 323–392. DOI: 10.1016/S0550-3213(02)00144-X. arXiv: hep-ph/0112108.

[57] Andrei V. Belitsky et al. "Twist three observables in deeply virtual Compton scattering on the nucleon". In: *Phys. Lett. B* 510 (2001), pp. 117–124. DOI: 10.1016/S0370-2693(01)00608-6. arXiv: hep-ph/0103343.

[58] A. Donnachie, J. Gravelis, and Graham Shaw. "Rho electroproduction and the hadronic contribution to deeply virtual Compton scattering". In: *Eur. Phys. J. C* 18 (2001), pp. 539–545. DOI: 10.1007/s100520100545. arXiv: hep-ph/0009235.

[59] A. Donnachie and Hans Gunter Dosch. "Diffractive exclusive photon production in deep inelastic scattering". In: *Phys. Lett. B* 502 (2001), pp. 74–78. DOI: 10.1016/S0370-2693(01)00171-X. arXiv: hep-ph/0010227.

[60] A. Freund, M. McDermott, and M. Strikman. "Modeling generalized parton distributions to describe deeply virtual Compton scattering data". In: *Phys. Rev. D* 67 (2003), p. 036001. DOI: 10.1103/PhysRevD.67.036001. arXiv: hep-ph/0208160.

[61] A. Gardestig, A. P. Szczepaniak, and J. T. Londergan. "Separation of soft and hard physics in deeply virtual Compton scattering". In: *Phys. Rev. D* 68 (2003), p. 034005. DOI: 10.1103/PhysRevD.68.034005. arXiv: hep-ph/0305210.

[62] A. Freund. "A Detailed QCD analysis of twist 3 effects in DVCS observables". In: *Phys. Rev. D* 68 (2003), p. 096006. DOI: 10.1103/PhysRevD.68.096006. arXiv: hep-ph/0306012.

[63] John C. Collins and Andreas Freund. "Proof of factorization for deeply virtual Compton scattering in QCD". In: *Phys. Rev. D* 59 (1999), p. 074009. DOI: 10.1103/PhysRevD.59.074009. arXiv: hep-ph/9801262.

[64] Xiang-Dong Ji and Jonathan Osborne. "One loop corrections and all order factorization in deeply virtual Compton scattering". In: *Phys. Rev. D* 58 (1998), p. 094018. DOI: 10.1103/PhysRevD.58.094018. arXiv: hep-ph/9801260.

[65] Stephen B. Libby and George F. Sterman. "Mass Divergences in Two Particle Inelastic Scattering". In: *Phys. Rev. D* 18 (1978), p. 4737. DOI: 10.1103/PhysRevD.18.4737.

[66] L. D. Landau. "On analytic properties of vertex parts in quantum field theory". In: *Nucl. Phys.* 13.1 (1959). Ed. by D. ter Haar, pp. 181–192. DOI: 10.1016/B978-0-08-010586-4.50103-6.

[67] S. Coleman and R. E. Norton. "Singularities in the physical region". In: *Nuovo Cim.* 38 (1965), pp. 438–442. DOI: 10.1007/BF02750472.

[68] John Collins. "A new and complete proof of the Landau condition for pinch singularities of Feynman graphs and other integrals". In: (July 2020). arXiv: 2007.04085 [hep-ph].

[69] John C. Collins, Leonid Frankfurt, and Mark Strikman. "Factorization for hard exclusive electroproduction of mesons in QCD". In: *Phys. Rev. D* 56 (1997), pp. 2982–3006. DOI: 10.1103/PhysRevD.56.2982. arXiv: hep-ph/9611433.

[70] A. V. Radyushkin. "Nonforward parton distributions". In: *Phys. Rev. D* 56 (1997), pp. 5524–5557. DOI: 10.1103/PhysRevD.56.5524. arXiv: hep-ph/9704207.

[71] Andrei V. Belitsky and Dieter Mueller. "Off forward gluonometry". In: *Phys. Lett. B* 486 (2000), pp. 369–377. DOI: 10.1016/S0370-2693(00)00773-5. arXiv: hep-ph/0005028.

[72] Markus Diehl and Thierry Gousset. "Time ordering in off diagonal parton distributions". In: *Phys. Lett. B* 428 (1998), pp. 359–370. DOI: 10.1016/S0370-2693(98)00439-0. arXiv: hep-ph/9801233.

[73] S. A. Larin. "The Renormalization of the axial anomaly in dimensional regularization". In: *Phys. Lett. B* 303 (1993), pp. 113–118. DOI: 10.1016/0370-2693(93)90053-K. arXiv: hep-ph/9302240.

[74] V. M. Braun et al. "Three-loop off-forward evolution kernel for axial-vector operators in Larin's scheme". In: *Phys. Rev. D* 103.9 (2021), p. 094018. DOI: 10.1103/PhysRevD.103.094018. arXiv: 2101.01471 [hep-ph].

[75] Erik Panzer. "Algorithms for the symbolic integration of hyperlogarithms with applications to Feynman integrals". In: *Comput. Phys. Commun.* 188 (2015), pp. 148–166. DOI: 10.1016/j.cpc.2014.10.019. arXiv: 1403.3385 [hep-th].

[76] Xiang-Dong Ji and Jonathan Osborne. "One loop QCD corrections to deeply virtual Compton scattering: The Parton helicity independent case". In: *Phys. Rev. D* 57 (1998), pp. 1337–1340. DOI: 10.1103/PhysRevD.57.R1337. arXiv: hep-ph/9707254.

[77] Andrei V. Belitsky and Dieter Mueller. "Predictions from conformal algebra for the deeply virtual Compton scattering". In: *Phys. Lett. B* 417 (1998), pp. 129–140. DOI: 10.1016/S0370-2693(97)01390-7. arXiv: hep-ph/9709379.

[78] L. Mankiewicz et al. "NLO corrections to deeply virtual Compton scattering". In: *Phys. Lett. B* 425 (1998). [Erratum: Phys.Lett.B 461, 423–423 (1999)], pp. 186–192. DOI: 10.1016/S0370-2693(98)00190-7. arXiv: hep-ph/9712251.

[79] Pervez Hoodbhoy and Xiang-Dong Ji. "Helicity flip off forward parton distributions of the nucleon". In: *Phys. Rev. D* 58 (1998), p. 054006. DOI: 10.1103/PhysRevD.58.054006. arXiv: hep-ph/9801369.

[80] Zhang Chen and Xiang-dong Ji. "Counting and tensorial properties of twist-two helicity-flip nucleon form-factors". In: *Phys. Rev. D* 71 (2005), p. 016003. DOI: 10.1103/PhysRevD.71.016003. arXiv: hep-ph/0404276.

[81] Andrei V. Belitsky, A. Freund, and Dieter Mueller. "Evolution kernels of skewed parton distributions: Method and two loop results". In: *Nucl. Phys. B* 574 (2000), pp. 347–406. DOI: 10.1016/S0550-3213(00)00012-2. arXiv: hep-ph/9912379.

[82] V. M. Braun et al. "Two-loop evolution equations for flavor-singlet light-ray operators". In: *JHEP* 02 (2019), p. 191. DOI: 10.1007/JHEP02(2019)191. arXiv: 1901.06172 [hep-ph].

[83] V. M. Braun et al. "Three-loop evolution equation for flavor-nonsinglet operators in off-forward kinematics". In: *JHEP* 06 (2017), p. 037. DOI: 10.1007/JHEP06(2017)037. arXiv: 1703.09532 [hep-ph].

[84] V. M. Braun, K. G. Chetyrkin, and A. N. Manashov. "NNLO anomalous dimension matrix for twist-two flavor-singlet operators". In: *Phys. Lett. B* 834 (2022), p. 137409. DOI: 10.1016/j.physletb.2022.137409. arXiv: 2205.08228 [hep-ph].

[85] T. Braunschweig, B. Geyer, and D. Robaschik. "Anomalous Dimensions of Flavor Singlet Light Cone Operators". In: *Annalen Phys.* 44 (1987), pp. 403–411.

[86] I. I. Balitsky and Vladimir M. Braun. "Evolution Equations for QCD String Operators". In: *Nucl. Phys. B* 311 (1989), pp. 541–584. DOI: 10.1016/0550-3213(89)90168-5.

[87] S. Moch, J. A. M. Vermaseren, and A. Vogt. "The Three-Loop Splitting Functions in QCD: The Helicity-Dependent Case". In: *Nucl. Phys. B* 889 (2014), pp. 351–400. DOI: 10.1016/j.nuclphysb.2014.10.016. arXiv: 1409.5131 [hep-ph].

[88] V. M. Braun et al. "Axial-vector contributions in two-photon reactions: Pion transition form factor and deeply-virtual Compton scattering at NNLO in QCD". In: *Phys. Rev. D* 104.9 (2021), p. 094007. DOI: 10.1103/PhysRevD.104.094007. arXiv: 2106.01437 [hep-ph].

[89] Jing Gao et al. "Next-to-Next-to-Leading-Order QCD Prediction for the Photon-Pion Form Factor". In: *Phys. Rev. Lett.* 128.6 (2022), p. 062003. DOI: 10.1103/PhysRevLett.128.062003. arXiv: 2106.01390 [hep-ph].

[90] Paulo Nogueira. "Automatic Feynman graph generation". In: *J. Comput. Phys.* 105 (1993), pp. 279–289. DOI: 10.1006/jcph.1993.1074.

[91] J. A. M. Vermaseren. "New features of FORM". In: (Oct. 2000). arXiv: math-ph/0010025.

[92] A. V. Smirnov and F. S. Chuharev. "FIRE6: Feynman Integral REduction with Modular Arithmetic". In: *Comput. Phys. Commun.* 247 (2020), p. 106877. DOI: 10.1016/j.cpc.2019.106877. arXiv: 1901.07808 [hep-ph].

[93] Johannes M. Henn. "Multiloop integrals in dimensional regularization made simple". In: *Phys. Rev. Lett.* 110 (2013), p. 251601. DOI: 10.1103/PhysRevLett.110.251601. arXiv: 1304.1806 [hep-th].

[94] M. C. Bergere and Yuk-Ming P. Lam. "ASYMPTOTIC EXPANSION OF FEYNMAN AMPLITUDES. Part 1: THE CONVERGENT CASE". In: *Commun. Math. Phys.* 39 (1974), p. 1. DOI: 10.1007/BF01609168.

[95] M. Czakon. "Automatized analytic continuation of Mellin-Barnes integrals". In: *Comput. Phys. Commun.* 175 (2006), pp. 559–571. DOI: 10.1016/j.cpc.2006.07.002. arXiv: hep-ph/0511200.

[96] V. M. Braun, G. P. Korchemsky, and Dieter Müller. "The Uses of conformal symmetry in QCD". In: *Prog. Part. Nucl. Phys.* 51 (2003), pp. 311–398. DOI: 10.1016/S0146-6410(03)90004-4. arXiv: hep-ph/0306057.

[97] Stanley J. Brodsky et al. "CONFORMAL SYMMETRY: EXCLUSIVE PROCESSES BEYOND LEADING ORDER". In: *Phys. Rev. D* 33 (1986), p. 1881. DOI: 10.1103/PhysRevD.33.1881.

[98] Dieter Mueller. "Constraints for anomalous dimensions of local light cone operators in phi**3 in six-dimensions theory". In: *Z. Phys. C* 49 (1991), pp. 293–300. DOI: 10.1007/BF01555504.

[99] Dieter Mueller. "Conformal constraints and the evolution of the nonsinglet meson distribution amplitude". In: *Phys. Rev. D* 49 (1994), pp. 2525–2535. DOI: 10.1103/PhysRevD.49.2525.

[100] Dieter Mueller. "Restricted conformal invariance in QCD and its predictive power for virtual two photon processes". In: *Phys. Rev. D* 58 (1998), p. 054005. DOI: 10.1103/PhysRevD.58.054005. arXiv: hep-ph/9704406.

[101] Andrei V. Belitsky and Dieter Mueller. "Next-to-leading order evolution of twist-2 conformal operators: The Abelian case". In: *Nucl. Phys. B* 527 (1998), pp. 207–234. DOI: 10.1016/S0550-3213(98)00310-1. arXiv: hep-ph/9802411.

[102] Andrei V. Belitsky and Dieter Mueller. "Broken conformal invariance and spectrum of anomalous dimensions in QCD". In: *Nucl. Phys. B* 537 (1999), pp. 397–442. DOI: 10.1016/S0550-3213(98)00677-4. arXiv: hep-ph/9804379.

[103] V. M. Braun et al. "Two-loop coefficient function for DVCS: vector contributions". In: *JHEP* 09 (2020). [Erratum: JHEP 02, 115 (2022)], p. 117. DOI: 10.1007/JHEP09(2020)117. arXiv: 2007.06348 [hep-ph].

[104] V. M. Braun et al. "Conformal symmetry of QCD in d-dimensions". In: *Phys. Lett. B* 793 (2019), pp. 78–84. DOI: 10.1016/j.physletb.2019.04.027. arXiv: 1810.04993 [hep-th].

[105] J. A. M. Vermaseren, A. Vogt, and S. Moch. "The Third-order QCD corrections to deep-inelastic scattering by photon exchange". In: *Nucl. Phys. B* 724 (2005), pp. 3–182. DOI: 10.1016/j.nuclphysb.2005.06.020. arXiv: hep-ph/0504242.

[106] V. M. Braun et al. "Two-loop conformal generators for leading-twist operators in QCD". In: *JHEP* 03 (2016), p. 142. DOI: 10.1007/JHEP03(2016)142. arXiv: 1601.05937 [hep-ph].

[107] V. M. Braun and A. N. Manashov. "Operator product expansion in QCD in off-forward kinematics: Separation of kinematic and dynamical contributions". In: *JHEP* 01 (2012), p. 085. DOI: 10.1007/JHEP01(2012)085. arXiv: 1111.6765 [hep-ph].

[108] I. V. Anikin and A. N. Manashov. "Higher twist nucleon distribution amplitudes in Wandzura-Wilczek approximation". In: *Phys. Rev. D* 89.1 (2014), p. 014011. DOI: 10.1103/PhysRevD.89.014011. arXiv: 1311.3584 [hep-ph].

[109] B. Basso and G. P. Korchemsky. "Anomalous dimensions of high-spin operators beyond the leading order". In: *Nucl. Phys. B* 775 (2007), pp. 1–30. DOI: 10.1016/j.nuclphysb.2007.03.044. arXiv: hep-th/0612247.

[110] Luis F. Alday, Agnese Bissi, and Tomasz Lukowski. "Large spin systematics in CFT". In: *JHEP* 11 (2015), p. 101. DOI: 10.1007/JHEP11(2015)101. arXiv: 1502.07707 [hep-th].

[111] Luis F. Alday and Alexander Zhiboedov. "An Algebraic Approach to the Analytic Bootstrap". In: *JHEP* 04 (2017), p. 157. DOI: 10.1007/JHEP04(2017)157. arXiv: 1510.08091 [hep-th].

[112] V. M. Braun, A. N. Manashov, and B. Pirnay. "Scale dependence of twist-three contributions to single spin asymmetries". In: *Phys. Rev. D* 80 (2009). [Erratum: Phys.Rev.D 86, 119902 (2012)], p. 114002. DOI: 10.1103/PhysRevD.80.114002. arXiv: 0909.3410 [hep-ph].

[113] Jakob Ablinger. "A Computer Algebra Toolbox for Harmonic Sums Related to Particle Physics". MA thesis. Linz U., 2009. arXiv: 1011.1176 [math-ph].

[114] Jakob Ablinger. "The package HarmonicSums: Computer Algebra and Analytic aspects of Nested Sums". In: *PoS* LL2014 (2014). Ed. by Martina Mende, p. 019. DOI: 10.22323/1.211.0019. arXiv: 1407.6180 [cs.SC].

[115] Jakob Ablinger, Johannes Blümlein, and Carsten Schneider. "Analytic and Algorithmic Aspects of Generalized Harmonic Sums and Polylogarithms". In: *J. Math. Phys.* 54 (2013), p. 082301. DOI: 10.1063/1.4811117. arXiv: 1302.0378 [math-ph].

[116] Claude Duhr. "Hopf algebras, coproducts and symbols: an application to Higgs boson amplitudes". In: *JHEP* 08 (2012), p. 043. DOI: 10.1007/JHEP08(2012)043. arXiv: 1203.0454 [hep-ph].

[117] D Maitre. "HPL, a mathematica implementation of the harmonic polylogarithms". In: *Comput. Phys. Commun.* 174 (2006), pp. 222–240. DOI: 10.1016/j.cpc.2005.10.008. arXiv: hep-ph/0507152.

[118] Xiangdong Ji. "Parton Physics on a Euclidean Lattice". In: *Phys. Rev. Lett.* 110 (2013), p. 262002. DOI: 10.1103/PhysRevLett.110.262002. arXiv: 1305.1539 [hep-ph].

[119] Xiangdong Ji. "Parton Physics from Large-Momentum Effective Field Theory". In: *Sci. China Phys. Mech. Astron.* 57 (2014), pp. 1407–1412. DOI: 10.1007/s11433-014-5492-3. arXiv: 1404.6680 [hep-ph].

[120] Kresimir Kumericki, Simonetta Liuti, and Herve Moutarde. "GPD phenomenology and DVCS fitting: Entering the high-precision era". In: *Eur. Phys. J. A* 52.6 (2016), p. 157. DOI: 10.1140/epja/i2016-16157-3. arXiv: 1602.02763 [hep-ph].

[121] Peter Kroll, Herve Moutarde, and Franck Sabatie. "From hard exclusive meson electroproduction to deeply virtual Compton scattering". In: *Eur. Phys. J. C* 73.1 (2013), p. 2278. DOI: 10.1140/epjc/s10052-013-2278-0. arXiv: 1210.6975 [hep-ph].

[122] I. V. Musatov and A. V. Radyushkin. "Evolution and models for skewed parton distributions". In: *Phys. Rev. D* 61 (2000), p. 074027. DOI: 10.1103/PhysRevD.61.074027. arXiv: hep-ph/9905376.

[123] Maxim V. Polyakov and C. Weiss. "Skewed and double distributions in pion and nucleon". In: *Phys. Rev. D* 60 (1999), p. 114017. DOI: 10.1103/PhysRevD.60.114017. arXiv: hep-ph/9902451.

[124] H. Abramowicz et al. "Combination of measurements of inclusive deep inelastic $e^{\pm}p$ scattering cross sections and QCD analysis of HERA data". In: *Eur. Phys. J. C* 75.12 (2015), p. 580. DOI: 10.1140/epjc/s10052-015-3710-4. arXiv: 1506.06042 [hep-ex].

[125] S. Alekhin et al. "Parton distribution functions, α_s, and heavy-quark masses for LHC Run II". In: *Phys. Rev. D* 96.1 (2017), p. 014011. DOI: 10.1103/PhysRevD.96.014011. arXiv: 1701.05838 [hep-ph].

[126] S. Alekhin, J. Blümlein, and S. Moch. "NLO PDFs from the ABMP16 fit". In: *Eur. Phys. J. C* 78.6 (2018), p. 477. DOI: 10.1140/epjc/s10052-018-5947-1. arXiv: 1803.07537 [hep-ph].

[127] T. Altinoluk et al. "Resumming soft and collinear contributions in deeply virtual Compton scattering". In: *JHEP* 10 (2012), p. 049. DOI: 10.1007/JHEP10(2012)049. arXiv: 1207.4609 [hep-ph].

[128] John Collins. *Foundations of perturbative QCD*. Vol. 32. Cambridge University Press, Nov. 2013. ISBN: 978-1-107-64525-7, 978-1-107-64525-7, 978-0-521-85533-4, 978-1-139-09782-6.

[129] Thomas Becher, Matthias Neubert, and Ben D. Pecjak. "Factorization and Momentum-Space Resummation in Deep-Inelastic Scattering". In: *JHEP* 01 (2007), p. 076. DOI: 10.1088/1126-6708/2007/01/076. arXiv: hep-ph/0607228.

[130] G. P. Korchemsky and A. V. Radyushkin. "Renormalization of the Wilson Loops Beyond the Leading Order". In: *Nucl. Phys. B* 283 (1987), pp. 342–364. DOI: 10.1016/0550-3213(87)90277-X.

[131] Edgar R. Berger, M. Diehl, and B. Pire. "Time - like Compton scattering: Exclusive photoproduction of lepton pairs". In: *Eur. Phys. J. C* 23 (2002), pp. 675–689. DOI: 10.1007/s100520200917. arXiv: hep-ph/0110062.

[132] Marie Boër, Michel Guidal, and Marc Vanderhaeghen. "Single and double polarization observables in timelike Compton scattering off proton". In: (Jan. 2015). arXiv: 1501.00270 [hep-ph].

[133] M. Guidal and M. Vanderhaeghen. "Double deeply virtual Compton scattering off the nucleon". In: *Phys. Rev. Lett.* 90 (2003), p. 012001. DOI: 10.1103/PhysRevLett.90.012001. arXiv: hep-ph/0208275.

[134] Andrei V. Belitsky and Dieter Mueller. "Exclusive electroproduction of lepton pairs as a probe of nucleon structure". In: *Phys. Rev. Lett.* 90 (2003), p. 022001. DOI: 10.1103/PhysRevLett.90.022001. arXiv: hep-ph/0210313.

[135] Andrei V. Belitsky and Dieter Mueller. "Probing generalized parton distributions with electroproduction of lepton pairs off the nucleon". In: *Phys. Rev. D* 68 (2003), p. 116005. DOI: 10.1103/PhysRevD.68.116005. arXiv: hep-ph/0307369.

[136] L. Mankiewicz, G. Piller, and T. Weigl. "Hard exclusive meson production and nonforward parton distributions". In: *Eur. Phys. J. C* 5 (1998), pp. 119–128. DOI: 10.1007/s100520050253. arXiv: hep-ph/9711227.

[137] L. Mankiewicz, G. Piller, and T. Weigl. "Hard leptoproduction of charged vector mesons". In: *Phys. Rev. D* 59 (1999), p. 017501. DOI: 10.1103/PhysRevD.59.017501. arXiv: hep-ph/9712508.

[138] L. L. Frankfurt et al. "Hard exclusive pseudoscalar meson electroproduction and spin structure of a nucleon". In: *Phys. Rev. D* 60 (1999), p. 014010. DOI: 10.1103/PhysRevD.60.014010. arXiv: hep-ph/9901429.

[139] L. L. Frankfurt et al. "Hard exclusive electroproduction of decuplet baryons in the large N(c) limit". In: *Phys. Rev. Lett.* 84 (2000), pp. 2589–2592. DOI: 10.1103/PhysRevLett.84.2589. arXiv: hep-ph/9911381.

[140] Michael I. Eides, Leonid L. Frankfurt, and Mark I. Strikman. "Hard exclusive electroproduction of pseudoscalar mesons and QCD axial anomaly". In: *Phys. Rev. D* 59 (1999), p. 114025. DOI: 10.1103/PhysRevD.59.114025. arXiv: hep-ph/9809277.

[141] L. Mankiewicz, G. Piller, and A. Radyushkin. "Hard exclusive electroproduction of pions". In: *Eur. Phys. J. C* 10 (1999), pp. 307–312. DOI: 10.1007/s100529900045. arXiv: hep-ph/9812467.

[142] M. Vanderhaeghen, Pierre A. M. Guichon, and M. Guidal. "Deeply virtual electroproduction of photons and mesons on the nucleon: Leading order amplitudes and power corrections". In: *Phys. Rev. D* 60 (1999), p. 094017. DOI: 10.1103/PhysRevD.60.094017. arXiv: hep-ph/9905372.

[143] Jian-Wei Qiu and Zhite Yu. "Single diffractive hard exclusive processes for the study of generalized parton distributions". In: *Phys. Rev. D* 107.1 (2023), p. 014007. DOI: 10.1103/PhysRevD.107.014007. arXiv: 2210.07995 [hep-ph].

A Integral operations on GPDs

In this Appendix we summarize a notation regarding integral operators that is used throughout this text.

Consider an unspecified space of functions Ω that depend on the momentum fraction variable x. Let $K : \Omega \to \Omega$ be a linear operator, defined by

$$(K * f)(x) = \int_{-\infty}^{\infty} dx' \; K(x, x') f(x'), \tag{A.1}$$

where $K(x, x')$ is a distribution-valued integration kernel and the action of K on f is denoted by the symbol $*$. Clearly, the algebra of such operators is associative and distributive with respect to the operations $+$ and $*$. Some obvious notations are as follows.

- The unit operator

$$\mathbb{I}(x, x') = \delta(x - x') \tag{A.2}$$

  is always denoted by $\mathbb{I} = 1$,

- for $n \in \mathbb{N}$ we denote

$$K^n = \underbrace{K * ... * K}_{n \text{ times}}, \tag{A.3}$$

- the commutator of two operators is defined by

$$[K_1, K_2] = K_1 * K_2 - K_2 * K_1. \tag{A.4}$$

A CF C can be viewed as in some sense dual to functions in Ω. I.e. formally $C : \Omega \to \mathbb{C}$ such that

$$C * f = \int_{-\infty}^{\infty} dx \; C(x) f(x). \tag{A.5}$$

For the case of the factorization theorem of DVCS, see e.g. Eqs. (2.47) and (2.55), the function f is a GPD, which is supported from -1 to 1, so integration is over this region. Furthermore we can identify $C(x) \to \frac{1}{\xi^j} C(x/\xi)$, where $j = 1$ for quarks and $j = 2$ for gluons. These details are usually omitted, since they are clear from the context. Correspondingly we can define the left action of K on CFs as

$$(C * K)(x) = \int_{-\infty}^{\infty} dx' \, C(x') K(x', x). \tag{A.6}$$

At many times it is beneficial to go from the above momentum fraction space to the light-ray position space, where we consider some space $\bar{\Omega}$ of functions of two positions $z_1, z_2 \in \mathbb{R}$ on the light-ray spanned by n. We can relate elements of Ω to $\bar{\Omega}$ by the analogue of Eq. (2.93), i.e.

$$f(z_1, z_2) = \int dx \; e^{i[(1+x)z_1 + (1-x)z_2]} \widetilde{f}(x), \tag{A.7}$$

where we have set the dimensionful scale P^+ to 1 and we also have set $\xi = 1$. These factors can always be reproduced from context.

In this sense, we can define the representation of K on $\bar{\Omega}$, denoted by $\mathcal{K}$. The corresponding action is also denoted by the symbol $*$. The action of $\mathcal{K}$ can be written as

$$(\mathcal{K} * f)(z_1, z_2) = \int_{\Delta_2} d(\alpha, \beta)\mathcal{K}(\alpha, \beta) f(\bar{\alpha} z_1 + \alpha z_2, \bar{\beta} z_2 + \beta z_1), \tag{A.8}$$

where $\Delta_2 = \{0 \leq \alpha \leq \bar{\beta} \leq 1\}$ and $\mathcal{K}(\alpha, \beta)$ is a distribution-valued integration kernel.

It is often useful to write the operator K in terms of $\mathcal{K}(\alpha, \beta)$. In Sec. 2.9 we prove the relation

$$(K * f)(x) = \int dy \ \mathrm{K}(1 + x, 1 - x|1 + y, 1 - y) f(y), \tag{A.9}$$

where

$$\mathrm{K}(x_1, x_2|y_1, y_2) = \int_{\Delta_2} d(\alpha, \beta) \ \mathcal{K}(\alpha, \beta)\delta(x_1 - \bar{\alpha} y_1 - \beta y_2), \tag{A.10}$$

subject to the constraint $x_1 + x_2 = y_1 + y_2$.

Another useful formula is for convolutions with the tree-level quark CF

$$C^{(0)}(x) = \frac{1}{1 - x} - \frac{1}{1 + x}, \tag{A.11}$$

which is given in Eq. (3.81) and the generalization in Eq. (3.82). We repeat

$$(C^{(0)} * K)(x) = \int_{\Delta_2} d(\alpha, \beta) \ \left(\frac{\mathcal{K}(\alpha, \beta)}{\bar{\alpha}(1 - x) + \beta(1 + x)} - (x \leftrightarrow -x) \right). \tag{A.12}$$

B Two-loop matching

To perform the two-loop matching we need explicit expressions for the $\mathcal{Z}$ factors at two-loop accuracy. They can be calculated directly, but are also widely available in the literature. Furthermore, they are directly related to the evolution kernel of the GPDs, see Eq. (2.91).

We present the following NLO results, which hold up to terms of $O(a_s^2)$.

$$\begin{aligned}
\mathcal{Z}_{\rm ns}(\alpha,\beta) &= \mathcal{Z}_{\rm ss}(\alpha,\beta) = \delta(\alpha)\delta(\beta) - a_s\frac{2}{\epsilon}C_F\Big\{1 + \Big[\frac{\bar\alpha}{\alpha}\Big]_+\delta(\beta) + \Big[\frac{\bar\beta}{\beta}\Big]_+\delta(\alpha) - \frac{1}{2}\delta(\alpha)\delta(\beta)\Big\},\\
\mathcal{Z}_{\rm sg}(\alpha,\beta) &= -a_s\frac{4}{\epsilon}n_f T_F(\bar\alpha\bar\beta + 3\alpha\beta),\\
\mathcal{Z}_{gs}(\alpha,\beta) &= -a_s\frac{2}{\epsilon}C_F\Big[2 + \delta(\alpha)\delta(\beta)\Big],\\
\mathcal{Z}_{gg}(\alpha,\beta) &= \delta(\alpha)\delta(\beta) - a_s\frac{2}{\epsilon}C_A\Big\{4(\bar\alpha\bar\beta + 2\alpha\beta)\\
&\qquad + \Big[\frac{\bar\alpha^2}{\alpha}\Big]_+\delta(\beta) + \Big[\frac{\bar\beta^2}{\beta}\Big]_+\delta(\alpha) + \frac{1}{2}(\beta_0 - 6C_A)\delta(\alpha)\delta(\beta)\Big\},
\end{aligned} \tag{B.1}$$

where the delta functions are defined such that $\int_0^1 d\alpha\ \delta(\alpha) = 1$ and the plus distribution is defined by $[f(\alpha)]_+ = f(\alpha) - \delta(\alpha)\int_0^1 d\beta\ f(\beta)$.

Consider the a_s^2 term in Eq. (2.79)

$$\begin{aligned}
C_q^{(2)}(y) &= \frac{\hat{\mathcal{V}}_q^{(2)}(1/y)}{y} - \int dx\ C_q^{(0)}(xy)\hat F_{q/q}^{(2)}(x,1/y) - \int dx\ C_q^{(1)}(xy)F_{q/q}^{(1)}(x,1/y)\\
&\qquad - y\int dx\ C_g^{(1)}(xy)\hat F_{g/q}^{(1)}(x,1/y).\\
C_g^{(2)}(y) &= \frac{\hat{\mathcal{V}}_g^{(2)}(1/y)}{2(y^2-1)} - \frac{y}{2(y^2-1)}\sum_q\int dx\ C_q^{(0)}(xy)\hat F_{q/g}^{(2)}(x,1/y)\\
&\qquad - \frac{y}{2(y^2-1)}\sum_q\int dx\ C_q^{(1)}(xy)\hat F_{q/g}^{(1)}(x,1/y)\\
&\qquad - \frac{y^2}{2(y^2-1)}\int dx\ C_g^{(1)}(xy)\hat F_{g/g}^{(1)}(x,1/y).
\end{aligned} \tag{B.2}$$

where $y = x/\xi = 1 - 2z$. In Eqs. (2.76) and (2.78) we have given the expressions for $\hat F_{q/q}$ and $\hat F_{q/g}$

in terms of the $\mathcal{Z}$-factors. The complete results read

$$\begin{aligned}
\hat{F}_{q/q'}(x,\xi) &= \int_{\Delta_2} d(\alpha,\beta)\ \Big[\delta_{qq'}\mathcal{Z}_{\rm ns}(\alpha,\beta)+\frac{1}{n_f}\mathcal{Z}_{\rm ps}(\alpha,\beta)\Big]\delta\Big(x-h(\alpha,\beta,\xi)\Big),\\
\hat{F}_{q/g}(x,\xi) &= -\frac{(1-\xi^2)}{2n_f}\int_{\Delta_2} d(\alpha,\beta)\ \mathcal{Z}_{sg}(\alpha,\beta)\Big[\delta'\Big(x-h(\alpha,\beta,\xi)\Big)+\delta'\Big(x+h(\alpha,\beta,\xi)\Big)\Big],\\
\hat{F}_{g/q}(x,\xi) &= \int_{\Delta_2} d(\alpha,\beta)\int_{-1}^{1} d\lambda\ \mathcal{Z}_{\rm gs}(\alpha,\beta)h(\alpha,\beta,\xi)\delta\Big(x-\lambda\, h(\alpha,\beta,\xi)\Big),\\
\hat{F}_{g/g}(x,\xi) &= (1-\xi^2)\int_{\Delta_2} d(\alpha,\beta)\ \mathcal{Z}_{gg}(\alpha,\beta)\Big[\delta\Big(x-h(\alpha,\beta,\xi)\Big)+\delta\Big(x+h(\alpha,\beta,\xi)\Big)\Big],
\end{aligned}\tag{B.3}$$

where

$$h(\alpha,\beta,\xi) = (1/2-\alpha)(1+\xi)+(1/2-\beta)(1-\xi).\tag{B.4}$$

All divergences on the right-hand-side of Eq. (B.2) must cancel, which is a great check of the calculation. To verify the cancellation of the simple $\frac{1}{\epsilon}$ poles, using the methods explained above, one must know the two-loop kernels $\mathcal{Z}^{(2)}_{\chi\chi'}$ in light-ray position space. These are trivially related to the two-loop evolution kernel in light-ray position space, see Eq. (2.88), which was calculated in Ref. [82]. Alternatively one can use the momentum fraction space representation for which the two-loop kernel was calculated in Ref. [81]. However, as mentioned before, this is more difficult, because momentum fraction space kernels are more complicated.

From Eq. (B.2) we can observe the occurence of finite subtractions. We present the results for the vector case. Denote $y = x/\xi = 1-2z$ and $\mathrm{H}_{i,j,\ldots} = \mathrm{H}_{i,j,\ldots}(z)$ are the HPLs introduced in Sec. 3.4.

The quark-in-quark finite IR subtraction

$$
\begin{aligned}
&-4z(1-z)/e_q^2\int dx\; C_q^{(1,1)}\hat{F}_{q/q}^{(1,-1)}(x,1/y)\\
&\quad= L^2\beta_0 C_F\Big[\mathrm{H}_1 z+\mathrm{H}_0(1-z)-3z+\frac{3}{2}\Big]\\
&\qquad L^2C_F^2\Big[4z\mathrm{H}_{1,1}+4(z-1)\mathrm{H}_{0,0}+2(z-1)\mathrm{H}_{1,0}+2\mathrm{H}_2 z+\mathrm{H}_0(4z-6)+\mathrm{H}_1(-4z-2)\\
&\qquad-2\zeta_2 z+9z-\frac{9}{2}\Big]\\
&\qquad+L\beta_0 C_F\Big[2z\mathrm{H}_{1,1}+2(z-1)\mathrm{H}_{0,0}+3\mathrm{H}_0 z+\mathrm{H}_1(3-3z)-18z+9\Big]\\
&\qquad+LC_F^2\Big[4z\mathrm{H}_{1,2}+4z\mathrm{H}_{2,1}+12z\mathrm{H}_{1,1,1}+(6-8z)\mathrm{H}_{0,0}+(2-8z)\mathrm{H}_{1,1}+(4-4z)\mathrm{H}_{2,0}\\
&\qquad-12(z-1)\mathrm{H}_{0,0,0}+(4-4z)\mathrm{H}_{1,0,0}+\mathrm{H}_1(-4\zeta_2 z-11z-7)+\mathrm{H}_0(11z-18)\\
&\qquad+\zeta_3(8-12z)+54z-27\Big]\\
&\qquad+\beta_0 C_F\Big[-3z\mathrm{H}_{0,0}+(3-3z)\mathrm{H}_{1,1}+(2-2z)\mathrm{H}_{0,0,0}+2z\mathrm{H}_{1,1,1}+\mathrm{H}_0(\zeta_2(z-1)+5z-1)\\
&\qquad+\mathrm{H}_1(-\zeta_2 z-5z+4)+\frac{3}{2}(\zeta_2-12)(2z-1)\Big]\\
&\qquad+C_F^2\Big[\mathrm{H}_{0,0}(-4\zeta_2(z-1)-5z+4)-2(\zeta_2+1)(z-1)\mathrm{H}_{1,0}+\mathrm{H}_{1,1}(-8\zeta_2 z-5z+1)\\
&\qquad+(6-6z)\mathrm{H}_{1,2}+6z\mathrm{H}_{2,0}+4(z-1)\mathrm{H}_{3,0}+(14z-6)\mathrm{H}_{0,0,0}+(8-14z)\mathrm{H}_{1,1,1}+4z\mathrm{H}_{1,1,2}\\
&\qquad+4z\mathrm{H}_{1,2,1}+4(z-1)\mathrm{H}_{2,0,0}+4z\mathrm{H}_{2,1,1}+16(z-1)\mathrm{H}_{0,0,0,0}+4(z-1)\mathrm{H}_{1,0,0,0}\\
&\qquad+16z\mathrm{H}_{1,1,1,1}-2(\zeta_2+1)\mathrm{H}_2 z+\mathrm{H}_1(2\zeta_2(5z-2)-(4\zeta_3+33)z)\\
&\qquad+\mathrm{H}_0(\zeta_2(6-4z)+(8\zeta_3+33)(z-1))+\frac{2\zeta_2^2 z}{5}+\zeta_2(\frac{9}{2}-7z)+6(2\zeta_3 z+18z-9)\Big].
\end{aligned}
\tag{B.5}
$$

The gluon-in-quark finite IR subtraction

$$
\begin{aligned}
&-\frac{yz(1-z)}{4C_F T_F\sum_{q'}e_{q'}^2}\int dx\; C_g^{(1,1)}(xy)\hat{F}_{g/q}^{(1,-1)}(x,1/y)\\
&\quad= L^2\Big[(z-1)\mathrm{H}_{1,0}+\frac{1}{2}\mathrm{H}_0(3-4z)z-\frac{1}{2}\mathrm{H}_1(z-1)(4z-1)+\mathrm{H}_2 z-\zeta_2 z\Big]\\
&\qquad+L\Big[z(4z-3)\mathrm{H}_{0,0}+2(z-1)(2z+1)\mathrm{H}_{1,0}+((5-4z)z-1)\mathrm{H}_{1,1}+2z\mathrm{H}_{2,1}+(2-2z)\mathrm{H}_{1,0,0}\\
&\qquad+2\mathrm{H}_0(3-4z)z-2\mathrm{H}_1(z-1)(4z-1)+2\mathrm{H}_2(3-2z)z+2z(\zeta_2(2z-3)-\zeta_3)\Big]\\
&\qquad+(-4z^2+2z+2)\mathrm{H}_{1,0,0}+(z-1)\mathrm{H}_{1,0}(-\zeta_2+8z+6)\\
&\qquad+2z(4z-3)\mathrm{H}_{0,0}-2(z-1)(4z-1)\mathrm{H}_{1,1}\\
&\qquad+2(3-2z)z\mathrm{H}_{2,1}+(3-4z)z\mathrm{H}_{0,0,0}+((5-4z)z-1)\mathrm{H}_{1,1,1}+2z\mathrm{H}_{2,1,1}+2(z-1)\mathrm{H}_{1,0,0,0}\\
&\qquad+\frac{1}{2}(\zeta_2-10)\mathrm{H}_0 z(4z-3)+\frac{1}{2}(\zeta_2-10)\mathrm{H}_1(z-1)(4z-1)-\mathrm{H}_2 z(\zeta_2+8z-14)\\
&\qquad+\frac{1}{5}\zeta_2 z(\zeta_2+40z-70)+2\zeta_3 z(2z-3).
\end{aligned}
\tag{B.6}
$$

The quark-in-gluon finite IR subtraction

$$
\begin{aligned}
&\frac{yz(1-z)}{4C_F T_F \sum_{q'} e_{q'}^2} \sum_q \int dx\; C_q^{(1,1)}(xy) \hat{F}_{q/g}^{(1,-1)}(x,1/y) \\
&\quad = L^2\Big[z^2 \mathrm{H}_{0,0} + (z-1)^2 \mathrm{H}_{1,1} - \frac{1}{2}\mathrm{H}_1(z+1)(z-1) + \frac{1}{2}\mathrm{H}_0(z-2)z + z(z-1)\Big] \\
&\qquad L\Big[-2z^2 \mathrm{H}_{0,0,0} + 3(z-1)^2 \mathrm{H}_{1,0} + 2(z-1)^2 \mathrm{H}_{1,1,1} + 2(z-2)(z-1)\mathrm{H}_{1,1} + 2z(z+1)\mathrm{H}_{0,0} \\
&\qquad + 3\mathrm{H}_2 z^2 - \mathrm{H}_1(9z-4)(z-1) + \mathrm{H}_0 z(9z-5) - 3\zeta_2 z^2\Big] \\
&\qquad + 3z^2 \mathrm{H}_{2,1} + 2z^2 \mathrm{H}_{0,0,0,0} - (z-1)\mathrm{H}_{1,1}(\zeta_2(z-1) + z + 4) \\
&\qquad - z\mathrm{H}_{0,0}(\zeta_2 z + z - 5) + 4(z-1)^2 \mathrm{H}_{1,0} \\
&\qquad - 3(z-1)^2 \mathrm{H}_{1,0,0} + 2(z-1)^2 \mathrm{H}_{1,1,1,1} + 2(z-2)(z-1)\mathrm{H}_{1,1,1} - 2z(z+1)\mathrm{H}_{0,0,0} \\
&\qquad + 4\mathrm{H}_2 z^2 + \frac{1}{2}\mathrm{H}_1(z-1)(\zeta_2(z+1) - 48z + 32) - \frac{1}{2}\mathrm{H}_0 z(\zeta_2(z-2) - 48z + 16) \\
&\qquad + z(-3\zeta_3 z + \zeta_2(1-5z) - 6z + 6).
\end{aligned} \tag{B.7}
$$

The gluon-in-gluon finite IR subtraction

$$
\begin{aligned}
&\frac{y^2 z(1-z)}{4T_F C_A} \sum_q \int dx\; C_g^{(1,1)}(xy) \hat{F}_{g/g}^{(1,-1)}(x,1/y) \\
&\quad = L^2\Big[z^2 \mathrm{H}_{0,0} + 3(z-1)^2 \mathrm{H}_{1,0} + (z-1)^2 \mathrm{H}_{1,1} + 3\mathrm{H}_2 z^2 + \mathrm{H}_0 z((5-4z)z - 4) \\
&\qquad + \mathrm{H}_1(z((7-4z)z - 6) + 3) - z(3\zeta_2 z + z - 1)\Big] \\
&\qquad + L\Big[2(4z^2 + z - 4)(z-1)\mathrm{H}_{1,0} - 2z^2 \mathrm{H}_{2,0} + 6z^2 \mathrm{H}_{2,1} - 4z^2 \mathrm{H}_{0,0,0} + 2(z-1)^2 \mathrm{H}_{1,2} \\
&\qquad - 6(z-1)^2 \mathrm{H}_{1,0,0} + 4(z-1)^2 \mathrm{H}_{1,1,1} - 2(4(z-1)z + 5)(z-1)\mathrm{H}_{1,1} + 2z(4(z-1)z + 5)\mathrm{H}_{0,0} \\
&\qquad - \mathrm{H}_1(z-1)(2\zeta_2(z-1) + z(16z-11) + 15) + \mathrm{H}_0 z((21-16z)z - 20) \\
&\qquad - 2\mathrm{H}_2 z(z(4z-9) + 1) + z(2\zeta_2(z(4z-9) + 1) - 5(2\zeta_3 z + z - 1))\Big] \\
&\qquad - 2(4z^2 + z - 4)(z-1)\mathrm{H}_{1,0,0} + 2z^2 \mathrm{H}_{3,0} + 2z^2 \mathrm{H}_{2,0,0} + 6z^2 \mathrm{H}_{2,1,1} + 6z^2 \mathrm{H}_{0,0,0,0} \\
&\qquad + (z-1)\mathrm{H}_{1,0}(-3\zeta_2(z-1) + 2z(8z+5) - 22) - (z-1)\mathrm{H}_{1,1}(3\zeta_2(z-1) + z(16z-17) + 25) \\
&\qquad + z\mathrm{H}_{0,0}(-\zeta_2 z + z(16z-15) + 24) + 2(z-1)^2 \mathrm{H}_{1,1,2} + 2(z-1)^2 \mathrm{H}_{1,2,1} + 6(z-1)^2 \mathrm{H}_{1,0,0,0} \\
&\qquad + 6(z-1)^2 \mathrm{H}_{1,1,1,1} + 2(z-2)(z-1)\mathrm{H}_{1,2} - 2(z(4z-5) + 7)(z-1)\mathrm{H}_{1,1,1} - 2z(z+1)\mathrm{H}_{2,0} \\
&\qquad - 2z(z(4z-9) + 1)\mathrm{H}_{2,1} - 2z(z(4z-3) + 6)\mathrm{H}_{0,0,0} + \frac{1}{2}\mathrm{H}_1(z-1)(-80z^2 + 2\zeta_2(z(4z-5) + 7) \\
&\qquad - 4\zeta_3(z-1) + 55z - 79) - \mathrm{H}_2 z(3\zeta_2 z + 2z(8z-21) + 4) + \frac{1}{2}\mathrm{H}_0 z(8\zeta_3 z + 2\zeta_2(z(4z-5) + 4) \\
&\qquad + 5(21-16z)z - 104) + \frac{1}{5}\zeta_2 z(3\zeta_2 z + 5z(16z-41) + 15) \\
&\qquad + 2\zeta_3 z(z(4z-11) - 1) - \frac{25}{2}z(z-1).
\end{aligned} \tag{B.8}
$$

C Explicit results for the two-loop vector CF

In this Appendix we collect explicit expressions for the vector CF at NNLO. For completeness, we repeat the expressions tree-level and one-loop expressions

$$
\begin{aligned}
C_q^{(0)} &= \frac{e_q^2(1-2z)}{2z(1-z)},\\
C_q^{(1)} &= \frac{e_q^2 C_F}{2z(1-z)}\Big\{L\Big[4(z\log(1-z)-(1-z)\log z)-3(1-2z)\Big]+(1-z)\log^2 z - z\log^2(1-z)\\
&\quad +3\Big[(1-z)\log(1-z)-z\log z\Big]-9(1-2z)\Big\},\\
C_g^{(1)} &= \frac{\Big(\sum_q e_q^2\Big)T_F}{4z^2(1-z)^2}\Big\{2L\Big[z^2\log z+(1-z)^2\log(1-z)\Big]-z^2\log^2 z-(1-z)^2\log^2(1-z)\\
&\quad +2\Big[z(1+z)\log z+(1-z)(2-z)\log(1-z)\Big]\Big\}.
\end{aligned}
\tag{C.1}
$$

We organize the two-loop result as follows

$$
\begin{aligned}
C_q^{(2)} &= \frac{1}{2z(1-z)}\Big[e_q^2 C_F\Big(C_F \mathrm{C}_{\mathrm{ns}}^{(F)} + C_A \mathrm{C}_{\mathrm{ns}}^{(A)} + \beta_0 \mathrm{C}_{\mathrm{ns}}^{(\beta_0)}\Big) + \Big(\sum_{q'} e_{q'}^2\Big) T_F C_F \mathrm{C}_{\mathrm{ps}}\Big],\\
C_g^{(2)} &= \frac{\Big(\sum_q e_q^2\Big)}{4z^2(1-z)^2} T_F\Big(C_F \mathrm{C}_g^{(F)} + C_A \mathrm{C}_g^{(A)}\Big).
\end{aligned}
\tag{C.2}
$$

In the following $\mathrm{H}_{i,j,\ldots} = \mathrm{H}_{i,j,\ldots}(z)$ are the HPLs introduced in Sec. 3.4. The C_F^2 contribution to the quark CF reads

$$
\begin{aligned}
\mathrm{C}_{\rm ns}^{(F)} = {} & L^2\Big[-4z\mathrm{H}_{1,1} - 4(z-1)\mathrm{H}_{0,0} - 2(z-1)\mathrm{H}_{1,0} - 2\mathrm{H}_2 z \\
& + \mathrm{H}_0(6-4z) + \mathrm{H}_1(4z+2) + 2\zeta_2 z - 9z + \frac{9}{2}\Big] \\
& + L\Big[-8z\mathrm{H}_{1,2} - 12z\mathrm{H}_{1,1,1} + (8z-6)\mathrm{H}_{0,0} - 8(z-1)\mathrm{H}_{1,0} + (8z-2)\mathrm{H}_{1,1} + 8(z-1)\mathrm{H}_{2,0} \\
& + 12(z-1)\mathrm{H}_{0,0,0} + 4(z+1)\mathrm{H}_{1,1,0} + \mathrm{H}_1\Big(4\zeta_2(3z+1) + 7z + 11\Big) - 8\mathrm{H}_2 z + \mathrm{H}_0(18-7z) \\
& - 4\mathrm{H}_3(z-2) + \zeta_2(6-4z) + 28\zeta_3(z-1) - 51z + \frac{51}{2}\Big] \\
& - 12(z-1)\mathrm{H}_{0,0,0,0} + (36-58z)\mathrm{H}_{1,0,0,0} + (40-70z)\mathrm{H}_{1,1,0,0} \\
& - 6(7z-6)\mathrm{H}_{1,1,1,0} - 12z\mathrm{H}_{1,1,1,1} - 24(z-1)\Big(2z^2 - z + 1\Big)\mathrm{H}_{1,1,0} \\
& - 2z\mathrm{H}_{0,0,0} + 4(3z-2)\mathrm{H}_{1,0,0} + 2(z-1)\mathrm{H}_{1,1,1} \\
& + (42-72z)\mathrm{H}_{1,1,2} + (28-38z)\mathrm{H}_{1,2,0} + (38-68z)\mathrm{H}_{1,2,1} \\
& + (46-68z)\mathrm{H}_{2,0,0} + (44-70z)\mathrm{H}_{2,1,0} \\
& + (38-58z)\mathrm{H}_{2,1,1} + \mathrm{H}_{1,0}\Big(48z^2 + \zeta_2(28-38z) - 44z + 10\Big) \\
& + 6(z-1)\Big(8z^2 - 4z + 3\Big)\mathrm{H}_{1,2} - 6z\Big(8z^2 - 12z + 7\Big)\mathrm{H}_{2,0} \\
& + \mathrm{H}_{1,1}\Big(\zeta_2(26z-2) + 25z - 7\Big) + \mathrm{H}_{0,0}\Big((60z-38)\mathrm{H}_{1,1} - 4\zeta_2 z + 25z - 18\Big) \\
& + (42-70z)\mathrm{H}_{1,3} + (4-12z)\mathrm{H}_{2,1} + (26-38z)\mathrm{H}_{2,2} + (46-72z)\mathrm{H}_{3,0} + (46-70z)\mathrm{H}_{3,1} \\
& + \mathrm{H}_2\Big(-48z^2 + \zeta_2(44-70z) + 52z - 14\Big) + 24\mathrm{H}_3 z\Big(2z^2 - 3z + 2\Big) + \mathrm{H}_4(22-42z) \\
& + \mathrm{H}_0\Big(\zeta_2\Big(\mathrm{H}_1(60z-38) - 48z^3 + 72z^2 - 44z + 6\Big) + \zeta_3(8z+4) + \frac{1}{2}(121-96z)z\Big) \\
& + \mathrm{H}_1\Big(\zeta_2\Big(-48z^3 + 72z^2 - 46z + 28\Big) + \frac{1}{2}\Big(-96z^2 + \zeta_3(44z-8) + 71z + 25\Big)\Big) \\
& + \zeta_2\Big(48z^2 - 76z + 26\Big) + \zeta_3\Big(144z^3 - 216z^2 + 154z - 69\Big) \\
& - \frac{1}{5}\zeta_2^2(31z-13) - \frac{331}{8}(2z-1). \qquad \text{(C.3)}
\end{aligned}
$$

The $C_F C_A$ contribution to the quark CF reads

$$
\begin{aligned}
\mathrm{C}_{\mathrm{ns}}^{(A)} = L\Big[&4z\mathrm{H}_{1,2} - 4z\mathrm{H}_{1,1,0} - 4(z-1)\mathrm{H}_{2,0} - \frac{4}{3}\mathrm{H}_0\Big(3\zeta_2(z-1) - 5z + 2\Big) \\
&- \frac{4}{3}\mathrm{H}_1\Big(3\zeta_2 z + 5z - 3\Big) + 4\mathrm{H}_3(z-1) - 12\zeta_3(z-1) + 2z - 1\Big] \\
&+ (30z-19)\mathrm{H}_{1,0,0,0} + (36z-21)\mathrm{H}_{1,1,0,0} + (20z-17)\mathrm{H}_{1,1,1,0} \\
&+ 2(z-1)\Big(12z^2 - 6z + 5\Big)\mathrm{H}_{1,1,0} + (36z-21)\mathrm{H}_{1,1,2} + 5(4z-3)\mathrm{H}_{1,2,0} \\
&+ (36z-19)\mathrm{H}_{1,2,1} + (36z-25)\mathrm{H}_{2,0,0} + (36z-23)\mathrm{H}_{2,1,0} + (30z-19)\mathrm{H}_{2,1,1} \\
&+ \mathrm{H}_{1,0}\Big(-24z^2 + 5\zeta_2(4z-3) + \frac{64z}{3} - \frac{4}{3}\Big) - 2(z-1)\Big(12z^2 - 6z + 5\Big)\mathrm{H}_{1,2} \\
&+ 2z\Big(12z^2 - 18z + 11\Big)\mathrm{H}_{2,0} + \mathrm{H}_{1,1}\Big(\zeta_2(2-10z) - \frac{38z}{3} + 10\Big) \\
&+ \mathrm{H}_{0,0}\Big((19-30z)\mathrm{H}_{1,1} + \frac{2}{3}\Big(\zeta_2(9z-6) - 19z + 4\Big)\Big) + (36z-21)\mathrm{H}_{1,3} \\
&+ (20z-13)\mathrm{H}_{2,2} + (36z-23)\mathrm{H}_{3,0} + (36z-23)\mathrm{H}_{3,1} \\
&+ \mathrm{H}_2\Big(24z^2 + \zeta_2(36z-23) - \frac{80z}{3} + 4\Big) \\
&+ \mathrm{H}_0\Big(2\zeta_2\Big(12z^2 - 18z + 11\Big)z + 24z^2 + \zeta_3(14-20z) - \frac{73z}{9} - \frac{32}{9}\Big) \\
&+ \mathrm{H}_1\Big(-\zeta_2\mathrm{H}_0(30z-19) + 2\zeta_2\Big(12z^3 - 18z^2 + 11z - 5\Big) + 24z^2 + 4\zeta_3 z - \frac{359z}{9} + \frac{37}{3}\Big) \\
&- 2\mathrm{H}_3 z\Big(12z^2 - 18z + 11\Big) + \mathrm{H}_4(20z-11) - \frac{2}{3}\zeta_2\Big(36z^2 - 50z + 11\Big) \\
&- 6\zeta_3\Big(12z^3 - 18z^2 + 19z - 9\Big) + \frac{1}{5}\zeta_2^2(13z+1) + \frac{73}{12}(2z-1). \qquad \text{(C.4)}
\end{aligned}
$$

The $\beta_0 C_F$ contribution to the quark CF reads

$$
\begin{aligned}
\mathrm{C}_{\mathrm{ns}}^{(\beta_0)} = L^2\Big[&-\mathrm{H}_1 z + \mathrm{H}_0(z-1) + 3z - \frac{3}{2}\Big] \\
&+ L\Big[-2z\mathrm{H}_{1,1} - 2(z-1)\mathrm{H}_{0,0} + 2(z-1)\mathrm{H}_{1,0} + 2\mathrm{H}_2 z + \frac{1}{3}\mathrm{H}_0(7z-10) - \frac{1}{3}\mathrm{H}_1(7z+3) \\
&+ 2\zeta_2(z-1) + 19z - \frac{19}{2}\Big] \\
&+ 2(z-1)\mathrm{H}_{0,0,0} + (2-2z)\mathrm{H}_{1,0,0} + (z-1)\mathrm{H}_{1,1,0} \\
&- 2z\mathrm{H}_{1,1,1} + \frac{1}{3}(10-7z)\mathrm{H}_{0,0} + \frac{2}{3}(4z-7)\mathrm{H}_{1,0} \\
&+ \Big(-\frac{7z}{3} - 1\Big)\mathrm{H}_{1,1} + 2z\mathrm{H}_{2,1} + \mathrm{H}_1\Big(\zeta_2(z-1) + \frac{1}{18}(31z-69)\Big) + \frac{1}{18}\mathrm{H}_0(-31z-38) \\
&+ \mathrm{H}_2\Big(\frac{8z}{3} + 2\Big) - \mathrm{H}_3 z + \frac{2}{3}\zeta_2(4z-7) + \zeta_3(z-1) + \frac{457}{24}(2z-1). \qquad \text{(C.5)}
\end{aligned}
$$

The pure singlet contribution to the quark CF reads

$$
\begin{aligned}
\mathrm{C}_{\rm ps} = {} & L^2\Big[-8(z-1)\mathrm{H}_{1,0} + 4\mathrm{H}_1\Big(4z^2-5z+1\Big) + 4\mathrm{H}_0 z(4z-3) - 8\mathrm{H}_2 z + 8\zeta_2 z\Big] \\
& + 8L\Big[-z(4z-3)\mathrm{H}_{0,0} - (z-1)(4z-1)\mathrm{H}_{1,0} + (z-1)(4z-1)\mathrm{H}_{1,1} \\
& - 2z\mathrm{H}_{2,1} + 2(z-1)\mathrm{H}_{1,0,0} - 2(z-1)\mathrm{H}_{1,1,0} - \Big(2\zeta_2-3\Big)\mathrm{H}_1(z-1) \\
& - 3\mathrm{H}_0 z + \mathrm{H}_2 z(4z-3) + 2\mathrm{H}_3 z - \zeta_2 z(4z-3)\Big] \\
& - 16(z-1)\mathrm{H}_{1,0,0,0} + 16(z-1)\mathrm{H}_{1,1,0,0} + (8-8z)\mathrm{H}_{1,1,1,0} + 8z(4z-3)\mathrm{H}_{0,0,0} \\
& + 8(z-1)(4z-1)\mathrm{H}_{1,0,0} - 4(z-1)(4z+5)\mathrm{H}_{1,1,0} + 8(z-1)(4z-1)\mathrm{H}_{1,1,1} - 16z\mathrm{H}_{2,1,1} \\
& - 16z^2\mathrm{H}_{2,0} - 8\Big(\zeta_2-3\Big)(z-1)\mathrm{H}_{1,1} - 16(z-1)^2\mathrm{H}_{1,2} + 24z\mathrm{H}_{0,0} + (4-4z)\mathrm{H}_{1,0} \\
& + 8z(4z-3)\mathrm{H}_{2,1} + 16z\mathrm{H}_{3,1} - 8\mathrm{H}_0 z\Big(2\zeta_2 z+5\Big) - 4\mathrm{H}_1(z-1)\Big(2\Big(\zeta_3-5\Big) + \zeta_2(4z+5)\Big) \\
& - 4\mathrm{H}_2 z - 4\mathrm{H}_3 z(4z-9) - 8\mathrm{H}_4 z + 4z\Big(2\zeta_2^2 + \zeta_2 - 3\zeta_3(4z+1)\Big). \qquad \text{(C.6)}
\end{aligned}
$$

The $C_F T_F$ contribution to the gluon CF reads

$$
\begin{aligned}
\mathrm{C}_g^{(F)} = {} & L^2\Big[-2\Big(z^2\mathrm{H}_{0,0} + (z-1)\Big((z-1)\mathrm{H}_{1,1} + z\Big)\Big) + \mathrm{H}_1\Big(z^2-1\Big) + \mathrm{H}_0(-(z-2))z\Big] \\
& + L\Big[8z^2\mathrm{H}_{0,0,0} - 4(z-1)^2\mathrm{H}_{1,0} - 8(z-1)^2\mathrm{H}_{1,1,1} - 4(z-3)(z-1)\mathrm{H}_{1,1} - 4z(z+2)\mathrm{H}_{0,0} \\
& - 4\mathrm{H}_2 z^2 + 4\mathrm{H}_1(z-1)\Big(\zeta_2(z-1) - 2z + 5\Big) \\
& - 4\mathrm{H}_0 z\Big(\zeta_2 z - 2z - 3\Big) + 4z\Big(\zeta_2 z - 4z + 4\Big)\Big] \\
& - 10z^2\mathrm{H}_{0,0,0,0} - 36z^2\mathrm{H}_{1,0,0,0} - 36z^2\mathrm{H}_{1,1,0,0} \\
& - 4\Big(7z^2 + 4z - 2\Big)\mathrm{H}_{1,1,1,0} - 10(z-1)^2\mathrm{H}_{1,1,1,1} \\
& + \Big(-8z^4 + 16z^3 - 5z^2 + 2z - 5\Big)\mathrm{H}_{1,1,0} \\
& - 2\Big(23z^2 - 10z + 5\Big)\mathrm{H}_{1,1,2} - 4\Big(7z^2 + 4z - 2\Big)\mathrm{H}_{1,2,0} \\
& + \Big(-34z^2 - 4z + 2\Big)\mathrm{H}_{1,2,1} - 34z^2\mathrm{H}_{2,0,0} - 44z^2\mathrm{H}_{2,1,0} - 36z^2\mathrm{H}_{2,1,1} + 4(z-1)^2\mathrm{H}_{1,0,0} \\
& - 10(z-2)(z-1)\mathrm{H}_{1,1,1} + 10z(z+1)\mathrm{H}_{0,0,0} \\
& + \mathrm{H}_{1,0}\Big(-4\zeta_2\Big(7z^2 + 4z - 2\Big) + 8z^3 - 11z^2 + 6z - 3\Big) - 4z^2\mathrm{H}_{2,1} - 28z^2\mathrm{H}_{2,2} - 46z^2\mathrm{H}_{3,0} \\
& - 36z^2\mathrm{H}_{3,1} + 8\Big(z^4 - 2z^3 + z\Big)\mathrm{H}_{1,2} - 4\Big(11z^2 - 4z + 2\Big)\mathrm{H}_{1,3} - 8\Big(z^4 - 2z^3 + z\Big)\mathrm{H}_{2,0} \\
& - 2z\mathrm{H}_{0,0}\Big(-18z\mathrm{H}_{1,1} + 3\zeta_2 z + 3z + 10\Big) + 2(z-1)\mathrm{H}_{1,1}\Big(6\zeta_2(z-1) - 3z + 13\Big) \\
& - \mathrm{H}_2 z\Big(8z^2 + 44\zeta_2 z - 13z + 8\Big) \\
& + 2\mathrm{H}_0 z\Big(\zeta_2\Big(18\mathrm{H}_1 z - 4z^3 + 8z^2 - 3z - 5\Big) - 4z^2 - 4\zeta_3 z + 23z + 9\Big) \\
& - \mathrm{H}_1(z-1)\Big(\zeta_2\Big(8z^3 - 8z^2 - 9z + 3\Big) + 8z^2 - 2\zeta_3(z-1) + 30z - 56\Big) - 28\mathrm{H}_4 z^2 \\
& + \mathrm{H}_3\Big(8z^3 - 16z^2 + 5z + 8\Big)z + z\Big(\zeta_2\Big(8z^2 - 13z + 8\Big) + \zeta_3\Big(24z^3 - 48z^2 - z + 24\Big) \\
& - 16\zeta_2^2 z - 36(z-1)\Big). \qquad \text{(C.7)}
\end{aligned}
$$

The $C_A T_F$ contribution to the gluon CF reads

$$
\begin{aligned}
\mathrm{C}_g^{(A)} = {} & 2L^2\Big[- z^2\mathrm{H}_{0,0} - 3(z-1)^2\mathrm{H}_{1,0} - (z-1)^2\mathrm{H}_{1,1} \\
& + \mathrm{H}_0 z\Big(4z^2 - 5z + 4\Big) + \mathrm{H}_1\Big(4z^3 - 7z^2 + 6z - 3\Big) - 3\mathrm{H}_2 z^2 + z\Big(3\zeta_2 z + z - 1\Big)\Big] \\
& + L\Big[16\Big(z^2 - z + 1\Big)(z-1)\mathrm{H}_{1,1} - 16z\Big(z^2 - z + 1\Big)\mathrm{H}_{0,0} \\
& + 4z^2\mathrm{H}_{2,0} + \Big(- 8z^2 - 8z + 4\Big)\mathrm{H}_{2,1} + 4z^2\mathrm{H}_{0,0,0} + 4\Big(2z^2 - 6z + 3\Big)\mathrm{H}_{1,0,0} \\
& - 8(2z+1)(z-1)^2\mathrm{H}_{1,0} - 4(z-1)^2\mathrm{H}_{1,2} - 8(z-1)^2\mathrm{H}_{1,1,0} \\
& - 4(z-1)^2\mathrm{H}_{1,1,1} + 8\mathrm{H}_2 z^2(2z-3) + 8\mathrm{H}_3 z^2 - 2\mathrm{H}_1(z-1)\Big(2\zeta_2(z-1) - 7(z+1)\Big) \\
& - 14\mathrm{H}_0(z-2)z - 2z\Big(4\zeta_2(2z-3)z - 8\zeta_3 z - 9z + 9\Big)\Big] \\
& - 2z^2\mathrm{H}_{0,0,0,0} + 2\Big(5z^2 - 6z + 3\Big)\mathrm{H}_{1,1,0,0} + 2\Big(z^2 + 6z - 3\Big)\mathrm{H}_{1,1,1,0} - 2(z-1)^2\mathrm{H}_{1,1,1,1} \\
& + 14(2z-1)\mathrm{H}_{1,0,0,0} + 2z\Big(8z^2 - 8z + 7\Big)\mathrm{H}_{0,0,0} + 2\Big(8z^3 - 14z^2 - z + 4\Big)\mathrm{H}_{1,0,0} \\
& - 2(z-1)\Big(4z^2 + 5z - 7\Big)\mathrm{H}_{1,1,0} + 2(z-1)\Big(8z^2 - 8z + 7\Big)\mathrm{H}_{1,1,1} \\
& + 2\Big(5z^2 - 2z + 1\Big)\mathrm{H}_{1,1,2} + 2\Big(5z^2 + 2z - 1\Big)\mathrm{H}_{1,2,0} \\
& + 2\Big(z^2 + 6z - 3\Big)\mathrm{H}_{1,2,1} + 2\Big(z^2 + 2z - 1\Big)\mathrm{H}_{2,0,0} + 2\Big(5z^2 + 2z - 1\Big)\mathrm{H}_{2,1,0} \\
& + (4 - 8z)\mathrm{H}_{2,1,1} + \mathrm{H}_{1,0}\Big(2\zeta_2\Big(5z^2 + 2z - 1\Big) - 5\Big(2z^2 - 5z + 3\Big)\Big) \\
& + \mathrm{H}_{0,0}\Big(\Big(- 6z^2 - 4z + 2\Big)\mathrm{H}_{1,1} + 2z\Big(4\zeta_2 z + 3z - 13\Big)\Big) + 2\Big(5z^2 - 2z + 1\Big)\mathrm{H}_{1,3} \\
& - 4z^2(2z-1)\mathrm{H}_{2,0} + 2\Big(8z^3 - 10z^2 - 5z + 3\Big)\mathrm{H}_{2,1} + 2\Big(5z^2 - 2z + 1\Big)\mathrm{H}_{2,2} \\
& + 2\Big(5z^2 + 2z - 1\Big)\mathrm{H}_{3,0} + 2\Big(5z^2 + 6z - 3\Big)\mathrm{H}_{3,1} - 4(2z-1)(z-1)^2\mathrm{H}_{1,2} \\
& + 2(3z + 10)(z-1)\mathrm{H}_{1,1} + \mathrm{H}_2\Big(2\zeta_2\Big(5z^2 + 2z - 1\Big) - 5z(2z+1)\Big) \\
& + \mathrm{H}_1\Big(- 2\zeta_2\Big(4z^3 - z^2 - 8z + 5\Big) + 4\zeta_3\Big(5z^2 - 4z + 2\Big) + 29z^2 - 8z - 21\Big) \\
& + \mathrm{H}_0\Big(- 2\zeta_2\mathrm{H}_1\Big(3z^2 + 2z - 1\Big) - z\Big(8\zeta_2 z^2 + 4\zeta_3 z + 29z - 50\Big)\Big) \\
& - 2\mathrm{H}_3 z\Big(4z^2 - 13z + 2\Big) + 2\mathrm{H}_4\Big(z^2 + 2z - 1\Big) \\
& + \frac{82}{5}\zeta_2^2 z^2 - 2\zeta_3 z\Big(12z^2 - 17z + 9\Big) \\
& \quad + 5\zeta_2 z(2z+1) + 37(z-1)z. \qquad \text{(C.8)}
\end{aligned}
$$

D Expressions for f and h functions

We collect the results for the functions f and h, defined in their bare form in Eqs. (5.14) and (5.15). The one- and two-loop expressions are

$$
\begin{aligned}
f^{(1)}(-\hat{s},\mu^2) &= C_F \log^2\frac{-\hat{s}}{\mu^2} + \bar{f}^{(1)},\\
f^{(2)}(-\hat{s},\mu^2) &= \frac{1}{2}C_F^2\log^4\frac{-\hat{s}}{\mu^2} - \frac{1}{3}\beta_0 C_F\log^3\frac{-\hat{s}}{\mu^2}\\
&\quad + \Big[-\Big(1+\frac{\pi^2}{6}\Big)C_F^2 + \Big(\frac{4}{3}-\frac{\pi^2}{3}\Big)C_F C_A + \frac{5}{3}\beta_0 C_F\Big]\log^2\frac{-\hat{s}}{\mu^2}\\
&\quad + \Big[C_F^2(\pi^2+4\zeta_3) - C_F C_A\Big(\frac{32}{9}-14\zeta_3\Big) - \frac{19}{9}\beta_0 C_F\Big]\log\frac{-\hat{s}}{\mu^2} + \bar{f}^{(2)},\\
h^{(1)}(Q^2,\mu^2) &= -C_F\log^2\frac{Q^2}{\mu^2} + 3C_F\log\frac{Q^2}{\mu^2} + \bar{h}^{(1)},\\
h^{(2)}(Q^2,\mu^2) &= \frac{1}{2}C_F^2\log^4\frac{Q^2}{\mu^2} + \Big(-3C_F^2+\frac{1}{3}\beta_0 C_F\Big)\log^3\frac{Q^2}{\mu^2}\\
&\quad + \Big[\Big(\frac{25}{2}-\frac{\pi^2}{6}\Big)C_F^2 - \Big(\frac{4}{3}-\frac{\pi^2}{6}\Big)C_F C_A - \frac{19}{6}\beta_0 C_F\Big]\log^2\frac{Q^2}{\mu^2}\\
&\quad + \Big[-\Big(\frac{45}{2}+\frac{3\pi^2}{2}-24\zeta_3\Big)C_F^2 + \Big(\frac{41}{9}-26\zeta_3\Big)C_F C_A\\
&\qquad + \Big(\frac{209}{18}+\frac{\pi^2}{3}\Big)\beta_0 C_F\Big]\log\frac{Q^2}{\mu^2} + \bar{h}^{(2)},
\end{aligned}
\tag{D.1}
$$

where $\bar{f}^{(1)} = -C_F(1+\pi^2/6)$ and $\bar{h}^{(1)} = -C_F(8-\pi^2/6)$. The on-shell massless Sudakov form factor h is known, see e.g. eq. (50) and (51) in Ref. [129], and I checked that the coefficients of the logarithms in $h^{(2)}$ obtained indirectly from $C_q^{(2)}$ agrees with those expressions. This is an important check of the formalism developed in Sec. 5.2.

Although $\bar{h}^{(2)}$ and $\bar{f}^{(2)}$ do not contribute at NNLL, we give the results for completeness. Note that they can not be determined by the methods in Sec. 5.4. However, $\bar{f}^{(2)}$ can be obtained from the result for $\bar{h}^{(2)}$, given in Ref. [129], and the constant term of $\hat{C}_q^{(2)}$, i.e. $\hat{\bar{C}}_q^{(2)} = \bar{h}^{(2)} + \bar{f}^{(2)} + \bar{h}^{(1)}\bar{f}^{(1)}$, which can be obtained from the result in Ref. [103] or App. C. I find that

$$
\begin{aligned}
\bar{f}^{(2)} &= C_F^2\Big(\frac{3}{2}-\frac{\pi^2}{3}+\frac{119\pi^4}{360}-39\zeta_3\Big) + C_F C_A\Big(\frac{95}{27}-\frac{4\pi^2}{9}-\frac{43\pi^4}{180}+18\zeta_3\Big)\\
&\quad + \beta_0 C_F\Big(-\frac{7}{54}-\frac{5\pi^2}{36}-\frac{2}{3}\zeta_3\Big),
\end{aligned}
\tag{D.2}
$$

$$
\begin{aligned}
\bar{h}^{(2)} &= C_F^2\Big(\frac{255}{8}+\frac{7\pi^2}{2}-\frac{83\pi^4}{360}-30\zeta_3\Big) + C_F C_A\Big(-\frac{1037}{108}-\frac{7\pi^2}{9}+\frac{11\pi^4}{45}+36\zeta_3\Big)\\
&\quad + \beta_0 C_F\Big(-\frac{4085}{216}-\frac{23\pi^2}{36}-\frac{1}{3}\zeta_3\Big).
\end{aligned}
\tag{D.3}
$$

We present the expressions for the anomalous dimensions defined in Eq. (5.28). As explained in Sec. 5.4 we have

$$\gamma_f^{(j)} = -\Gamma_{\rm cusp}^{(j)} \log \frac{-\hat{s}}{\mu^2} + \bar{\gamma}_f^{(j)}, \qquad \gamma_h^{(j)} = \Gamma_{\rm cusp}^{(j)} \log \frac{Q^2}{\mu^2} + \bar{\gamma}_h^{(j)}. \tag{D.4}$$

The expressions for the constant terms are $\bar{\gamma}_f^{(1)} = 0,\ \bar{\gamma}_h^{(1)} = -6C_F$ and

$$\begin{aligned}
\bar{\gamma}_f^{(2)} &= -2(\pi^2 + 4\zeta_3)C_F^2 + \Big(\frac{64}{9} - 28\zeta_3\Big)C_F C_A + \Big(\frac{56}{9} + \frac{1}{3}\pi^2\Big)\beta_0 C_F, \\
\bar{\gamma}_h^{(2)} &= -\Big(3 - 4\pi^2 + 48\zeta_3\Big)C_F^2 - \Big(\frac{82}{9} - 52\zeta_3\Big)C_F C_A - \Big(\frac{65}{9} + \pi^2\Big)\beta_0 C_F.
\end{aligned} \tag{D.5}$$

Acknowledgements

I thank my supervisor Vladimir Braun for his excellent supervision and for sharing with me his immense experience. Also thanks to Alexander Manashov and Yao Ji for instructing me on many of the highly technical aspects of my research.
I also thank my mother and my girlfriend Bine for their support in my personal life.

Declaration of primary Authorship

I hereby confirm that I have authored this dissertation independently and without use of others than the indicated sources. All passages which are literally or in general matter taken out of publications or other sources are marked as such.

Regensburg, March 10, 2023 .....